EXPERIMENTAL INVESTIGATIONS ON DRILLING OF CORTICAL BONE

A Thesis submitted in the fulfillment of the requirement for the award of the degree of

DOCTOR OF PHILOSOPY
IN
MECHANICAL ENGINEERING

Submitted by

GURMEET SINGH

Roll No. 901308002

Under the supervision of

Dr. Vivek Jain
Associate Professor
MED, TIET, Patiala

Dr. Dheeraj Gupta
Associate Professor
MED, TIET, Patiala

DEPARTMENT OF MECHANICAL ENGINEERING

THAPAR INSTITUTE OF ENGINEERING & TECHNOLOGY, PATIALA-147004,
(Deemed to be University)
INDIA

SEPTEMBER – 2019

CERTIFICATE

I, Gurmeet Singh, Roll. No. 901308002, hereby declares that the thesis entitled **"Experimental Investigations on Drilling of Cortical Bone"** submitted to the Department of Mechanical Engineering at Thapar Institute of Engineering & Technology, Patiala, Punjab, for the award of the degree of **Doctor of Philosophy**, is a record of original bonafide research work carried out by me under the supervision of **Dr. Vivek Jain** and **Dr. Dheeraj Gupta**. All the requirements for the submission of this thesis have been fulfilled as per institute norms.

The results presented in this thesis have not been submitted elsewhere for the award of a degree or diploma.

Gurmeet Singh

Roll. No. 901308002

27/9/19

Dr. Vivek Jain

Associate Professor

Department of Mechanical Engineering

Thapar Institute of Engineering & Technology

27/09/19

Dr. Dheeraj Gupta

Associate Professor

Department of Mechanical Engineering

Thapar Institute of Engineering & Technology

Date:

Place: Thapar Institute of Engineering & Technology, Patiala-147004, Punjab, India.

ACKNOWLEDGEMENT

First and foremost, I wish to thank my supervisors **Dr. Vivek Jain** and **Dr. Dheeraj Gupta** for their valuable support, supervision, guidance and belief in me. I am thankful for the positive suggestions, and meticulous guidance that helped me to improve my scientific writing and carry out the new research. I feel really motivated and honored to work under their guidance throughout my entire Ph.D. work.

I wholeheartedly thank the doctoral committee members **Dr. T.P.Singh** (Chairman, Doctoral committee), **Dr. S. K. Mohapatra** (Ex-Chairman, Doctoral committee), **Dr. Dheeraj Gupta, Dr. Vivek Jain, Dr. V.K.Singla, Dr. A.K.Singh**, and **Dr. Mandeep Singh** for the feedback and reviews that were given on my research proposal and progress monitoring presentations. Their guidance was beneficial for me to improve my research work. I am also thankful to **Dr. Tarun Nanda** and **Dr. Gagandeep Bhardwaj** our Ph.D. coordinators for their approachability and keeping me informed with all the relevant communication throughout E-mails.

A special thanks to the office of Mechanical Engineering Department for providing all the facilities required for research work. Thanks to all my lab mates, colleagues and friends for their support and a very special and sincere thanks to Mr. Ankit Sharma, Mr. Apoorv Jain, who had helped me a lot during my research work. I am thankful to the office staff of the ME department at Thapar Institute of Engineering & Technology for their help and cooperation throughout my study.

I would like to thank my wife, **Mrs. Priyanka K. Chauhan**, Assistant Professor, Maharishi Markandeshwer University, Mullana-Amlaba, to share her knowledge related to the field of medicine and her understanding with continuous support during my thesis work.

I am sincere thankful to **Dr. Abhimanyu Sharma**, MD, Assistant Professor, Maharishi Markandeshwer University, Mullana-Amlaba for shearing het experience and knowledge in the field of orthopedics and guidance during histopathology study of drilled bone specimens.

A special thanks to **Mr. Gian Singh (Ex-Drawing Instructor, TIET), Mr. Lalit Kumar (Foreman Instructor, TIET), Mr. Satpal Singh, Mr. Dilkaran Singh, Dr. Debabarata Deb (Assistant Professor, SPMS, TIET), Dr. Himani Pal** for their unconditional support and knowledge at various steps of my research work.

A huge thanks goes to my parents, Mr. Laxman Chand Pal, Mrs. Kiran Raj Pal and parents-in-law, Mr. Mahinder Singh Chauhan, Mrs. Prabha Chauhan, My Brother Mr. Pushpinder Pal who always encouraged me and stood by me. I thank all my family and relatives who had supported and cared for me during this period of time. I wish to thank all those who have helped me directly or indirectly in this journey of my life.

Finally, I bow and thank the Almighty, without whom I could have not completed this journey of completing my research work for the highest degree in the engineering discipline.

(Gurmeet Singh)

ABSTRACT

The implication of machining for bone is widely accepted during the different orthopedic, dental and neuro surgeries. There are some mechanical and thermal damages observed, while machining bone for some specific reasons.This secondary damage to the bone cells and tissues may cause failure to the bone joint. Heat generation around the drill site may lead to osteonecrosis and further the body part may get collapse. Novel techniques are regularly encouraging in orthopedic, dental and neuro surgeries to minimize the thermal and mechanical invasive and improve the quality and efficiency. Ultrasonic assisted drilling method is one from these techniques, in which ultrasonic vibrations are superimposed on rotating tool.The main concern with bone drilling process is to reduce the damages to the bone tissues around the drill site by means of some technological improvements.

In this study, experimental examinations have been done to understand the behavior of bone to thermal and mechanical damage around the drill site with respect to the different drilling parameters and experimental conditions. The experiments included the measuring of heat generation around the drill site, thrust forces during drilling process, diametric delamination of drilled holes and pullout study of bone-screw joint. In order to justify the ultrasonic assisted bone drilling (UABD), a comparison of ultrasonic assisted bone drilling (UABD) process with conventional bone drilling (CBD) process for above said outcomes has been done. The conduct of drilling parameters i.e rotational speed (rpm), Feed rate (mm/min), drill point angle (degree), drill helix angle (degree) was evaluated and analyzed on various levels using Taguchi optimization. From the optimization, most favorable condition of drilling parameters has been found to control the different bone drilling outcomes studied in this thesis. Further, ANOVA analysis was used to check the percentage contribution of each involved parameter on the output

which was optimized individually. The effectiveness of the selected parameters with their levels has also evaluated by calculating P-value in ANOVA table. The parameters considered to be significant when $P \leq 0.05$ for Rotational speed, Feed rate and drill specifications (Point angle and helix angle).

Thereafter, microscopic characterization techniques i.e Histopathology and Scanning Electron Microscope (SEM) were employed to understand the thermal and mechanical damage with respect to the exposed temperature and thrust forces to the bone during experiments. Damaged osteocytes were observed in histopathology study and confirmed that increasing heat generation and thermal damage around the drill siteis directly interpersonal.SEM was used to detect the surface topography in view of surface damage and microcracks generated during the drilling related to the mechanical damage. Finite element analysis (FEA) is conducted and model is developed using DEFORM 3D software to compare the results for ultrasonic assisted bone drilling (UABD) and conventional bone drilling (CBD) process.

The main focus of the study is on the mechanistic behavior of different bone drilling parameters under the influence of ultrasonic assisted tooling conditions and influence of individual parameters on desired responses help to draw the final conclusions and recommendations for its applications in orthopedic surgeries.

Keywords: *Bone drilling, Ultrasonic assisted drilling(UAD), Heat generation, Thrust forces, Pullout, Osteonecrosis, Histopathology, Scanning electron microscopy(SEM), Finite element analysis(FEA).*

CONTENTS

LIST OF FIGURES

LIST OF TABLES

LIST OF ABBREVATIONS

BMD	Bone Mineral Density
AWIJ	Abrasive Water Injection Jet
TEZ	Thermal Effected Zone
SEM	Scanning Electrode Microscopy
RTD	Resistance Thermometer
CMM	Coordinate Measuring Machine
S/N	Signal-to-Noise
ANOVA	Analysis of Variance
SS	Sum of Square
CI	Confidence Interval
DOF	Degree of Freedom
FEA	Finite Element Analysis
CBD	Conventional Bone Drilling
UABD	Ultrasonic Assisted bone drilling

CHAPTER 1: INTRODUCTION

1.1 BONE HISTOLOGY

Bone is an inherent hard body tissue, give impulsive strength and support to the human body for its day-to-day routine. Bone is a connective tissue found in all Vertebrates i.e. consisting of inter-cellular calcified material. Hard bones help to connect the body parts and give relative motion and movement to them. As per structural classification, bones are majorly classified in two types: i) Cortical bone (Compact bone), II) Cancellous bone (Spongy bone) [1-3]. The hard structure, which mainly supports the body and protects the organs, is the cortical bone and inner spongy structure is cancellous bone. The density of cortical bone is around 50 percent more than the cancellous bone [4-5]. The hard structure of bone is covered with a fibrous membrane called periosteum. This layer contains blood vessels, nerves and lymphatic vessels helps to supply blood and oxygen to the bone. The inner hollow surface called medullary cavity, is also covered with membranous lining called endosteum and helps in bone growth, repair and remodeling of bone[6-7]. The detailed structure of femor is shown in figure 1.1.

Damage to the bone in terms of cracks and fracture is a common hazard to the human from ancient time. The reason for these fractures may be unconventional loading conditions or sometime excessive loading due to accidents. The chances of bone fracture will be more if the bones are already suffered with any diseases. According to Rodan GA (1992) [2] tissues of bones are continuously in the phase of resorbed and rebuilt and a disturbance in this balance will causes the several diseases. When bone met any excessive damage in terms of diseases or fracture the remodeling process abort and self-healing process of bone tissues get disturbed [8-9].

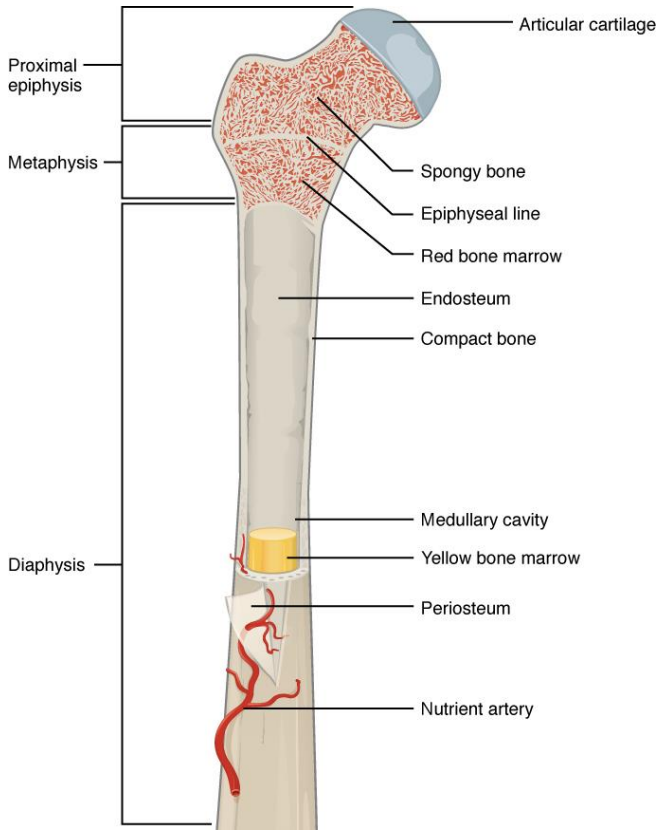

Figure 1.1: Basic Anatomy of Long Bones (Femor and Tebia)[11]

1.2 BONE FRACTURES AND TYPES OF TREATMENT

Fractures are the mainly dislocation or parting off the hard bone tissues, due to some accidents, unconventional jerks or injuries. Due to the inherent property i.e. remodeling of bone tissues, it will heal itself or need to fix it on its anatomical position. If it is not done, the bone may get remodeled in the deformed position. Basically, long bone (femor and tebia) majorly faces the fracture problem. Fractures in these bones are classified on the basis of location, fracture length, direction and complexity [10-11]. The major classification of bone fractures are illustrated in figure 1.2.

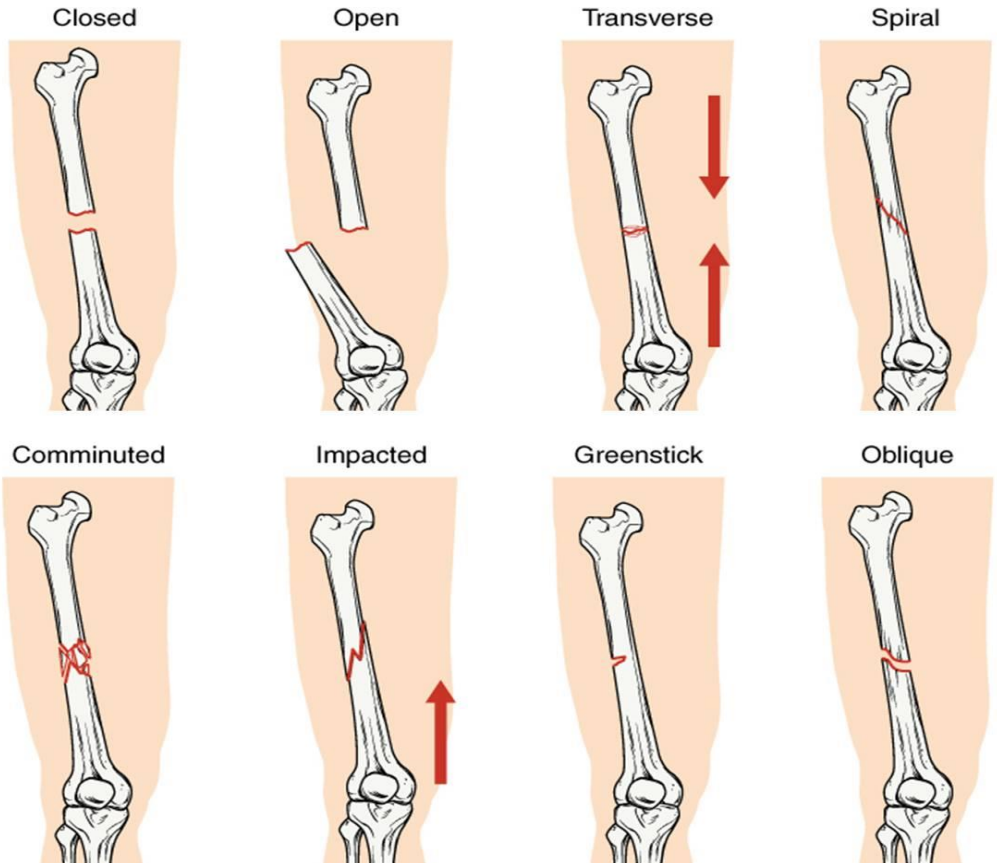

Figure1.2: Classification of Fractures in Bone on the Basis of Features and Level of Cracks in Bone[11]

This fixation of fractured bone at their original anatomical position is carried out in two ways [3,11];

i) Closed Reduction

ii) Open Reduction

Closed reduction process is used when fractures are minor or hair lined. The fractured bone is fixed to its original position, or immobilize for some time to speed up the remodeling process of bone tissues without any surgical intervention, the process is named as closed reduction. On the other hand, open reductions involves surgical intervention to find the fractured bone and reset them at their position with the help of wires, nails or implants.

1.3 PROPERTIES OF BONE

Human bone is a material which shows relative different mechanical properties, with respect to age, sex and ethnicity. The mechanical properties of bone is further depend upon the levels of structural elements and there organization [12-13]. Keveny et al.(1994)[14] reported the behavior of bone in their study and observed different reaction of bone while undergone compressive and tensile forces. Bone is generally a composite material in which fibers are rooted in irregular cage of organic matrix with some pores and liquid within it. Cortical bones are considered to be a transversely anisotropic material. Some authors stated it as standard fiber-rod and some considered it as a platelet-reinforced material [15-17]. Pidaparti et al. [16] recommended the compact bones can be treating as simple reinforced compositie, if the accurate properties of the mineral and collagen of the structure are known. Bones are the main reason for strength of body, thus its mechanical behavior is particularly important to understand the fracture risk in bones. While walking, femor and tebia are continuously under the compressive loading i.e. liable to the increased risk of fractures in these bones. The mechanical properties of bone must be quantified to understand the behavior of bones in different loading and machining conditions. The density of bone is within the range of 1.7 to 2.0 g/cm^3 and Porosity of 30% to 90%[18]. As it described earlier that bone shows different properties under different loading conditions and directions. The quasi-static tensile strength of bone was examined experimentally and large variations in results i.e. 100 to 200MPa and failure strain of 0.4% to 4% [19-21]. The fracture mechanics of bone is different than the isotropic material and the main reason for this is the hierarchical structure and its composition. Mechanical properties of cortical bone reported in different research articles are shown in table 1.1.

Table1.1: Mechanical properties of cortical bone [18-24]

Properties	**Value**
Tensile Strength	45-150 MPa
Compressive Strength	130-200 MPa
Young's Modulus	10-17GPa
Elasticity	1.5%
Shear Modulus	3MPa
Poisson's Ratio	0.4
Hardness	70.36 HRC
Toughness	350 J/m^2
Thermal conductivity	0.38-0.58 W/mK
Density	1800 kg/m^3
Specific heat	1300 J/kgK

1.4 BONE DRILLING: PROCESS, COMPLICATIONS AND CONSEQUENCES

From the ancient civilization, human skeletons need repair and rehabilitation when faced any major damage to any body part. Bone drilling was described in ancient, Greek and Roman medicine. From the modern civilization, orthopedics, dental, neurosurgery, plastics and reconstructive, craniomaxillofacial, ear nose and throat etc. surgeries are performed all over the world. From the studies, it was reported that in the United States only approximately 300,000 knee arthroplasties are performed per year [25]. During orthopedic surgery various operations on bone are performed like drilling, sawing, boring, grooving, grafting, shearing etc. From all these operations, drilling is a major operation performed on bone during orthopedic surgery.

Drilling of bones is a mechanical process and comes in action when open reduction method of Rehabilitation and repair of bones are required. This kind of fracture treatment is used only in case of major fracture. The open reduction process immobilizes the bone by the means of implants and screws. Figure 1.3 shows the fractured bone undergoes healing with a direct approach. This method of treatment is more secure and stabilizes, then the conventional approach.

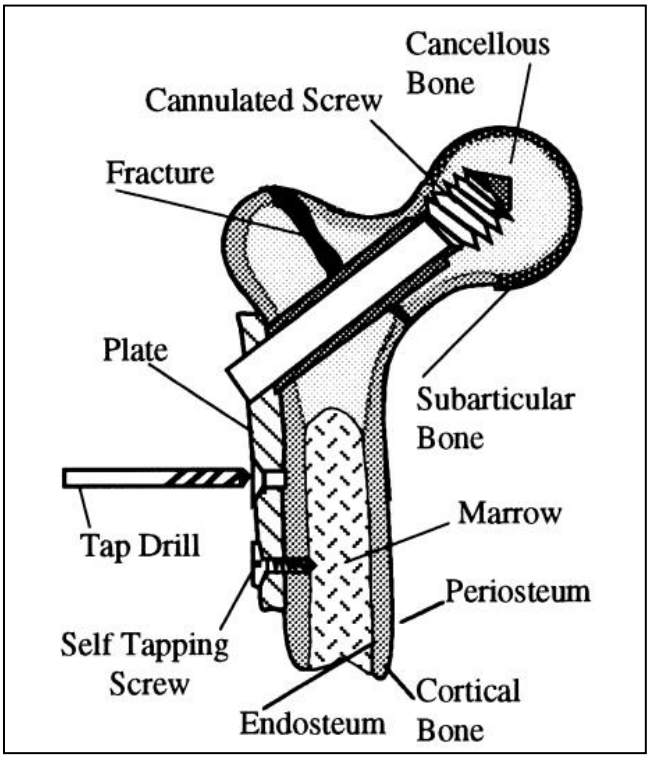

Figure 1.3: Drilling of bone in femoral fracture surgery [26]

Along with all these advantages, some minuses with the drilling of bones are like heat generation, hole accuracy, drill wander etc. Also, other unpredictable situations can occur due to the non-homogeneous structure of the bone material itself. Existing of foreign elements in the body for a long time may cause some other problem like infection and slow blood circulation. Pin site care is given to the patient to avoid these problems. The origin of these side effects arise from the heat generated during the bone drilling process. So, the orthopedic surgeon tries mostly

to cure fracture without surgery. In current medical practice, portable mechanical drilling setup is used to drill the bones. The drilling performed on bone with a wide range of rotational speeds, i.e. 400 to 15000 RPM [24].

It was noticed that the major problem during the open reduction is heat generation and micro-cracks during bone drilling. Drilling through bone is most likely to the mechanical drilling process. During drilling, the mechanical energy is converted into thermal energy. Initially the temperature rises due to frictional forces between tool and bone material. Later thermal energy produces due to plastic deformation and shear failure of bone. Rise in temperature depends on major drilling parameters like, rotational speed, feed rate, axial thrust force, initial drill bit temperature, drill diameter, and irrigation system. As the bone is a poor conductor of heat, and fresh cortical bone has a thermal conductivity of 0.38-0.58 W/mK [27] so the heat accumulated at the localized point of drilling only. Due to low thermal conductivity, temperature rises rapidly within the bone. If the temperature rises beyond the threshold limit, then the irreversible death of bone cell is observed. Threshold limit is suggested as 45°C by Olson et.al. (2011) and exposing of bone above this will leads to the irreversible death of bone cell is known as thermal necrosis or osteonecrosis [28]. After fixation, major forces act on the fixation screw of the implanted device in the bone. So it needs to make sure that screw must fit into the place or grasp the bone within the drilled hole. But the stability of the joint depends upon the anchorage strength of screw with the bone. This anchorage strength of screw with bone is leading to loosening, because of osteonecrosis and cracks in the drilled walls of bone. It is reported that, the implant failure rate for lower leg osteosynthesis is around 2.1-7.1% [29]. Thus, the method of internal fixation of fracture for fast recovery is helpful only if the osteonecrosis and cracks are avoided.

During the bone drilling the temperature should be maintained as low as possible for the safety of bone and tissue from the necrosis. During the year, 1984 Eriksson et al [30] performed histological, histochemical and vital microscopic study in the rabbit and concluded that a threshold of 47°C for 60s to cause thermal necrosis of the cortical bone. Lundskog [31] conducted his study on rabbit and found that temperature of 50°C for 30s induced irreversible death of the bone cell. Krause et al. [32] performed the study on the cutting of bone; author found that thermal necrosis occurred when the temperature reached around 50°C. It was reported that protein cannot be generated when the temperature increased above 70°C. Further, it was noticed that the temperature can reach up to 170°-259°C if the optimum drilling parameter or irrigations are not used [64]. Majority of the researchers reported that, average temperature of 47°C for 60s as threshold level, above which the necrosis of the human bones will take place [30,40,43-45].

Hole accuracy, drill wander and micro cracks are the other problems arising during the bone drilling process [3,24,29]. The axial penetration forces should not be too much because in some patients it may cause further fractures. Drill bit can be broken frequently if the forces and torque during the drilling increased above a certain threshold value. To penetrate in bone with a breakage drill bit needs more force. Furthermore, drilling forces are the main source of heat generation during bone drilling [33], which could increase the temperature during the bone drilling and increased in temperature can be the reason for thermal necrosis. Moreover, the axial large drilling forces could promote the microcrack formation if these forces exceed the threshold. Elastic modulus and bone stiffness is decreased, because increase in the level of micro cracks. These micro cracks could cause fatigue damages in bone, because the increase of micro-cracks can decrease the bone stiffness and the elastic modulus [34-36]. Therefore, rapid accumulation of

micro-cracks will increase the bone fragility and lead to stress fractures or this could yield prosthetic or bone failure [37]. Hence, there is an increasing demand to minimize the cutting force in order to avoid injuries to nerves in the treated area.

1.5 MOTIVATION TOWARDS THE RESEARCH

Millions of the surgeries performed in the world, in which bone encountered mechanical drilling process during open reduction process. Some orthopedic abnormalities like fractures, trauma or disease are intervened using fixing of implants or any other supporting agent. Drilling of bones was an ancient practice and used around 500B.C. for different purpose related to orthopedics. In modern medicine, drilling is employed to fix the implants on fractured bones, interamedullary canal along the anatomical axis for total knee anthroplasty during the treatment of osteoarthritis. It is also used in the treatment of osteochondral lesions by subchondral drilling or osteochondral allografting technique. The overall success rate of these all surgical procedures and remodeling time of bone tissues are majorly depend upon the invasion induced to the bone during the drilling process. Drilling is a mechanical machining process in which a drill tool used to create a cylindrical cavity in the bone used for fastens the screw while supporting the fracture bone with metallic implants. During this mechanical process large mechanical forces developed during the shear deformation of bone. The large residual mechanical forces and friction in between the chips and rake face of tool cause the heat generation and micro-cracks surrounding the drill site. The low thermal conductivity of bone also plays a vital role as it does not allow the heat to dissipate within the bone i.e. increases the local heating around the drill site. The increase in temperature around the drill site may result in the form of temporary or permanent decay of tissues i.e. loos of blood and oxygen to that specific part will get disturbed and finally leads to the thermal osteonecrosis.

Along with the thermal damage, mechanical damage was also observed to the bone surrounding in term of micro cracks in the bone. Which may get prolong with the time and can cause the low anchorage strength of fixed screws and may be a reason of secondary damage to the bone and joints.

From previous studies, it was observed that the excessive heat generation may damage the bone in term of osteonecrosis. The amount of heat in terms of temperature and its expose time with bone is the countable head for judging the level of osteonecrosis in bone. Some experimental observation has been conducted on different species including human bone and their results for osteonecrosis are as follows in table 1.2.

Table1.2: Investigation on threshold for osteonecrosis of bone

Authors(Years)	**Species Investigated**	**Conclusions**
Moritz and henriques (1946)[38]	Pig	Above 70^{o}C causes immediate damage
Bonfield and li (1968)[39]	Dog	After 56^{o}C bone cells dead
Lundskog (1972)[31]	Rabbit	55^{o}C for 30s induced irreversible death
Eriksson & albrektson (1983)[40]	Rabbit	47^{o}C for 1 min causes thermal necrosis
Augustin et.al. (2009)[41]	Goat	Above 47^{o}C necrosis observed
Olson et.al.(2011)[28]	Human bone	At 45^{o}C bone cells starts burning

It has been observed that bone fractures are very common, and hence it needs better care while drilling so the problems associated with bone drilling like thermal necrosis, hole accuracy and

microcracks should be eliminated. Therefore, a better understanding about the drilling process and parameters behavior will definitely help the orthopedic surgeon to take the steps for sustainable surgery. Studies conducted so far are helpful up to some extent, but the limitation is within technique used for drilling. An innovative ultrasonic-assisted drilling technique introduced for bone drilling and possesses minimal damage to the bone. The ultrasonic-assisted drilling technique is a hybrid drilling technique, where the tool contact is not regular with the bone. This detachment of tool is at ultrasonic level and provides aerodynamic cooling during the process. The discontinuous action of tool also help to reduce the stress developed at the interface of tool and workpeice. However, the technique is in investigating stage and the parametric study with different drilling parameters can contribute a positive impact and support for its commercial use in orthopedic surgery. The basic motivation for carrying this work is primarily to drill the bone with minimum invasive to the bone tissues (thermal and mechanical) for application in orthopedic surgeries.

1.6 THESIS OVERVIEW

The structure of present work organized in different chapters as following:

Chapter 1: This chapter introduces the bone, bone structure and its function within the body. Different fractures in the bone and the role of mechanical machining process in treatment of orthopedic fractures is also highlighted. The developments in the orthopedic surgery for efficient bone drilling process are explained. Some historic developments and research about the damages (mechanical and thermal) induced during drilling are highlighted. Further, it includes how an inefficient drilling of bones may cause some post-operative complications and affects the sustainability of orthopedic surgery. The complications during the bone drilling drive through the

motivation of the work progress in the field of bone drilling and how an efficient bone drilling using some novel technique which can reduce the damage is outlined.

Chapter 2: A comprehensive literature of orthopedic bone drilling process and its outcome has been reviewed. The detailed study about the effect of drilling parameters on aftereffects of bone drilling is focused. Literature review has been categorized according to the various types of studies related to the bone drilling process. i.e. threshold level of osteonecrosis, effect of process parameters on bone drilling outputs, factors affecting the hole quality and sustainability, and unconventional drilling attempts for orthopedic surgeries. All available bone drilling processes are also reviewed and their feasibility check has also been explained. On the basis of literature review, research gaps have been identified and formulate the objectives for the present work. Finally, the methodology and detailed work plan for the research has been overviewed.

Chapter 3: Include the experimental process in detailed. The selection of bone for experimental process has been introduced and the selection of process parameters which is to be studied under experimental condition has been discussed. On the basis of selected parameters the L25 orthogonal array experimental process has been designed. The development of ultrasonic assisted drilling setup for experimental purpose has been explained and further the other required equipment (dynamometer, temperature data logger) for experiment is being explained. Experimental observations with respect to the each experiment performed have been presented. Further, the drilled holes were studied for the delamination, Scanning Electron microscopy (SEM), and histopathology examination of bone specimens for the drilled hole accuracy, hole quality and osteonecrosis in drilled bone specimens respectively.

Chapter 4: The experimental observation had undergone the statistical calculation as per taguchi optimization technique and ANOVA calculation to get the optimized set of parameters for

desired output of bone drilling. The Taguchi calculation for lowest heat generation, lowest thrust force is being calculated and the results were analyzed. The effect of parameters on drilled hole accuracy, hole quality and osteonecrosis were also analyzed through the characterization of bone samples.

Chapter 5: explained and discuss the results of each experimental output with respect to the change in parameters. The concept behind the change of experimental out with change of respective parameter has been explored and discussed with the reference of available literature. The chapter also discussed about the characterization of drilled holes under Scanning electron microscopy (SEM) and histopathology.

Chapter 6: The bone drilling model using simulation software Deform 3D has been developed. The study of conventional drilling and ultrasonic assisted bone drilling is carried out using the developed model. The temperature rise during both the drilling techniques has been discussed and the results compared. The importance of use of simulation software in orthopedic surgery is also discussed.

Chapter 7: The results obtained from experimentation and simulation summaries further to draw the key findings of the research in terms of conclusions. The possible scope of future work in this area is also outlined.

In the end of the thesis, references, appendix and papers published related to this project is listed.

1.7 SUMMARY

In order to drill the bone successfully for fixing implants to support the fractured bone the conventional drilling techniques is still in practice. However, some developments are introduced to make the bone drilling more efficient i.e. making machine portable and handy for easy control of feed motion as per requirement, use of guide ways to fix the position and direction of tool. But

the main technique used to cut the material from the drill site is still the same. The above said technique and the cutting action of this technique is the main reason for the consequences faced by the bone. Therefore, the unconventional non-thermal approach must be introduced to reduce the damage to the bone. The recent demand of more sustainable orthopedic surgeries target to reduces these damages to the maximum extent. The threshold limit for thermal damage is highlighted and discussed. The use of ultrasonic- assisted drilling technique is introduced which is a prominent and efficient method to reduce the damages. The requirement and motivation of the present work is also discussed with the organizational structure of the thesis.

CHAPTER 2: LITERATURE REVIEW

2.1 BONE DRILLING: REVIEW

The requirement of drilling the bone for treatment of orthopedic surgeries invites some after effects. These effects are so serious that they must be eliminated or minimized for a viable and effective surgery. Osteonecrosis is the major issue faced by the bone and most of the researchers focus their research toward this. Heat generation during the bone drilling is the main cause for the osteonecrosis in a healthy bone and is considered as the preliminary damage to the bone. Further, the micro cracks in the drilled walls exaggerate and turns in to large voids which may lead to the lower axial pullout of screw considered as secondary damage to the bone.

The drilling conditions are the main reason for these damages and these were studied in the old literature available [3,24-50]. On the basis of available literature the review can be divided in the following sections.

- Determination of threshold level for osteonecrosis in bones.
- Effect of different drilling parameters on the damage in bone drilling.
- Study about other factors that affect the drilling quality and sustainability.
- Feasibility and practicality of unconventional bone drilling techniques.

2.1.1 Threshold level for osteonecrosis in bones

Osteonecrosis in the bone is a type of disease, in which the supply of fresh blood is aborted. The lacking of blood will forced the bone tissues to get damaged and further failure and trauma of the particular body part. High temperature rise in bone drilling is the main concern for the osteonecrosis. Thermal necrosis in the bone tissues was examined in terms of the diminution of osteocytes. Evaporation of lacuna from osteocytes during drilling increases the chances of

osteonecrosis and the osteoclastic resorption will occur which affects the strength of bone. The necrotic bone in the body act as a foreign element and body did not feed it further. The major concern of the studies is to find out the level of temperature up to which bone can withstand without affecting the osteocytes. Healthy and enriched osteocytes give strength to the bone. Various studies have been carried out to check the response of lacunas within the osteocytes with respect to the temperature rise. Initially, Bonfield and Li(1968) [39] reported that temperature more than 50°C causes irreversible changes in the morphology of bone. Lundskog (1972) [31] studied experimentally to investigate the thermal properties of bone and threshold level of temperature for osteonecrosis in bone. Study was performed on rabbit bone and results concluded that the heat generation of 55°C for 30s only damaged the bone cell permanently. Franssen Bas et al (2008) [42] conducted experimental investigation on rabbit bone drilling with K-wires to study the behavior of changes in osteocytes and observe that the increase drilling time directly increase the damage around the drill site. The damage has been observed in terms of distance up to which the osteocytes get damaged shown in figure 2.1.

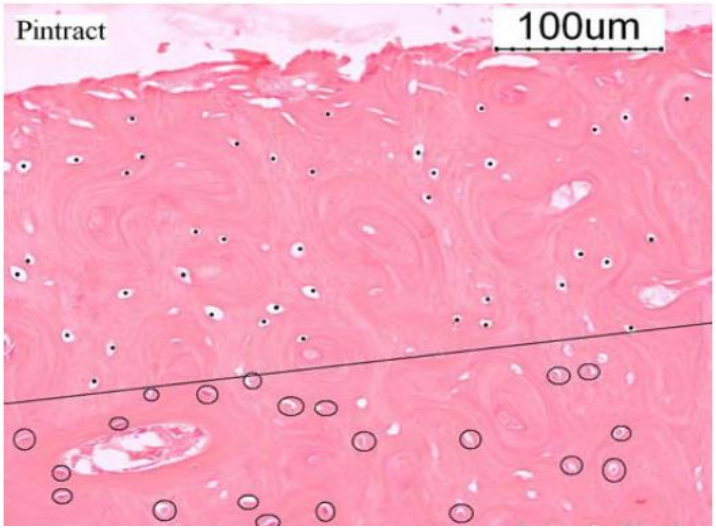

Figure 2.1: Empty osteocytes marked above the margin line [42]

Eriksson et al. (1984) [42] performed histological microscopic investigation to study the level of threshold temperature for thermal necrosis in bone. Results show that the temperature of 47°C for 1 min causes losses to the bone up to the structural level. It was also stated that heating up to 44°C does not show any significant effect on bone. In other studies, Eriksson et al. (1982,1983,1984,1986)[40,42-45] confirmed that the threshold level for the thermal injuries for bone is 47 °C. Karaca et al. (2011)[46] also performed drilling experiment on bovine bone and studied the effect of parameters and results were studied histologically and results reported in terms of evaporated lacunas from osteocytes. Images shown in figure 2.2 observe the effect of heat generation in bone morphology.

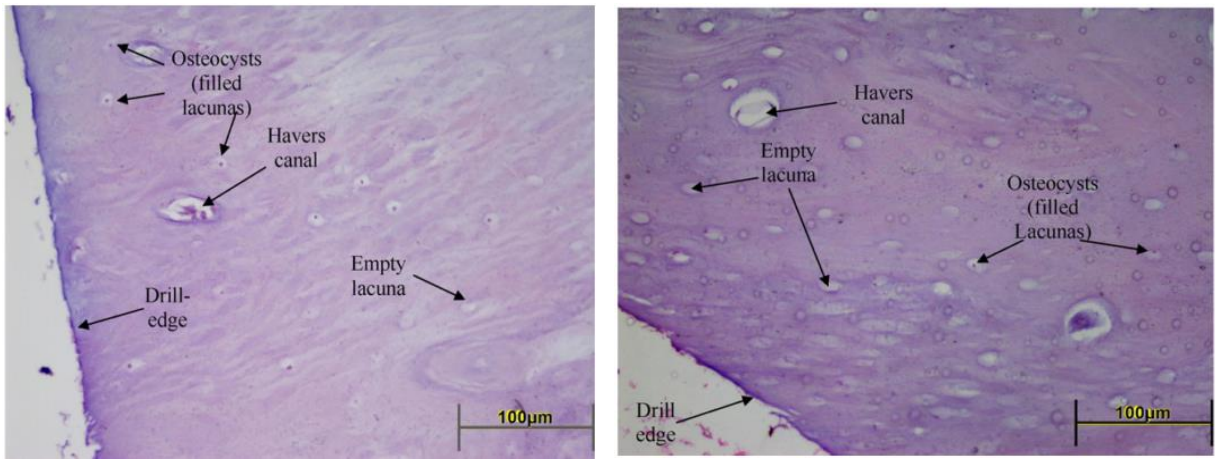

Figure 2.2: Histopathology images of drilled bone specimens (A) temp exposed 47.7 °C, (B) temp exposed 54°C. [46]

2.1.2 Effect of different drilling parameters on damage in bone drilling

The mechanical drilling of materials is a thermo mechanical process in which a mechanical shearing of material removes the material in form of small chips. The shearing of material initiates the heat generation and develops with the continuation of the process. Further, the removal of chips and friction between the drilled wall and tool increase the temperature rise

[3,27,47-48]. This rise in temperature during drilling is a major source of thermal damage around the drill site. The heat dissipation is also very slow due to the low thermal conductivity of bone [3,27,49] and the collective damage is done around the drill site within the minimum peripheral distance. If this heat possibly distributed within the material then the heat encountered by per section of the bone will be minimum and hence decrease the thermal attack. During bone drilling, different drilling parameters, drill design and specifications must be chosen wisely so that the heat generation must be as low as possible. Different drilling combinations and parametric studies were conducted and reported the effect of specific drilling parameter in terms of thermal and mechanical Damage.

(a) Rotational Speed:

The effect of rotational speed has been studied individually by the various researchers [50-69]. Thompson, (1958) [50] experimentally performed in vivo skeletal pin insertion in the bone using the rotational speed of 125 rpm to 2000 rpm and measured the heat at a distance of 2.5 mm and 5.00 mm. It was observed that the increasing rotational speed of drill bit generates more heat in bone. The result of increasing the heat generation with increasing rotational speed were confirmed by some other researchers with different bone drilling conditions and parametric range [29-30,43-45,51-53]. Vaughan and Peyton (1951) [51] investigated the behavior of heat generation in cutting of tooth under the variable drilling conditions using fisher burr tool. The behavior of rotational speed has been studied from 1100 to 11,300 rpm and results show (in figure 2.3) that increasing rotational speed develops high temperature during drilling. Kalidindi (2004) [53] studied the low rotational speed (1200-2200rpm) on drilling of cortical bone. However, the difference in rotational speed is very low but still there is variation of 5°C in temperature rise has been recorded. Some studies also followed the concept of increasing

temperature with rotational speed [54-67]. Mathematical, numerical and finite element model also approved the concept of increasing heat generation with increasing rotational speed [27,47-48,68-69] (shown in figure 2.4). The concept of frictional energy plays the role on increasing heat generation. The frictional energy linearly increases with increase the rotational speed and thus, converted in to heat and directly leads to the higher temperature.

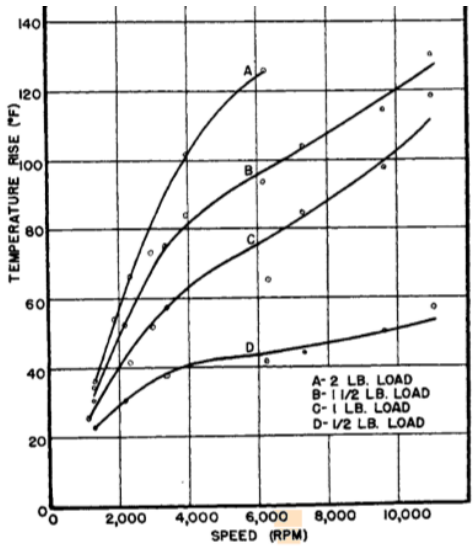

Figure 2.3: Behavior of temperature on increasing rotational speed in bone drilling [51]

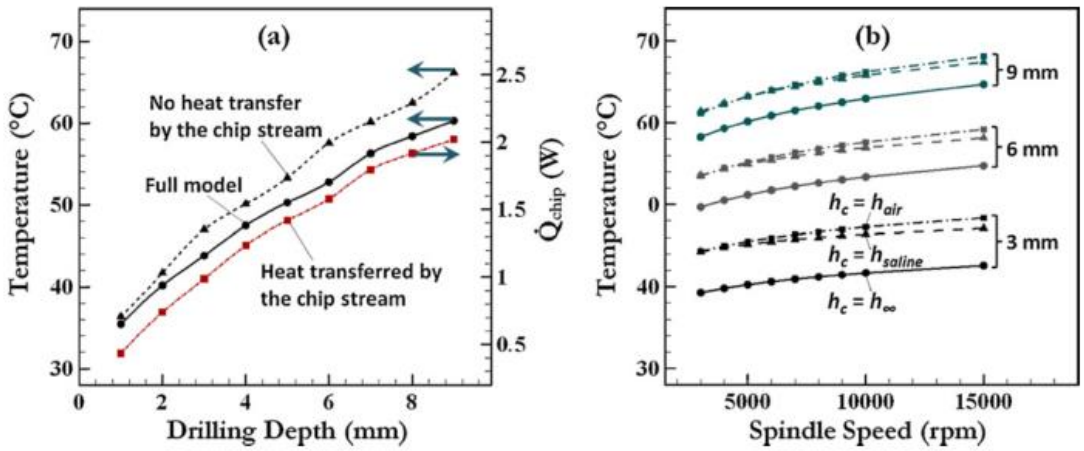

Figure 2.4: Heat generation in bone drilling using numerical thermal model and experimental study [47]

However, the increasing rotational speed may give an efficient cutting of bone and helps to minimize the thrust forces and toque developed during the drilling. Alam et al (2011); Wang et al. (2013) [70,71] stated experimentally, that the friction coefficient at the interface of cutting surface and drill tool decreases with increase in rotational speed (in figure 2.5). An easy and efficient shear deformation was observed with higher rotational speed, results in the form of thinner chips and less thrust forces. Further, Lee et al. (2011,2012)[48,66] studied the effect of drill depth on force and torque, found that the drill depth is also a prominent factor and while going in depth, the results may differ for thrust force and torque at different drilling depths. Increasing drill depth, rapidly increase the drilling forces and torque due to fine chipping mechanism with higher rotational speed (shown in figure 2.6).

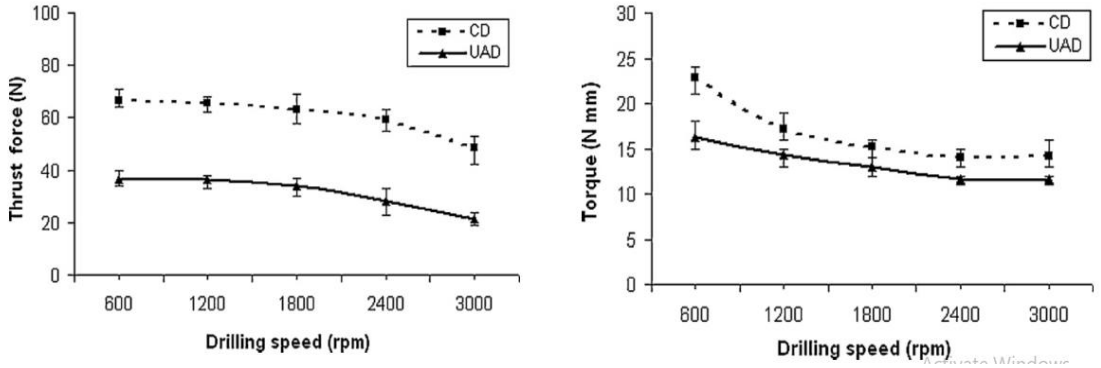

Figure 2.5: Effect of rotational speed on thrust force and torque [70]

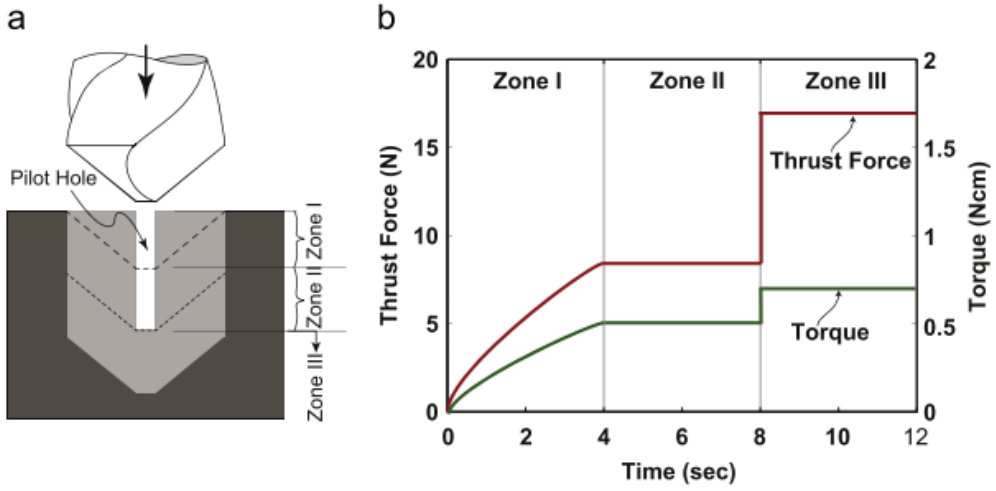

Figure 2.6: Development of drilling forces at different drilling depth [48]

Small and fine chips of bone material get packed in the flutes in spite of the withdrawing, ultimately increase the forces exerted by the drill bit [48]. The mathematical model developed by Lee et al. (2012) [48] confirms that increasing drilling depth increase the thrust forces and torque. However, Soriano et al. (2012) study the torque developed within the range of 50-500rpm, shows that drill depth does not affect significantly in bone drilling. But the range of rotational speed was very compact in this experiment and used three flute drill bit which ejaculate the chips at faster rate than standard two flute drill bit. Many studies (Rafel 1962, Abouzgia and James, 1995, Sharawy et al., 2002) agree with this concept and support this experimentally and analytically [72-74]. Further it was found by (Alam et al., 2011; Xu et al., 2014) that the forces increases with rotational speed up to a certain value and then starting decreases with increase in rotational speed of drilling tool[65,70]. The level up to which the forces start decreasing can be different with drilling conditions. The above experimental, analytical investigations stated that the rotational speed affects the bone drilling thermally and mechanically. The optimal combination of parameters is a solution and results may vary with the drilling conditions [72-73]. But in general, the increasing rotational speed increases the damage thermally and decreases the damage mechanically.

(b) Feed Rate:

Feed rate is a drilling parameter which allows the specific thickness of the material to be cut during per revolution of cutting tool. A higher feed rate in drilling allows a deep cut, which results in the form of high shearing stress development and thus, a high thrust force and toque may be observed (Alam et al, 2011, Soriano et al., 2012; Wang et al., 2013; Xu et al., 2014; Lughmani, 2013)[65,70,77,78,82]. The effect of feed rate on thrust forces were verified by the finite element simulation process and behavior of feed rate was studied experimentally also

[70,81] (shown in figure 2.7 and 2.8) . The higher forces developed with the high feed rate also increases the frictional forces between drill walls and cutting tool.

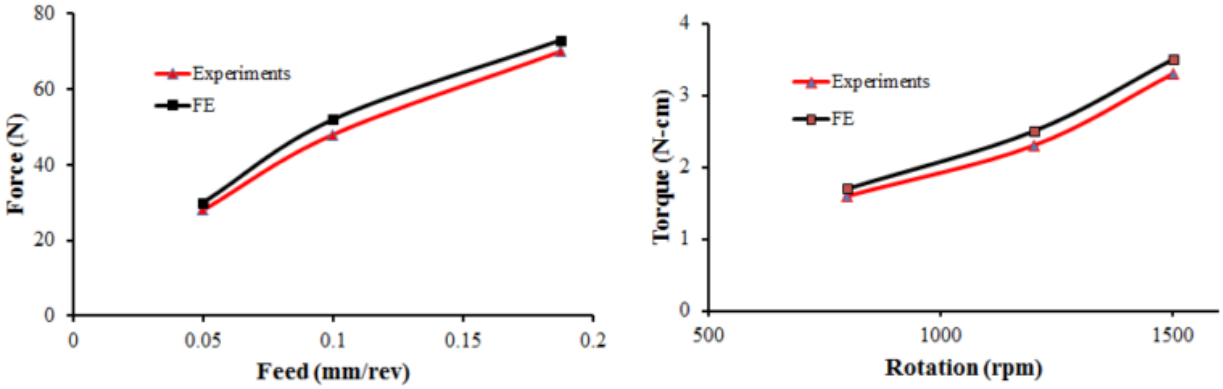

Figure 2.7: Forces and torque measurment during the drilling of bone process [81]

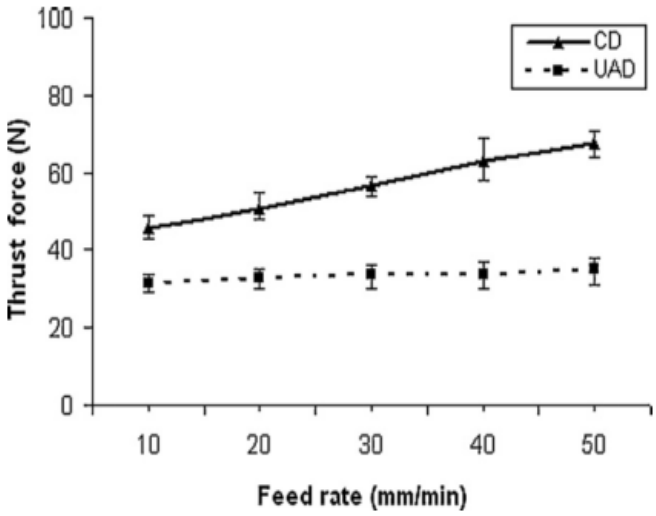

Figure 2.8: Effect on thrust force with increasing feed rate [70]

The mechanistic model developed by lee et al (2012) [48] also shows that the increasing feed rate directly associated with the high thrust force and toque at marginal high speeds. In terms of thermal losses, with the above said reason where frictional forces increases with high feed rate,

the heat generation also increase with the increase in feed rate (Pandey and Panda, 2014,2015; Brisman, 1996; Lee et al., 2011; Alam et al., 2015)[48,60,66,75-76,81](in figure 2.9 and 2.10).

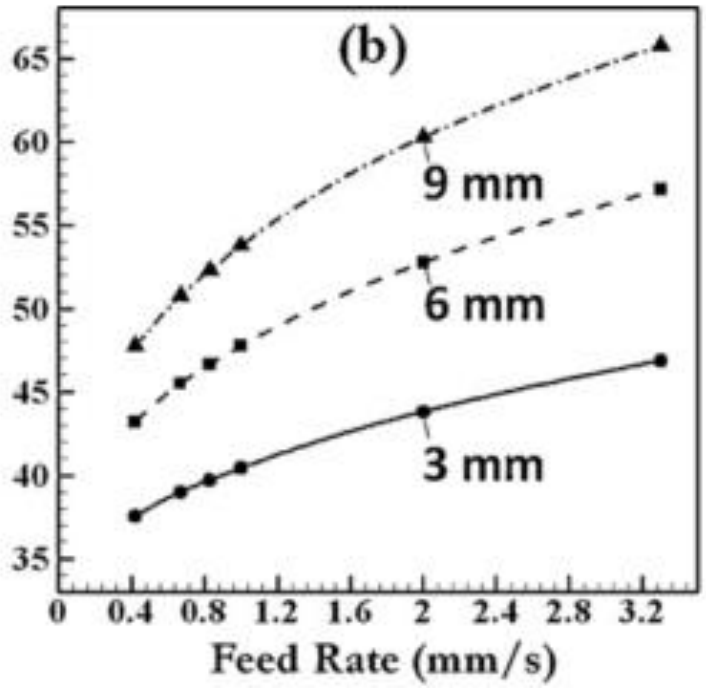

Figure 2.9: Effect of feed rate on increasing temperature [48]

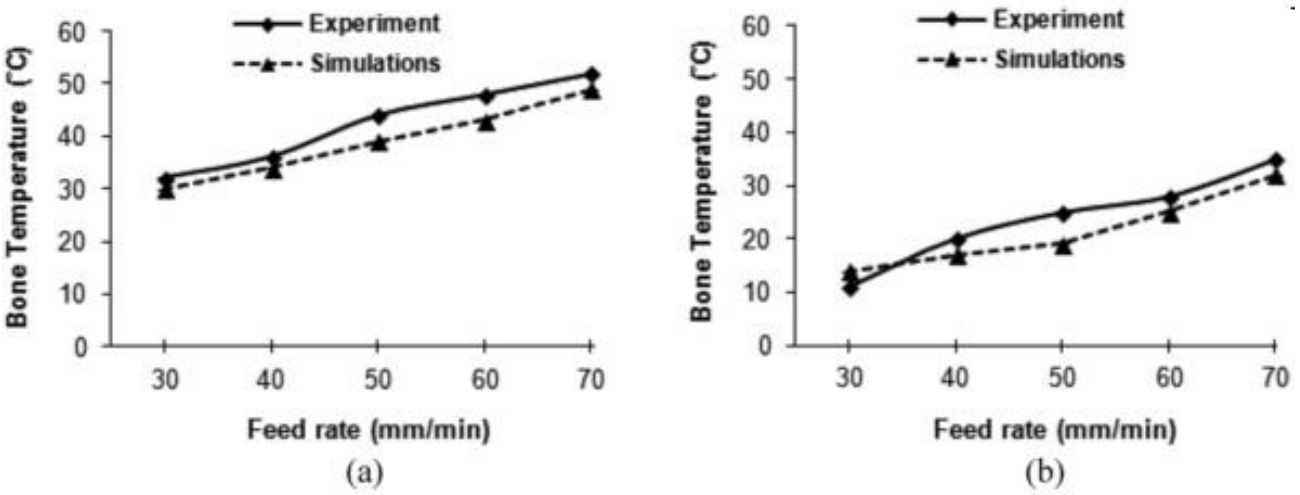

Figure 2.10: Effect of feed rate on increasing in temperature with feed rate (a) Initial temperature 25°C, (b) Initial temperature: 5°C

The generated heat during drilling is distributed within the bone and increasing feed rate of tool give less time to transmit the generated heat to the bone. Thus, the thermal losses in term of

osteonecrosis may be less with the high feed rate. The temperature measured at distance of drill site is measured less by several researchers with increasing the feed rate (Krause, 1987; Toews et al., 1999; Augustin et al, 2008; Soriano et al., 2012; Karaca et al., 2013; Xu et al., 2014; Tai et al., 2015)[61,65,79-82]. However, this effect has been observed when the study has been done with a wide range of feed rate (10-150mm/min). In a short span of feed rates, where the difference of drilling time is comparatively less, the effect is not significant. Therefore, the selection of optimal solution was suggested by the researcher to get balance these two mechanisms affecting the thermal lose to the bone during bone drilling.

(c) Drill bit Specifications:

Design of drill bit is a complex structure directly involved in bone drilling and affects the thermally and mechanically to the bone and its surrounding. The structural view of drill bit shown in figure 2.11, having a specific diameter with shank, flutes, helix angle, point angle, chisel edge, cutting lip and flank face are the essential structural body parts in a standard drill bit.

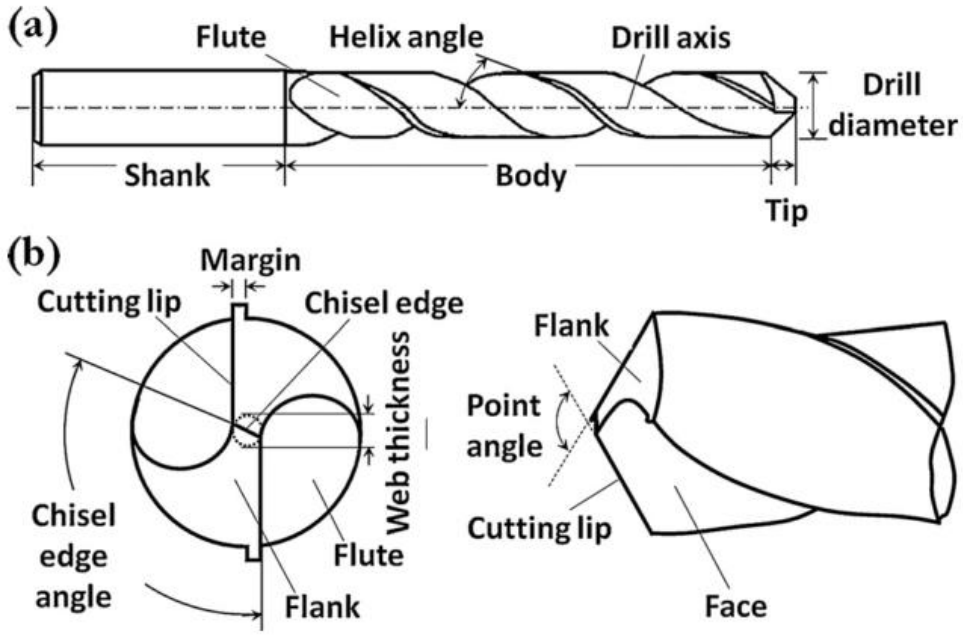

Figure 2.11: Detailed drawing showing the structured elements of drill bit [47]

The commercially available and in practice surgical drill bits are within the range of 0.4-4.5mm and used subjected to the requirement. Different structural parts of the drill bit play their role during drilling differently and shown their behavior in terms of their effect on thermal and mechanical lose. These all aspects have been studied separately by different researchers. These studies reveled that heat generation and drilling forces in bone drilling is directly proportional to the drill diameter [27,57,66-67] . Increasing drill diameter directly increases the surface contact of drill and bone; eventually increase the frictional forces and higher material removal per revolution of drill bit. Increasing drill hole size also affect the strength of bone. However, selection of drill bit is completely depend upon the level of fracture in bone, size of bone and implant need to be fixed on the fractured bone. From the above said experimental studies, it is evident that the size of drill bit should not be increased unnecessarily.

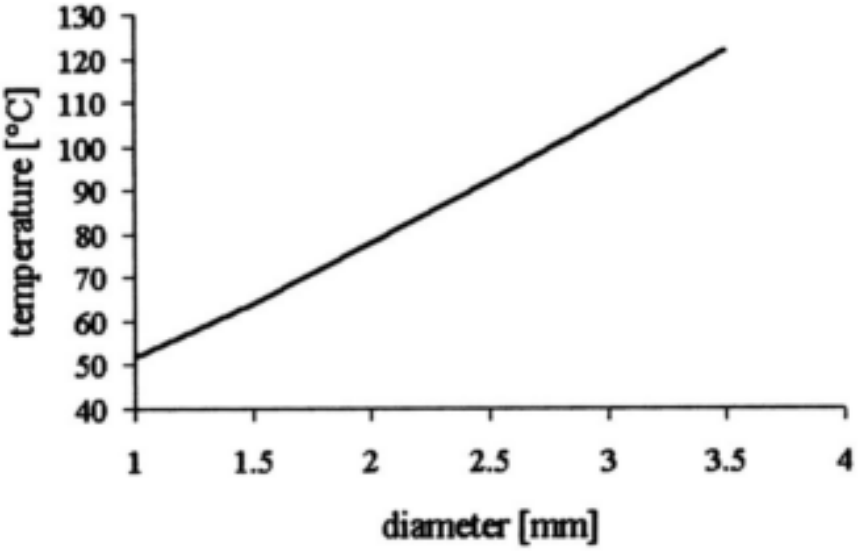

Figure 2.12: Change in temperature with respect to diameter [27]

The next feature of drill bit which is directly and primarily involved in the drilling of bone is chisel edge and point angle of drill bit [3,75]. The first encounter of bone with drill bit was with

chisel edge of drill bit. The edge formed at the connection of the cutting lips [3,80]. While rotating the drill bit at its axis, the edge starts the cutting action and developed thrust forces at the contact point. The wider chisel edge increases the primary shear deformation and thus, resulting in the form of excess heat generation [3,86-87]. While limiting the chisel edge may weaken the drill causing breakage of tool tip at high rotational speed and feed rate [3]. Natali et al.1996 [37] used a split point drill bit to reduce the chisel edge surface area results in the form of better cutting action with a positive rake angle (shown in figure 2.13). The split point of drill bit also helps to get accurate position on the uneven surface of bone and reduces the chips into small sections for easy discharge through drill flutes [37]. Overall, concluded that decline the chisel edge reflects in the form of less heat generation and reduces the thrust forces with better accuracy in the positioning on bone for desired hole.

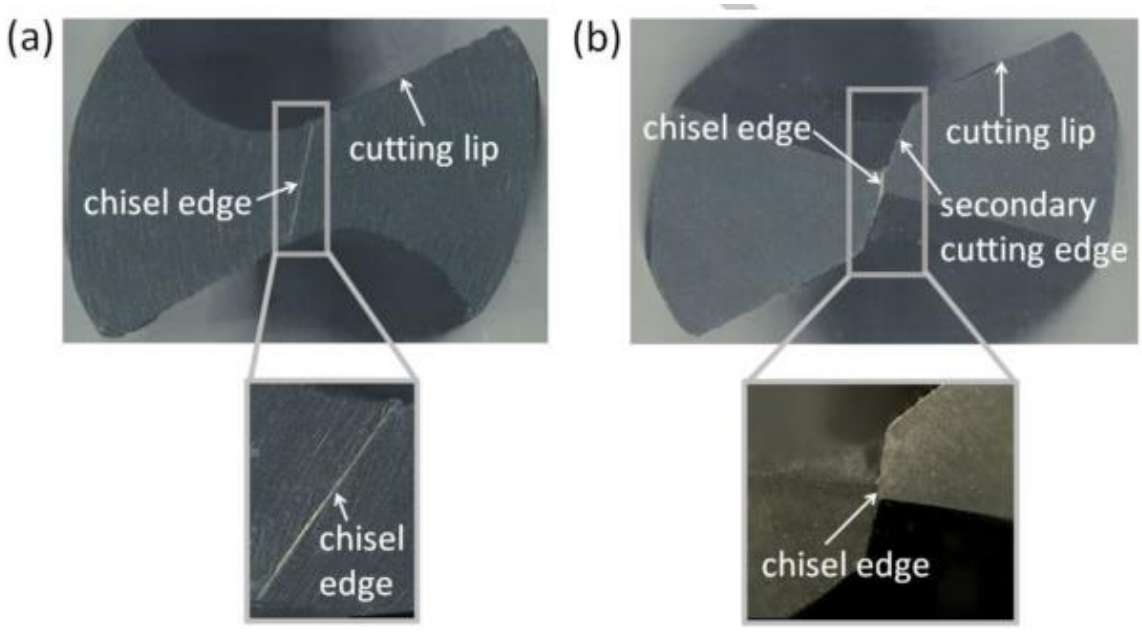

Figure 2.13: Chisel edges of drill bits: (a): standard drill bit; (b): split point drill bit[3,37,87]

Point angle of the drill bit is angle formed by extending the projections of drill cutting edges concentric with the plane of longitudinal axis [3,87]. The point angle of tool help to get pokes the drill in the material and its cutting edges start removing material in form of chips. An optimum point angle is essential to minimize the damage in the bone drilling. Point angle gives the inclination to the cutting edges of drill bit and the material is to be removed with per revolution of tool is to be changing with varying point angle. Small point angle are more accurate, tool tip prevent the tool dislocation even with less loading conditions. Low point angle of tool provides small chipping of material with initiation of drilling. Thus, decreases the shear stress and results in the form of less heat generation at the time of first stage of drilling. Whereas, higher point angle gives complete contact of cutting edge as quick then the lower point angle tool and generates high heat generation. From literature, there are conflicting remarks on the point angle of tool in case of bone drilling. Bechtol et al. (1959) [88] conducted experimental investigation and observed that the drilling with point angle (90º) lower than the standard (118º) gives less damage to the bone. Jacobs and berry (1976) [89] also suggest that point angle lower than the standard drill point angle should be used in case of bone drilling. Hillery and Shuaib (1999)[26] suggested that there is no significant differences in the performance of temperature generation while drilling with low range of point angle (70º,80º,90º). On the other side, Saha et al. (1982); Natali et al. (1996); Karmani and Lam(2004); Franworth and Burton(1974); Sneath(1964) suggested the point angle of 118º to 140º for better drilling performance in terms of torque, rate of penetration and hole quality [37,57,90-92]. Recently, Alam et al.(2018) [93] investigated experimentally the effect of point angle (90º,118º) specifically for bone drilling and observed that point angle of 90 produces less thrust forces and less heat generation in bone drilling. Lee et

al. 2011 confirms the effect of point angle mathematically and suggest low point angle for less damage in bone drilling [47].

The cutting face of the drill bit includes the rake angle of the cutting lip, clearance angle and flank face[3,47]. Rake angle is the angle formed by the rake face and a perpendicular plane passing through the cutting surface of the workpiece [3,87](shown in figure 2.14). The rake face of the tool is directly involved in the cutting action and the material removed by the cutting edge slides over this. The material removal and chip formation is interlinked with the rake angle. Jacob et al. (1976); Saha et al. (1982); Hillery and Shuaib (1999) [26,57,89] conduct experiments to check the significance of rake angle in case of bone drilling. Heat generation in bone drilling is also a factor controlled by the rake angle of the drill bit. Movement of chip over the rake face generates frictional energy and thus converted and transmitted in to heat. Lee et al. (2011); Jacob et al. (1976); Wiggins and Malkin (1976) observed that drilling forces during bone drilling decreases with an increase in positive rake angle of cutting tool [47,89,94]. Saha et al(1982) [57] observed that increasing the rake angle increase the cutting efficiency with high drilling energy generated; i.e. further converted to heat also. Hillery and Shuaib 1999; Plaskos et al., 2003; Yeager et al., 2008; Soriano et al., 2013 suggested 20-30º rake angle for efficient drilling with low forces and easy clearance of chips[26,95-97].

From figure 2.11(b), the flank face of the drill bit is the area adjacent to the cutting edge at the tool tip. This area makes contact with the workpiece and responsible for high frictional energy [3,87]. The angle given to the flank face to avoid unnecessary contact with the workpiece during drilling is the clearance angle in drilling tool. The clearance angle must be fixed as per the requirement and type of material to be drilled. In case of bone drilling, the researchers tried to control this factor for minimum thermal damage. Farnworth and Burton (1974) [91] conducted

experimental study on cortical bovine bone and suggested that 15 degree clearance angle provides better and efficient drilling. Saha et al. (1982) [57] supports his results and suggested 15 degree as optimum clearance angle for bone drilling. Karmani and Lam (2004) [90] investigate for the optimum drill design and suggested that 12-15º clearance angle is perfect for drilling the bone.

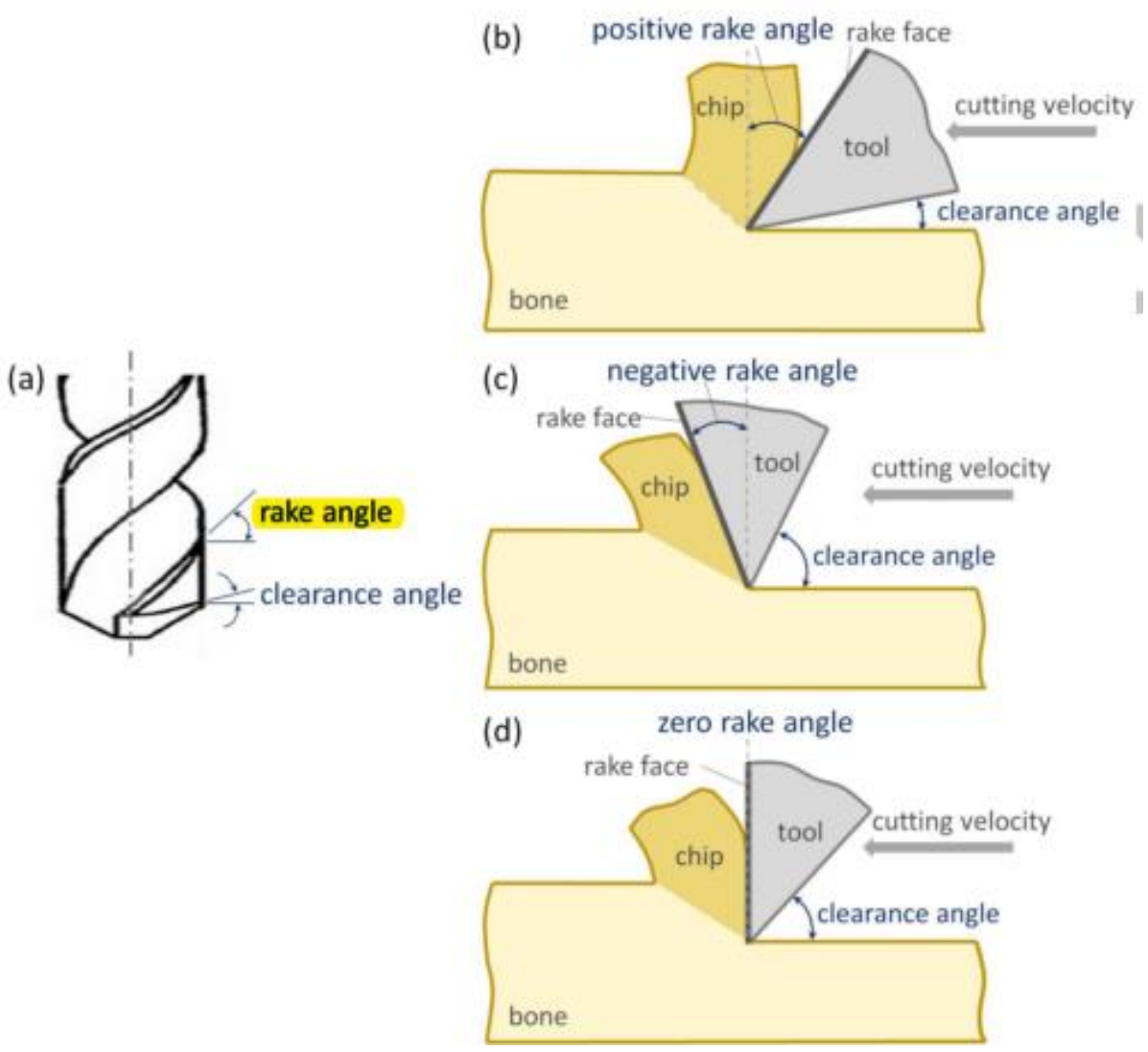

Figure 2.14: Representations of rake angle and clearance angle of drill bit [87]

Flutes and helix angle of the drill bit is the main constituent of the body section (figure 2.11(a)) of the drill bit. Flutes are the spiral curved structure on the body of the drill bit gives an easy and quick dispose of the chips from the drilled holes. Sharp edges of the flutes also give a reaming effect on the drilled walls of the hole. Majorly, two fluted drill bits are in practice and used commercially and research purpose also. These two flutes are cut on the either sides of the drill bit body to make symmetry in the structure of the body. A three flute drill bit was introduced by Bertollo et al. (2008) [98] in case of bone drilling and examined there effect on the bone drilling. Results were compared with the standard two flute drill bit. From comparative study, it was concluded that the three flute drill bit improve the drilling efficiency and accuracy in drilling quality. Bertollo et al. (2008) [98] also concluded that the three flute drill bit can replace the requirement of drill-jigs and guides as it also help to reduce the skiving effect of drill bit. But the three flute drill bit can reduce the strength of drill bit and may break within the bone during drilling which may cause trauma. In another study, bertollo et al. (2008,2010) [98,99] suggested that the three flute drill does not make any significant difference in decrease in heat generation during bone drilling but give an efficient and stress free drilling and easy evacuation of chips.

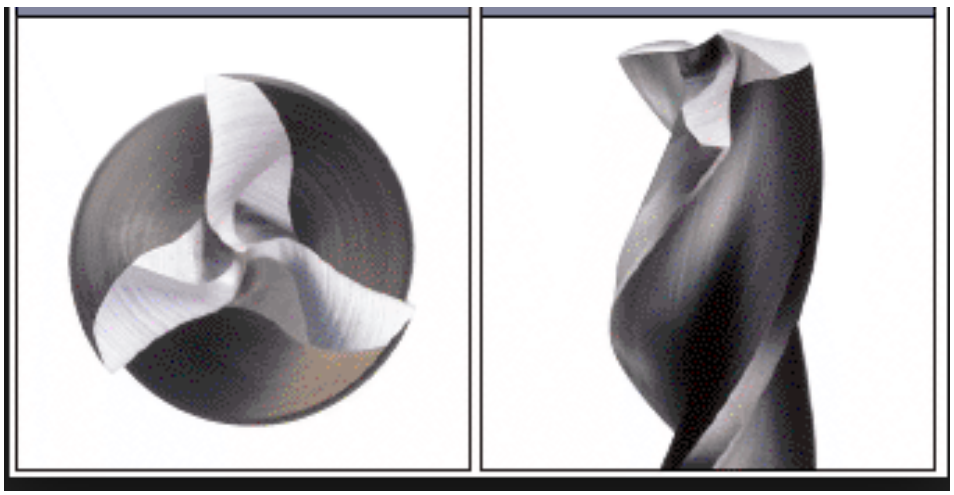

Figure 2.15: Drill tip of three flute drill bit [3]

Helix angle of the drill bit is the angle formed by the flutes with the central axis of the drill bit[3]. Helix angle and rake angle of drill bit are in agreement in case of drill bit. Higher helix angle naturally increases the rake angle of drill bit. Helix angle of drill bit can be varied with an angle of 10º to 40º and also term as slow, standard and quick in broad sense (shown in figure 2.16). A slow helix angle of drill bit prolonged the flutes length with higher number of spiral shape around the drill body. Whereas decreasing the helix angle give a straight and short flute in the drill bit.

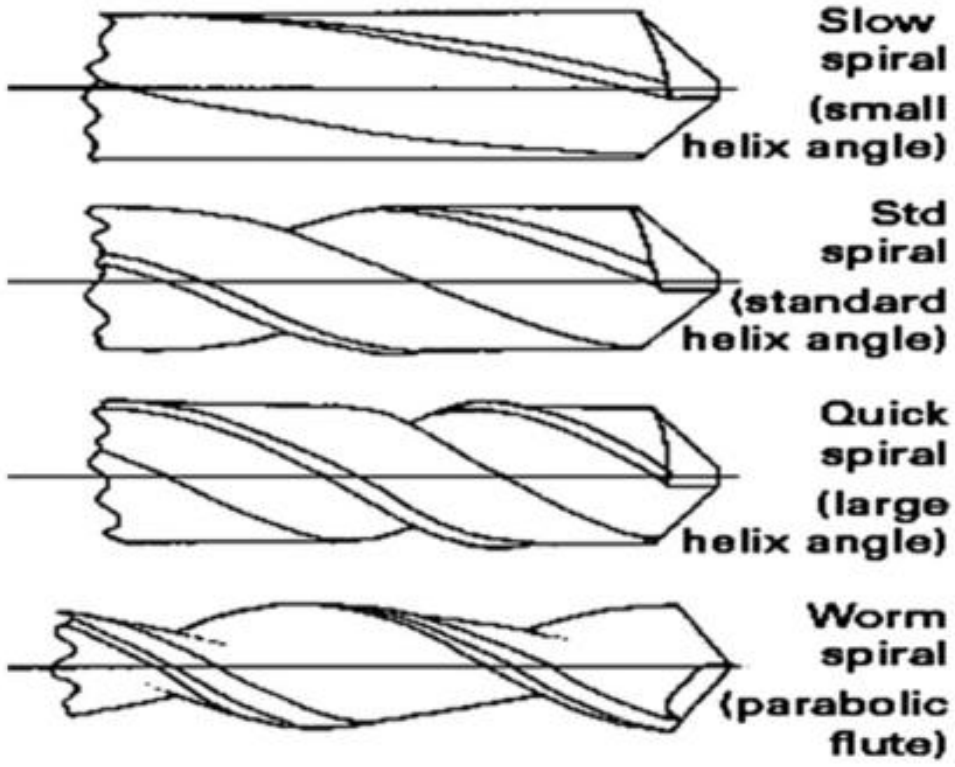

Figure 2.16: Representation of drill helix angle [3]

The function of flutes is to evacuate the chips during drilling and helix angle of drill bit is a function of evacuation of chips through the drill bit. From previous studies it was found that, the drill helix angle signifies its role with the drilling conditions. If bone is dry, a quick or standard helix angle is suggested with a concept that dry and short chips can easily evacuated through the

narrow or spiral path also. But in actual condition, where bone is fresh and circulated with blood including bone marrow within it, the evacuation of chips will be difficult. A clear and open path through the flutes is required for easy evacuation of the chips. Farnworth and burton (1974)[91] found experimentally that 27-30 degree helix angle is good for executing the orthopedic drilling operations. Wiggins and Malkin (1976) [94] also suggested this range for minimum torque and specific cutting energy. Davidson and James (2003) [27] suggested that the increasing helix angle significantly decreases the heat generation in bone drilling. Lee et al.(2011)[47] also confirms these results for minimizing the heat generation with increasing the helix angle with mathematical model and experimental analysis .

Further, the wear of drill bit is also a factor which can affect the drilling damage in orthopedic drilling operations. The regular use of drill bit in orthopedic surgery may result in the form of worn off the cutting lip, edge of the drill bit. Matthews and Hirsch (1972)[55] warned that the multiple use of drill bit increases the chances of excessive thrust forces and heat generation due to worn cutting edges of drill bit. Jochum and Reichart (2000) [100] conducted experimental study on pig mandibles and suggested that drill bit used more than 40 times increases the heat generation significantly. Same kind of results was presented by Allan et al. (2005) [101] while comparing the three drill bits with different level of wear shown in figure 2.17. From observation, it was concluded that drill wear increases the temperature significantly. Chacon et al.(2006); Ercoli et al.(2004);Misir et al. (2009); Oliveira et al.(2011)[102-105] supported the concept that drill bit wear increases the thermal and mechanical damage in case of bone drilling. However, the number of safe uses for a particular drill bit is depending upon the drilling diameter, depth and type of bone.

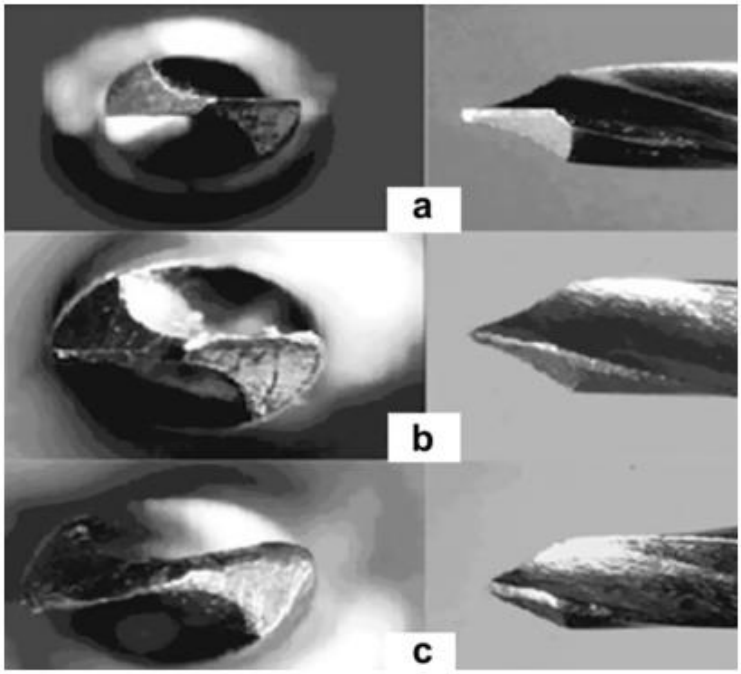

Figure 2.17: SEM images of drill bits used (a) fresh tool, (b) used 600 times, (c) several months used [3]

2.1.3 Factors affecting the drilling quality and sustainability

Other than the drilling parameters, some factors which affect the drilled hole quality and sustainability are studied by researchers. These factors are also important and must be taken care when drill the bone in orthopedic surgery. Predrilling/step drilling, cooling system, in-vitro and in-vivo experimental conditions are the factors which affects directly or indirectly as a function of quality of holes and sustainability of bone.

Predrilling or step drilling is a way to control the thermal damage and also reduces the shear stress developed during the cutting mechanism of bone. In order to drill the hole in two steps, initially bone is to be drilled with the drill bit of smaller diameter than required, after that a drill bit of required diameter is used to enlarge the hole to the required dimension. The effect of predrilling in case of bone drilling was studied experimentally. Udiljak et al. (2007) [106]

develop a step drill having a sudden change in diameter of drill bit shown in figure 2.18. A comparison have been made using these drill bits and observed that the heat generation with step drill bit is considerable low as compared to the drilling with conventional drill bit.

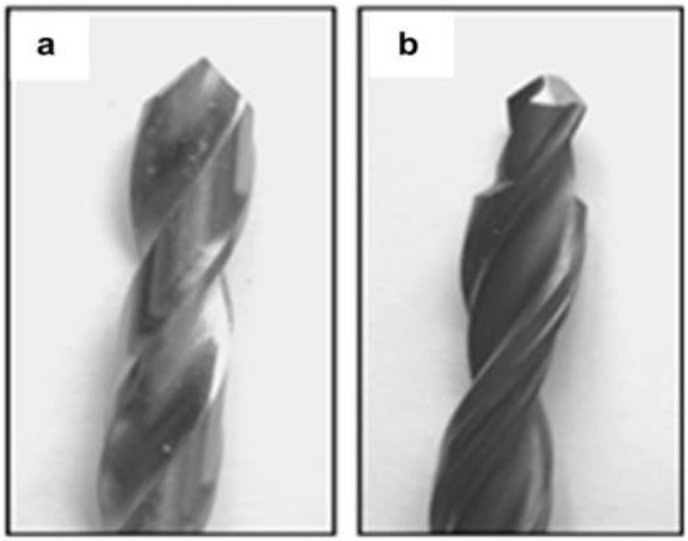

Figure 2.18: (a) Standard drill bit; (b) Step drill [3]

Saha et al. (1982); Lee et al. (2012) reported that the pilot hole of the diameter equal to chisel edge of final used drill bit will reduced the thrust forces up to 50 % and creates a fine smooth hole[48,57]. Matthews and Hirsch, 1972; Branemark; Albright et al., 1978; Itay and Tsur suggested that step drilling in bone help to maintain the drilling temperature lower than the standard condition due to gradually removal of material with low thrust and frictional forces[55,107-108].

Cooling system during drilling of bone is a responsible factor for controlling the heat generation. The effect of cooling around the drill site was studied through experimental investigations. There two kind of cooling system used in bone drilling (schematic shown in figure 2.19):

- Internal cooling
- External cooling

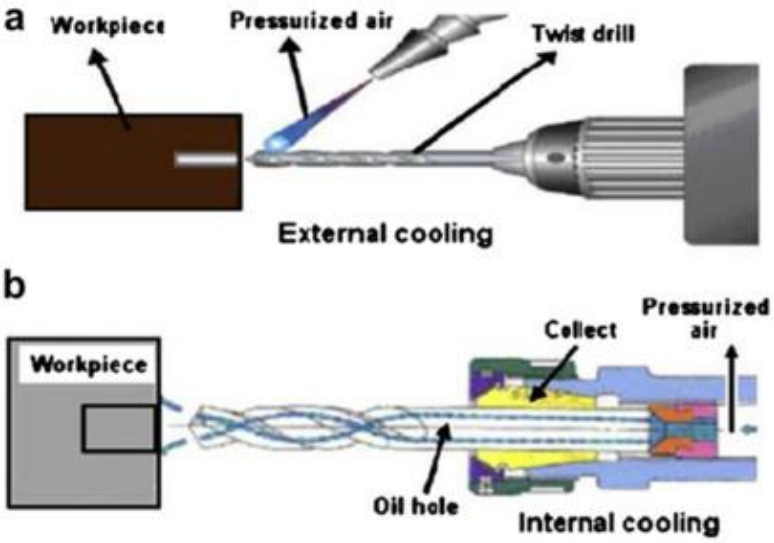

Figure 2.19: (a): internal cooling system; (b); external cooling system [3]

Internal cooling process involves the use of drill bit having channels with the drill bit and an efficient cooling has been achieved as the coolant directly target the shearing area of bone and help to resolve the heat generation with the flow of coolant. Image of internal cooled drill bit shown in figure 2.20.

Figure 2.20: Internal cooled enabled drill bit

However, in case of external cooling process, flow of coolant through the means of external feeding system around the drill site was facilitated. In external cooling process there is no direct contact of coolant with shear zone of bone. Most of the coolant strike with the chipping surface

and drill tool in this process. Thus, the efficiency of the external coolant system is marginal low as compared to the internal coolant process. In general, coolant also provides the lubrication effect and helps to reduce the frictional forces and easy evacuation of the chips. Matthews and Hirsch (1972) [55] examined experimentally on human cortical bone with different flow rate of coolant (300,500,1000 ml/min). Results show that higher flow rate of coolant helps to control the heat generation at much lower level. Kirschner and Meyer, (1975); Lavelle and Wedgwood, (1980) [109-110] compared the external and internal cooling system while processing the dental drilling. Results expressed the interest in internal cooling process with benefits of low heat generation as compared to the external cooling system. In general agreement, it is very obvious that coolant helps to minimize the heat generation, with dependency of depth of drill, temperature of coolant is the main considerable factors. Coolant definitely helps to control the heat generation but it can also be a reason for infection to the bone and its surrounded sections [26,111].

In other factors, which can be considered is the experimental drilling condition, i.e. in-vitro or in-vivo investigation of the bone drilling process. Majority of the experiments were carried out on in-vitro condition where only bone is replying back to the external factors. Whereas, in actual condition flow of blood and other fluids in the bone may get dissipate some amount of heat during drilling process. Wootton et al. (1976) [112] recommended that the concept of heat dissipation with blood flow is correct but within the cortical portion of bone the level of blood is very low and moreover, due to moist structure of bone coagulation of chips was noticed which increases the frictional energy and increases the heat . Thus, the effect of experimentation on live bone can be countered. Matthews and Hirsch (1972) [55] compared the in-vitro (studies or experiment performed in lab, virtual environment or on parts taken from living organism) and in-

vivo (studies or experiment performed on living organism) drilling conditions and observed that there is no significant difference of the blood flow around the drill site on drilling temperature. They also reported that the ambient body temperature condition should be maintained to get the accurate results that can replicate to the in-vivo drilling process. Lee (2011); Lee et al. (2012) studied that the influence of bone mineral density (BMD) is a factor which cannot be neglect while choosing the drilling parameters and drilling conditions [66-67]. However, the density factor is fixed in the real situation and the effect of bone mineral density on heat generation must be evaluated. Karaca et al. (2011) [46] investigate the effect of increasing BMD on heat generation and observed that the increasing BMD increase the heat generation in bone drilling. Increasing BMD make the bone more compact in structure and also increases the hardness of bone. Mitsuishi et al. (2004); Ong and Bouazza-Marouf, (1998) [113-114] also supports these findings of increasing temperature with bone density because of the increases in shearing energy and thrust forces.

Orthopedic bone drilling is a complex structure in which a single factor does not control the output. This complex structure of drilling process may be the reason for confliction in results with the above discussed drilling parameters. On the basis of these findings it is difficult to streamline the favorable drilling parameters and drill specifications for controlling the mechanical and thermal damage to the bone. Pandey and Panda (2013); Lee et al. (2018) [3,87] also suggested in the review process that the results were found conflicting and an optimal parametric combination must be found with respect to the drilling condition. In order to study the combined effect of drilling parameters (Pandey and Panda (2012, 2014)) [115,116] investigated the drilling parameters (Rotational speed and Feed rate) for thermal and mechanical damage (i.e. forces and temperature). Li et al. (2016); Gok et al. (2014); Ueda et al. (2010); Izamshah et al.

(2016); Akhbar et al. (2018) also conducted experimental studies and optimize the different drilling parameters and optimize the drilling conditions with respect to the response output[117-121]. Initially, optimization for each response output has been done separately, and parametric involvement in terms of percentage contribution has been evaluated using ANOVA analysis. Later on, it was realized that the optimal combination of one response may differ from the other response and in real time situation improvement of one response cannot be justified with the deterioration of other one. Thus a multi response optimization was also introduced by Pandey and Panda (2013, 2014, 2015] [75, 76,122] for optimization of thermal and mechanical responses (temperature, forces and surface roughness) in a single attempt.

2.1.4 Feasibility and practicality of unconventional bone drilling techniques

Drilling of bone during the orthopedic open reduction process is an unavoidable task and the after effects on the bone were studied by many research groups to minimize the thermal and mechanical loses to the bone and its surrounding. Mainly, the previous studies target the drilling parameters, drill specification and drilling conditions to control the damage in bone drilling. Later on, some optimization techniques were employed to get the combined optimal drilling conditions for minimizing the thermal and mechanical losses to the bone during surgery. However, the basic concept behind the drilling technique was same and that is the main reason for the losses encountered to the bone. Cutting of material with continuous shear deformation is the primary reason for the high heat generation in bone drilling [3,27,47-48]. Further heat is generated in the form of frictional energy developed in between the flank and rake face of tool and bone chips. In general, the further chances of improvement in the bone drilling process are very less with the current established conventional technique. In order to avoid the direct contact of cutting tool to the bone, unconventional bone drilling techniques were employed to check the

feasibility with the bone. Initially, water jet and abrasive water jet techniques were used to cut the bone. Schwieger et al. (2004) [123] used abrasive waterjet material cutting technique, used high speed abrasive particles to remove the material from the desired location and create a cavity in the workpiece material. Abrasive waterjet drilling technique is a non-thermal machining technique and mostly used to cut the materials with high hardness. Lactose-monohydrate was used as abrasive which is a bio-compatible material. Different water pressure and abrasive feed rate were studied and the results show that increasing feed rate of abrasive particles increase the surface roughness of drilled holes. Although the above said technique give favorable results in terms of thermal damage but the shape of drilled hole is challenge i.e. increasing cutting gap angle (shown in figure 2.20) make this technique unfit for use it in present conditions. Thus, suggested to improve the cutting quality by a further parameter optimization, the abrasive water jet may be the cutting technique of the future for robotic usage.

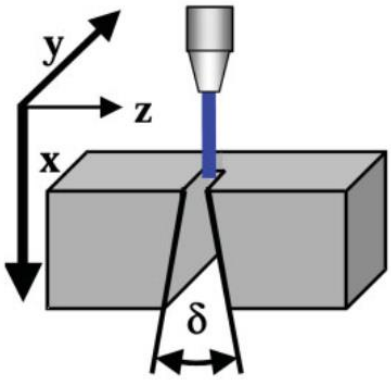

Figure 2.21: Unfavorable cutting gap angle in abrasive waterjet cutting system [123]

Biskup et al. (2006) [124] studied the heat generation during abrasive water injection jet (AWIJ) osteotomies was measured by thermocouples that were inserted into the cortical hollow bone segments of cattle. The influence of parameters like pressure, traverse rate, abrasive flow rate and abrasive material are shown in this paper together with the influence of the location of

thermocouples, which represents an increment of the bone tissue. Taking parameters in account as : Abrasive material: Garnet , biocompatible abrasives, Pressure: 300 MPa, Abrasive flow rate: 6 g/s, Orifice/focus-diameter : 0.25 / 0.8 mm, Traverse rate : 100 mm/min. After experimentation, it was evident that bone cell damage was completely removed using AWIJ. From results it was revealed that with lower pressure and lower abrasive feed rate less temperature rise in bone surrounding. Dunnen et al. (2013) [125] also used the non-conventional method of drilling for bone. Water jet is used as a tool instead of solid twist drill rotating at high speed. During experimentation, 210 holes were drilled in porcine femora with waterjet diameters of 0.3, 0.4, 0.5 and 0.6 mm at a pressure of 700 bar and a 5s jet time. Hole depths, diameters and bone architectural properties were determined using microCT scans. The depth of the hole as a result of waterjet drilling in bone is correlated to the waterjet diameter and the local BV/TV. For pure waterjet drilling of cortical bone, a nozzle of 0.5mm is recommended to ensure penetration, whereas for articular bone, a nozzle diameter of 0.2mm suffices. The study gives the descriptive mathematical equation able to predict the hole depth and diameter based on the local structural properties of the bone at given waterjet diameters. Eshet et al (2006) [126] shows the feasibility of bone drilling using microwave energy. The microwave drill uses a near-field focused energy having power under 200 W at 2.45 GHz frequency having drilling speed 1 mm/s. From optical and scanning electron microscopy it is evident that microwave drilled hole are substantially smoother than the holes drilled by mechanical drilling machine. Researchers found that microwave drilling helps to control the formation of debris and rupture of bone vasculature during drilling. However, carburizing of bone near by the drilled point shows some damage to the bone tissue. Whereas no further damage to the bone (mirocarcks or rapture of bone tissue) in the non-carburizing zone was reported.

These above said technique are found less practical and thus, reported as not feasible to use to drill the bone in-vivo conditions. Drill cutting gap angle, use of abrasive particles and continuous flow of water inn waterjet drilling technique and the requirement of heavy set up machine are some of the key factors which make this technique non-feasible. However, researchers reported that some modification in process, technique or setup can make a fore step for using these techniques for drilling of bones.

In another attempt, in the year of 2009, ultrasonic-assisted drilling technique were employed first time to satisfy the needs of a damage free bone drilling [127,128]. The use of ultrasonic vibrations ($\leq$ 20 kHz) coupled with the conventional rotating drill bit and other functions of conventional drilling keeps constant. The basic concept of this technique is same as conventional drilling but there is no continuous contact of drill tool and bone. The relieving time in between the each successive contact reduces the resultant stresses and followed to low heat generation was also reported [24,111]. All other factors like drilling time, drill hole shape remain same in the conventional drilling i.e the feasibility of this technique make it possible for practical use. Alam et al. (2009) [24] conducted experimental investigations to check the surface roughness of drilled holes and compared the results with conventional drilled bone samples, results observed shows the significance and importance of use ultrasonic vibrations in drilled of bone. Ito et al. (2009) [129] use bone curette to create a cavity in spinal surgery and reported that the use of ultrasonic bone curette on the place of conventional burr is more safe and minimum damage to the spinal bone. Further, Alam et al. (2011) [70] compared the technique for force and torque developed during the drilling of bone. Results observed that the development of force and torque during the bone drilling is also in controlled manner. This means the ultrasonic-assisted drilling of bone help to maintain the drilling process free from the mechanical damage. Alam et al.

(2015) [78] measured the temperature also during the bone drilling and compared it with conventional and proves that the ultrasonic-assisted bone drilling also helps to control the thermal damage also [85]. Wang et al. (2014) [130] performed experiment with various vibration level (5, 10,15 and 20kHz) and suggested that the increasing ultrasonic vibrations helps to maintain the minimum temperature during the bone drilling. A finite element simulation of the process in ANSYS validates the experimental results. Wang et al. (2013) [71] compared the results of conventional and vibrational drilling process for microcracks developed in the bone surrounding with the help of scanning electron microscopy (SEM) and report that the vibrational drilling of bones help to get minimal mirocracks damage. Recently, Gupta et al. (2016) [131] performed experimental investigations using the rotary ultrasonic drilling technique, in this technique a cylindrical tool of abrasive coated is used instead of the drill bit and observations were made on the basis of experimental procedure on porcine bone. Gupta et al. (2017) [111,132] also suggested that the rotary ultrasonic drilling of bone improved the pullout force and give minimum thermal damage to the bone as shown in figure 2.22 & 2.23**.**

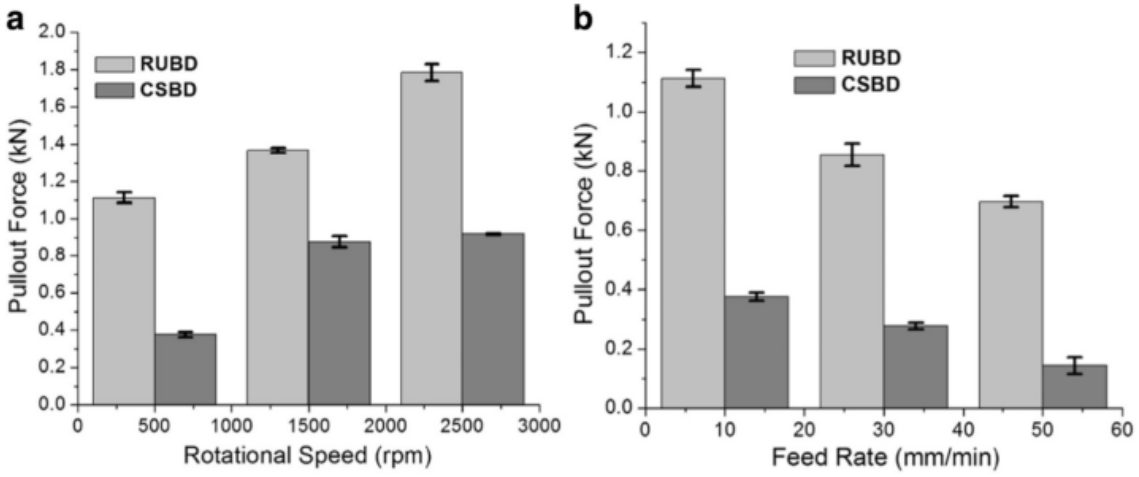

Figure 2.22: Measurement of axial pullout of bone screw joint with respect to rotational speed and feed rate [132]

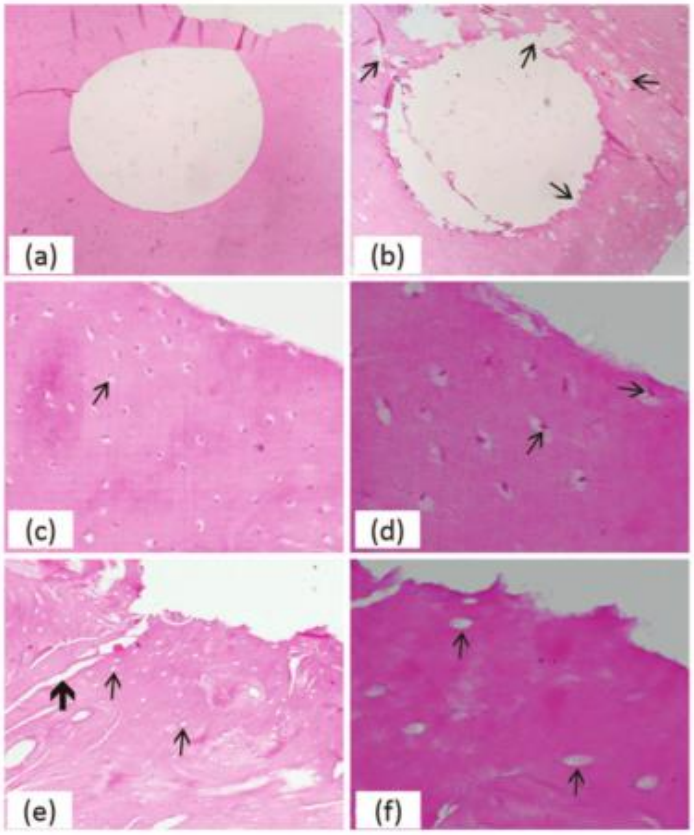

Figure 2.23: Histopathology of drilled bone samples for investigation of osteonecrosis [111]

2.2 RESEARCH GAPS & ANALYSIS

From the comprehensive literature review of the bone drilling process adopted in the orthopedic surgeries it comes in limelight that there are some imperfections which may damage the bone thermally and mechanically during the orthopedic surgery beyond the limit. Studies related to the hybrid techniques of drilling and measuring there outcomes are the major shortcoming observed in the literature. Thus, brief research gaps are listed below:

- ***Non-Conventional/Hybrid Machining:*** Very few attempts were made with the non-conventional or hybrid machining of bones. Hence there is great need to check their feasibility, so that they can be used clinically.

- Non-conventional way of cutting shows some of the advantages in bone drilling but still they are lacking in operational efficiency.
- Various parameters of drilling have been studied in previous articles but no attempts have been made with ultrasonic actuation of conventional drilling by varying its geometry.

- **Axial Pullout:** Studies on design of screw are explained for pullout of bone screw joint, No pull out studies compare the conventional and hybrid way of drilling.
- **FEA Simulation:** Further, a simulation study is requiring showing the effectiveness of hybrid drilling as compare to conventional drilling.
- **Histopathology:** morphological study of drilled bone specimen to understand the effect of heat on bone structure in terms of evaporated lacunas.

2.3 SCOPE OF THE WORK AND OBJECTIVES FOR THE STUDY

The sustainability of an orthopedic surgery is a major concern and mainly depends upon the damages expressed to the bone during drilling. Thermal and mechanical damage observed during the drilling of bones affecting the sustainability of the bone screw joint in the long run. The researchers are continuously contributing to minimize these loses. Study of drilling parameters for some individual conditions, parametric optimization, modification in drilling techniques and numerical modeling of drilling processes is the path breaking developments in order to achieve the sound and sustainable orthopedic surgeries.

On the basis of available literature, feasibility of the current techniques and practicality of their use, the ultrasonic –assisted drilling technique shows its importance in terms of maintaining the

thermal and mechanical loses minimum as compared to the conventional drilling process. The available literature shows the perfection of ultrasonic-assisted drilling technique in the following way better than the conventional process:

- Discontinuous shear deformation of material leads to minimal thermal invasive to the bone and its surrounding
- Control the force and torque developed during the drilling process and resulting in the form of minimum mechanical damage.
- Better control over the drilled hole quality in terms of surface finish and delamination or drill wander.
- Better axial pullout force of bone screw joint in case of ultrasonic-assisted drilled holes.

These Inherent characteristics of ultrasonic-assisted drilling provide a way out to get rid of the damages caused by the conventional bone drilling and give a fine and damage free drilled holes with better sustainability to the orthopedic surgeries. The available literature on ultrasonic-assisted bone drilling shows the cutting edge impact of this technique over the conventional drilling process. Majorly, the study has been done to compare the ultrasonic-assisted drilling process with conventional one. Recently few attempts have been made to study the effect of vibrations and amplitude of drilling on accessing thermal and mechanical damage. The behavior of drilling parameters under the effect of ultrasonic vibrations needs to be explored and some drill specifications playing key factors in the heat generation and forces need to be studied. The variation of these drill specifications, when studied with the effect of ultrasonic vibrations is the one of the major core objective. The level of damage under different temperature levels is still undercover and can be considered for the thrust research area for the present study. There is no attempt has been done for the simulation process of ultrasonic assisted bone drilling process. The

feasibility and practicality of the simulation process for Ultrasonic assisted bone drilling process and comparison of observation with conventional bone drilling process should be considered. On the basis of available literature, scope of work and to improve the practicality of ultrasonic-assisted drilling of bone, the following objectives were decided to attain in this study.

- To study the hole accuracy, hole quality during the drilling of cortical bone.
- To evaluate the damaged area, thermal effected zone (TEZ) along the drilling site using SEM, histopathology images.
- To examine the pullout strength of the bone - screw joint after drilling.
- To simulate the drilling and generate thermal model for application in to orthopaedic surgery.

2.4 WORK METHODOLOGY

In order to achieve the objective of the study, the following work plan (shown in figure 2.24) has been proposed and followed throughout the process.

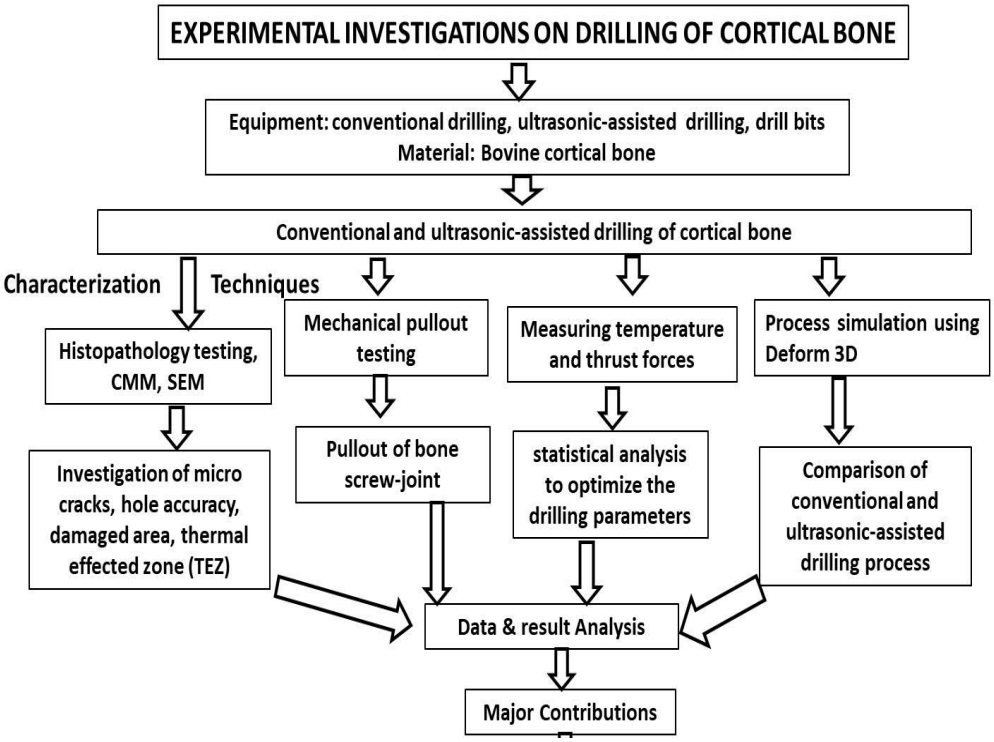

Figure 2.24: Work flow process followed for the study

2.5 SUMMARY

The sustainability of bone screw joint is a main factor that is to be prime concern over the orthopedic surgeries. The damages caused by the drilling process and producing inadequate drilled holes in the bone may lead to the second damage to the already fractured bone. In this chapter, a comprehensive study of the literature has been carried out and tried to understand the behavior of each drilling factor while drilling the bone under various drilling conditions. The review of literature shows that the conflicting behavior of drilling parameter needs to find the optimal solution with respect to the drilling conditions. Few parametric studies have also been reviewed for thermal and mechanical damage under the influence of in-vitro environment. Unconventional drilling techniques are also studied in the review process, from them most of the techniques shows impracticality and non-feasible for the drilling of bone in real situation during surgery.

While reviewing ultrasonic-assisted drilling of bone shows some feasibility for the process and also shows the practicality of this technique during the surgical intervention. The technique already shows the improvement over the conventional process in terms of mechanical and thermal damage.

CHAPTER 3: DRILLING SETUP AND EXPERIMENTATION

3.1 ULTRASONIC ACTUATORS

Ultrasonic sensors are the electro-mechanical devices converted the electric signals to the ultrasonic vibrations and vice-versa. There are three types of the devices;

(i) Transmitters

(ii) Receivers

(iii) Transceivers

Transmitters are the devices which convert the electrical signals to the ultrasonic waves or vibrations. Receivers do the opposite function and convert the ultrasonic vibrations to the electric signals and Transceivers are able to do the both function. The ultrasonic transducer used for the machining purpose is either piezoelectric or magnetostrictive. The piezoelectric transducer consist of piezoelectric crystals i.e. Quartz, Topaz, Berlinite, Sucrose, Rochelle salt and lead titanate etc. There are some syntactic crystals and ceramics available act like piezoelectric materials. When high voltage AC current passed through the electrons on the either sides of the piezoelectric crystals generates high potential difference and causing vibration in it.

3.2 ULTRASONIC-ASSISTED DRILLING SETUP

To develop the ultrasonic-assisted drilling setup, a piezoelectric ultrasonic transducer of frequency 20 kHz was procured and the further development has been done as per the process and CNC machine requirement. The ultrasonic transducer consists of the piezoelectric crystals that can convert the electric signals to the ultrasonic vibrations. The specifications of the transducer are as follows in table 3.1.

Table 3.1 Technical specifications of ultrasonic transducer

SPECIFICATIONS	RANGE
Input Power	800 watt
Frequency	20 kHz
Input Voltage	220V
Power Supply	AC 5A
Amplitude	4-20 µm

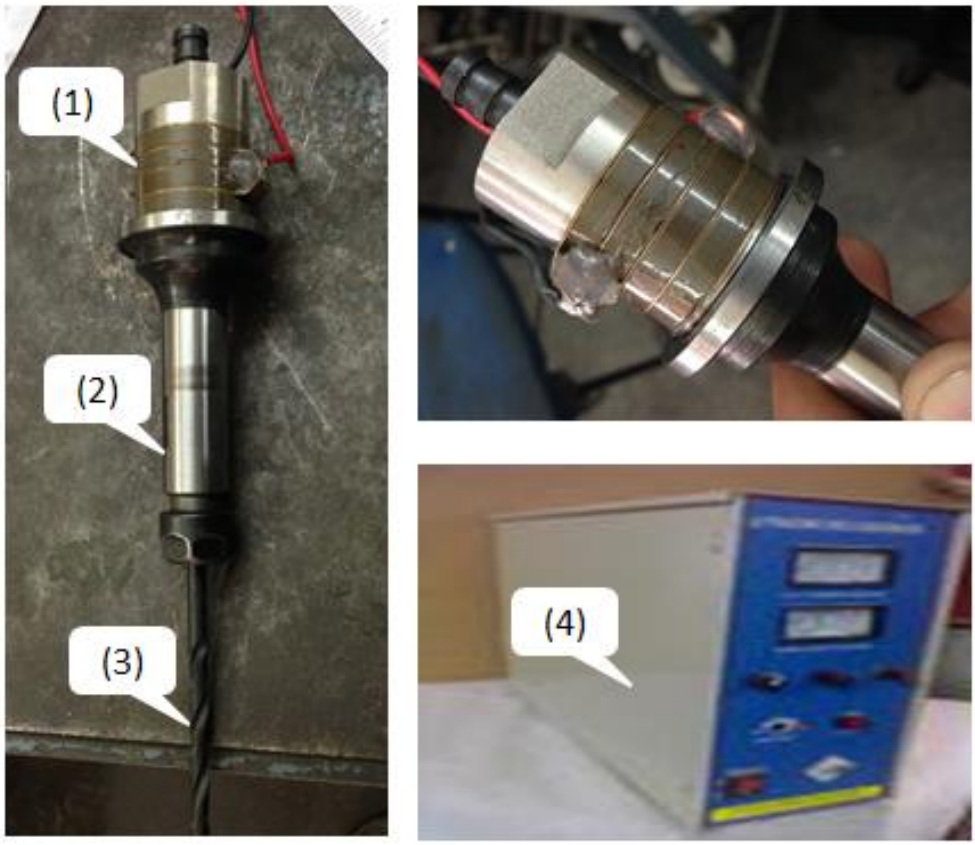

Figure 3.1: Ultrasonic actuating device: (1): Ultrasonic transducer; (2): Horn attached; (3) Drill bit; (4): AC transformer unit

The ultrasonic transducer has been further coupled with the CNC adapter by the help of coupling assembly made by a non-conducting material. Two slip rings of copper were fixed over the main housing of assembly to transmit the power terminal from transducer. A detailed drawing of assembly and developed assembly setup is shown in figure 3.2. The connection of slip rings connected with the AC transformer by the means of carbon Bushes (Shown in figure 3.3).

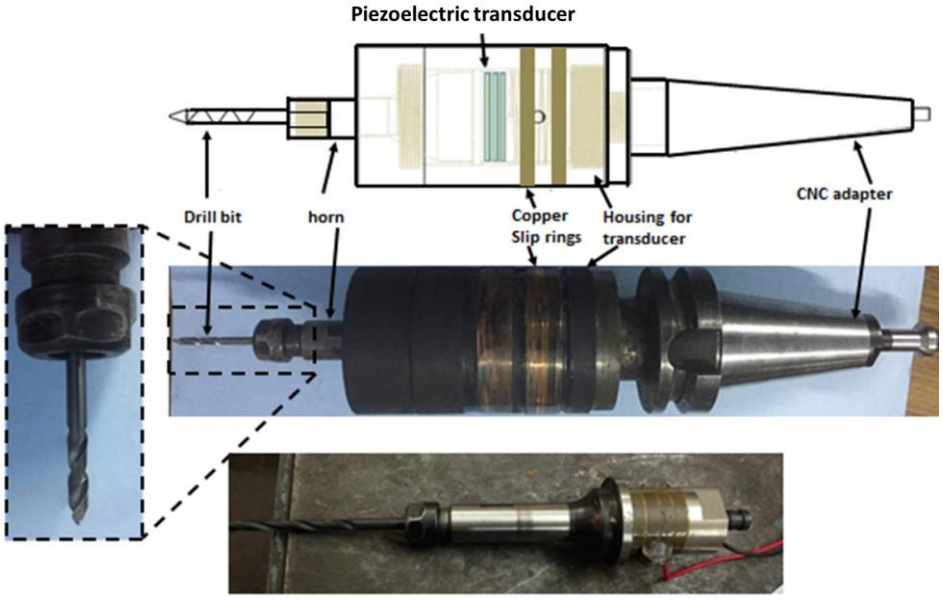

Figure 3.2: Developed ultrasonic-assisted drilling tool coupling of transducer and CNC Adapter

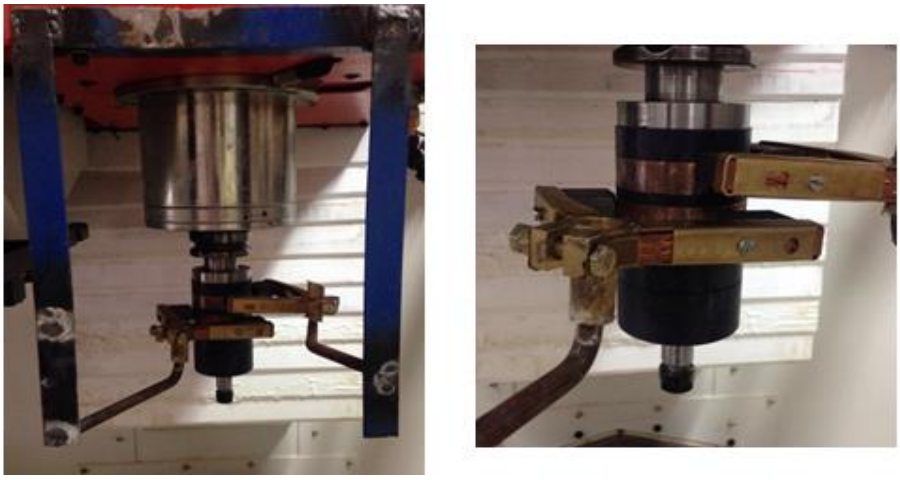

Figure 3.3: Ultrasonic-assisted drilling setup fixed on CNC machine with power supply arrangement

3.3 BONE SPECIMEN SELECTION

In order to study the drilling process of bone, experimentation was performed on the bovine cortical bone. Selection of bone specimen for experimentation is a challenging task in this type of study. Bovine bone is used for the experimentation purpose in place of human bone [24,28-29,46-48,68-70,75-78,131-132] because experimentation on human bones is not permitted and bovine bones have similar properties as human bone [24,28-29,46-48,68-70,75-78,131-132]. The statement showing the similarity of mechanical properties for bovine bone and human bone are as follows in table 3.2. No animal was harmed specifically for the experimentation purpose. The cortical bovine bone is easily available from local slaughter and experimentation was performed on the same day within the couple of hours so that the mechanical and physical properties of bone specimens must not be disturbed for better results [24,28-29]. The bone specimen acquired from slaughter house is matured animal of age 10-14 Year. Thus, the results from this study may get reflected to the human age group of 20-45 year. The properties of human bone for this age group are comparatively remaining same and free from any diseases [133]. The change in bone properties was observed in the form of osteoporosis or other structural diseases after the age of 50 [133-135]. Osteoporosis or other structural diseases are not only the case of aging, but it was considered to simplify the problem and focus on the drilling process and study of different drilling parameters only. Most of other bone decay causes also recorded after the age of 50 mostly in different studies [133-139]. These terms are taken care of while selecting the bone specimens. The bone specimen acquired from slaughter house is shown in figure 3.4. The outer edges of bones helping in fixing the joints called Epiphysis and mid-section of bone is named as diaphysis. The excess meat on the bone is cleaned up and thawed in saline solution until the experimentation process to procure the properties and structure of bone intact.

Table 3.2: Similarity for the properties of bovine bone and human bone [24,28-29,46-48,68-70,75-78,131-132]

Bone Property	**Bone type**	
	Bovine Bone	**Human Bone**
Tensile strength (MPa)	40-150	40-145
Compressive strength (MPa)	140-250	130-200
Young's modulus (GPa)	10-22	10-17
Shear modulus (MPa)	3	3
Density (kg/m^3)	1950-2100	1800-2000
Poisson's ratio	0.33	0.4
Specific heat (J/kgK)	1300	1330
Thermal conductivity (W/mK)	0.1-0.3	0.1-0.43

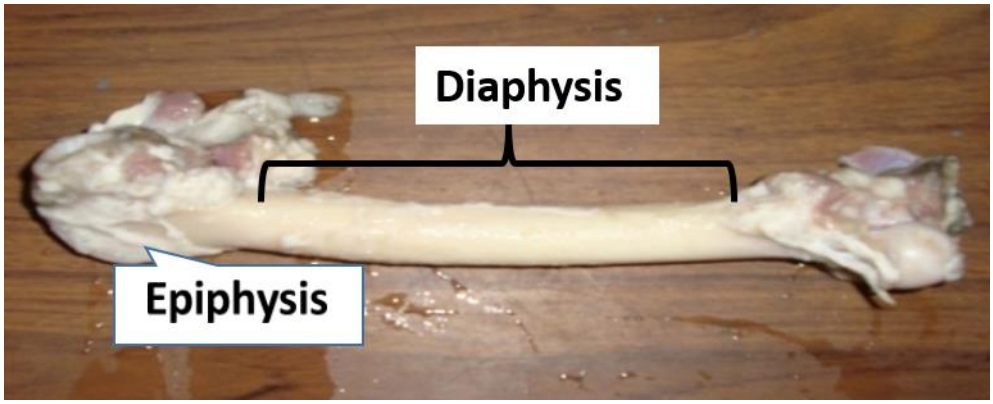

Figure 3.4: Bone specimen acquired from slaughter house

3.4 SPECIMEN PREPRATION

The bovine bone obtained from the slaughter house is shown in figure 3.5. This bone is filled with the bone marrow inside the hollow section of bone, Cancellous bone in the epiphysis ends of the bone. The study targeted the drilling of cortical bone only, having high density and most hart tissue present in the body. Therefore, this section of bone is tough to machine or drill during the surgeries. For the purpose, the bone specimen has been sawed from the ends and inner bone marrow has been squeeze out from the cortical bone. The cut section of diaphysis drilled with two 8 mm diameter holes at a distance of 11cm to get fixed it on the dynamometer. The step wise process of specimen preparation is shown in the figure 3.5.

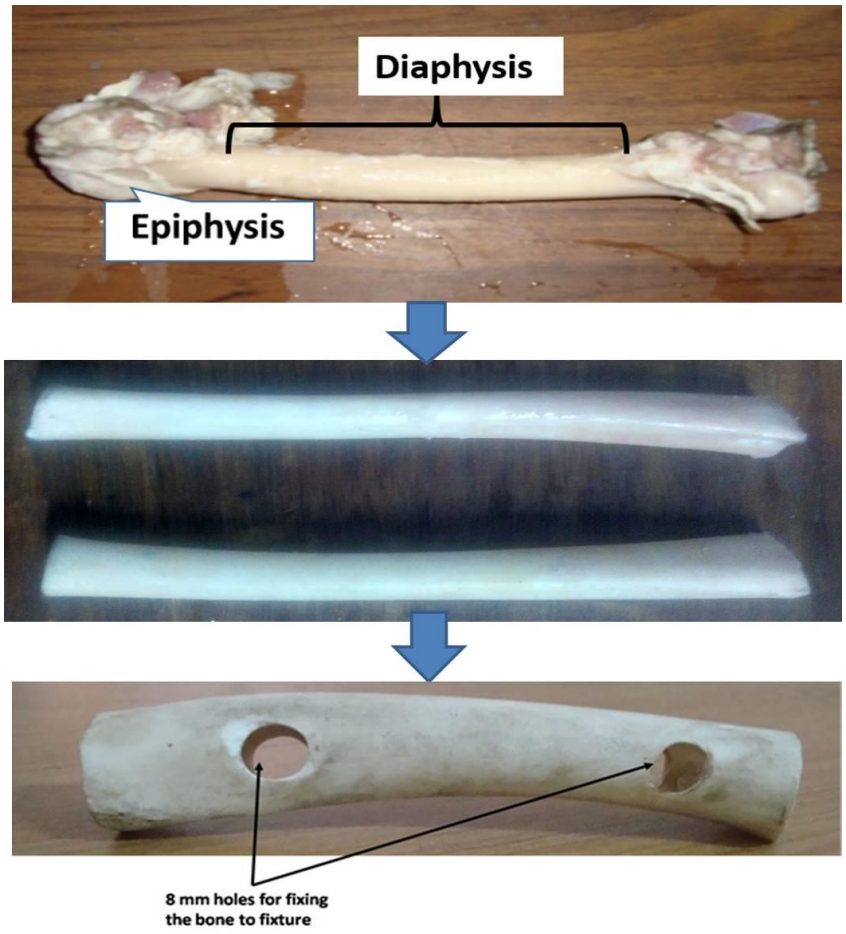

Figure 3.5: Specimen preparation process for experimentation

3.5 DYNAMOMETER SETUP FOR FORCES MEASURMENT

Specimens prepared for experimentation were fixed over the dynamometer for measuring the forces during different experimental combinations by the means of fixing screws. A dynamometer fixed on the machine bed connected to the decoder with display unit connected to the computer system give results in form of forces on desired interval of time. Graph has been generated automatically for a particular experimental condition. The setup of dynamometer displayed in figure 3.6. The graph generated for an experiment is also shown in figure 3.7 and excel file for each individual experimental run has been saved and calculate the average thrust forces in Z direction was calculated. Forces developed during drilling are associated with the mechanical damage and micro cracks initiated in the drilled walls.

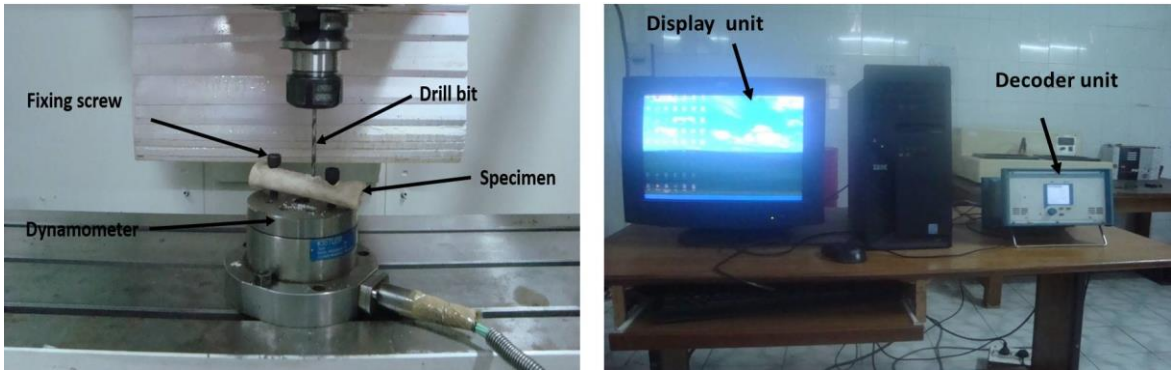

Figure 3.6: Dynamometer fixed on machine bed, connected to decoder unit and display unit

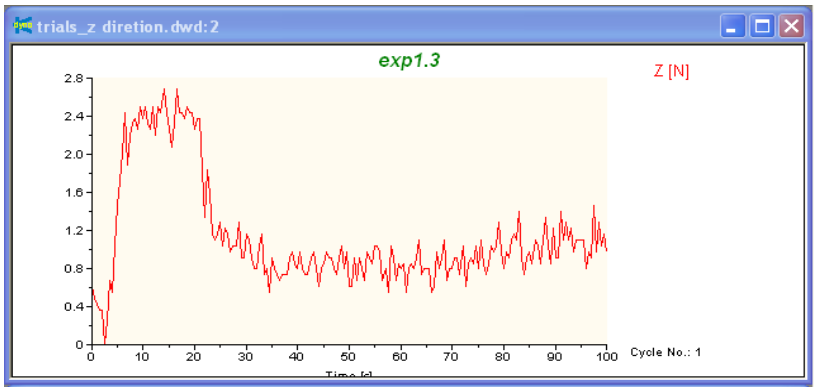

Figure 3.7: Graph generated for thrust forces in Z direction during drilling

3.6 THERMOCOUPLE FOR TEMPERATURE MEASUREMENT

Thermal damage during drilling of bone is a major concern and the experimentation is also performed to understand the behavior of different drilling parameters on heat generation during bone drilling. To measure the temperature during drilling a PT100 RTD sensor is used. PT100 RTD sensors are the resistance temperature detector working on the principle that resistance of a material is a function of temperature. During practice of temperature measurement, current is transmitted through the small piece of metal having a specific resistance value. When temperature rises, the resistance of a particular metal piece is changed with the change of temperature and measured by the system. The level of resistance decreased is converted into the temperature at that point. PT stands for platinum in this term and pure platinum material having a resistance of 100Ω at 0ºC. There is a linear relation in between the temperature and resistance of platinum make it suitable for the RTD purpose. Platinum RTD sensor is capable of measuring the temperature within the range of -270 ºC to 900 ºC. RTD sensor connected to a digital meter which shows the instant temperature on display and a logging system help to record the temperature per second interval of time saved in data card connected to the digital meter. Thermal conductivity of bone is very low and flow of temperature within the bone during the drilling process is very low, makes very high thermal losses around the drill site. From literature, it is observed that the 0.5 mm distance from the drilled wall edge is the most affected distance thus thermocouple fixed at a distance of 0.5 mm from the holed edge to measure the temperature during drilling. A schematic representation of RTD sensor placement and setup of thermocouple during experimentation is shows in figure 3.8 (A&B).

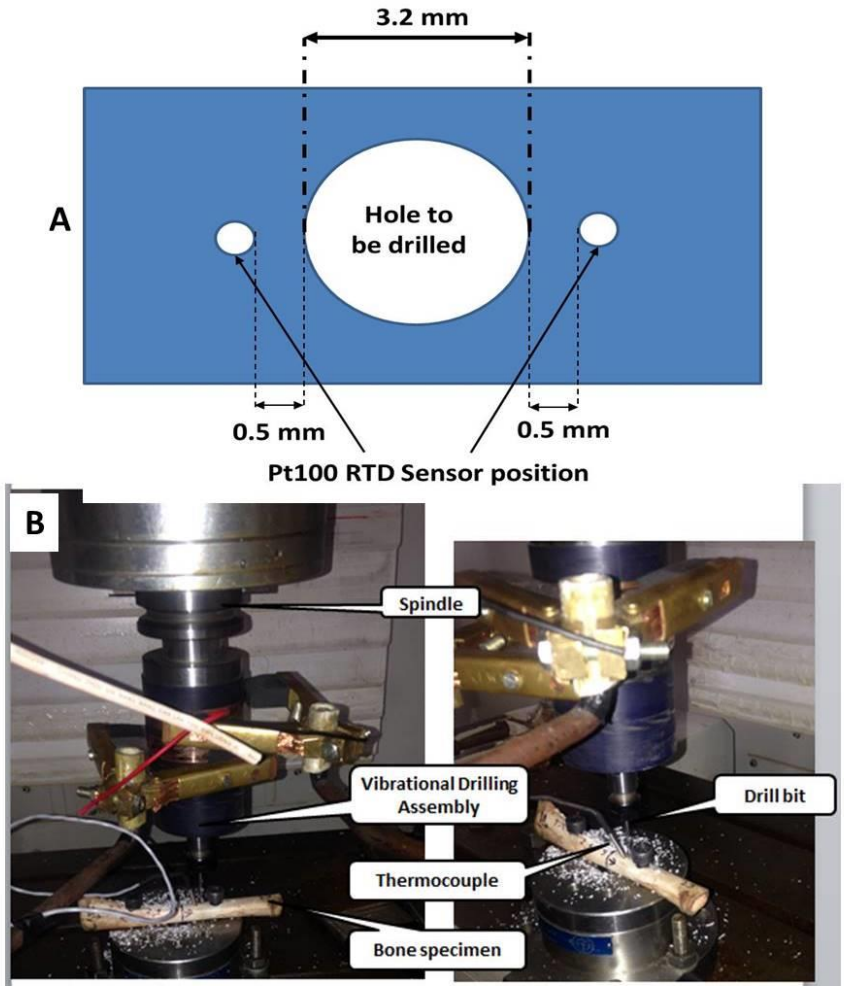

Figure 3.8(A&B): (A): Schematic representation of position of RTD sensor around the hole; (B): measurement of temperature by thermocouple during drilling

3.7 CMM FOR MEASUREMENT OF DELAMINATION IN DRILLED HOLES

Coordinate measuring machine (CMM) was used to study the delamination in diameter of drilled holes. Coordinate measuring machine is mechanical, optical, or laser-guided equipment used to measure the physical geometry or geometrical irregularities of an object. CMM having a probe easily move in X,Y,Z directions with the specified range. Directional movements connected with a three-dimensional cartesian coordinate system. When probe connect the object generates a point coordinates for that particular point and process continues with the movement of probe and

generates various points coordinates as required. Further, the generated points help to get the results in desired unit, value, or shape. Image showing the measuring diameter on CMM is shown in figure 3.9. Further, to measure the delamination in diameter measured using the equation below.

$$D_p = \left(\frac{D_{max} - D}{\mathrm{D}}\right) \times 100$$

Where, D_{max} is the maximum diameter of the hole measured, D is the minimum diameter/drill diameter, D_p is the percentage delamination in diameter.

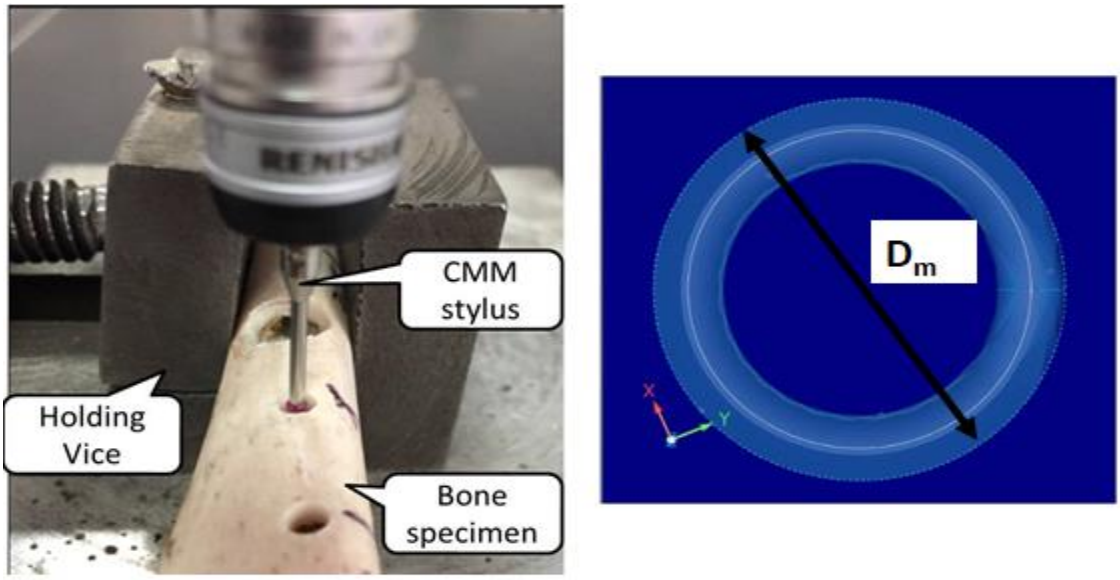

Figure 3.9: Measuring diameter of drilled holes using CMM machine

3.8 SCANNING ELECTRON MICROSCOPY (SEM) FOR DRILLED HOLE QUALITY

To observe the mechanical damage and irregularities like hole cracks, pits and voids in the drilled holes are observed using the scanning electron microscopy investigation. In SEM, electron beam passed through the anode and magnetic lens. Further, beams get converges

through the scanning coils, backscattered electron detector, and finally fall on the specimen. A secondary electron decoder used to analyze the image further and decoder sends it to the screen in an image format. Complete SEM process was carried out in vacuum and to analyze the non-conducting material a layer of gold is coated over the specimen by the help of spray coating process. Sectioning of drilled bone specimens were cut and specimen prepared for SEM analyses are also shown in figure 3.10.

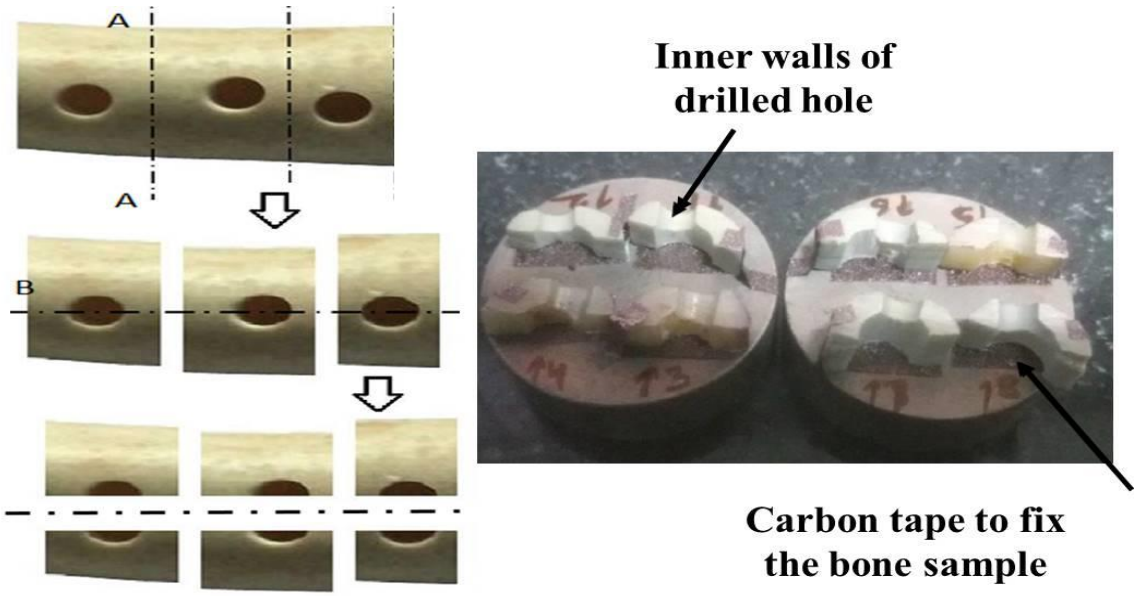

Figure 3.10: Gold plated specimens ready for scanning electron microscopy (SEM)

3.9 HISTOPATHOLOGY OF BONE SPECIMEN

Histopathology of drilled bone samples enabled to check the level of thermal damage to the bone. In histopathology, Some standard preparations were executed before the morphological investigations. The drilled bone site was divided transversely into small pieces. Small sections of bones were sliced from the drilled site. The drilled bone site was divided transversely into small pieces. The prepared bone tissue samples were wrapped with a sponge and labeled. They were then kept in a solution of 10% nitric acid for 3-5 days for decalcification and then sections were

treated with 10 vol% formaldehyde diluted in distilled water before embedding and microtomy [140-142]. The samples were checked after every 2 day intervals to see whether decalcification was achieved. Each time the chemical solution was changed for a fresh one [140-142]. After the decalcification process was finished, macro sections were taken from the specimens by the use of a microtome cutting apparatus. The specimens were cut and sliced by a microtome into micro sections of thickness of 4-6 um and stained by hematoxyline–eosine and they were then processed and mounted with D.P.X. before labeling. The histograms of sections were taken from the drill site by an optical microscope (NIKON). In the histograms, the damaged or necrotic zone at the drill site was evaluated for different drilling parameters by considering the volume of the nonviable and viable osteocyte within lacuna. From histopathology the following comparative statement has been observed. The follow-up of process is shown in figure3.11.

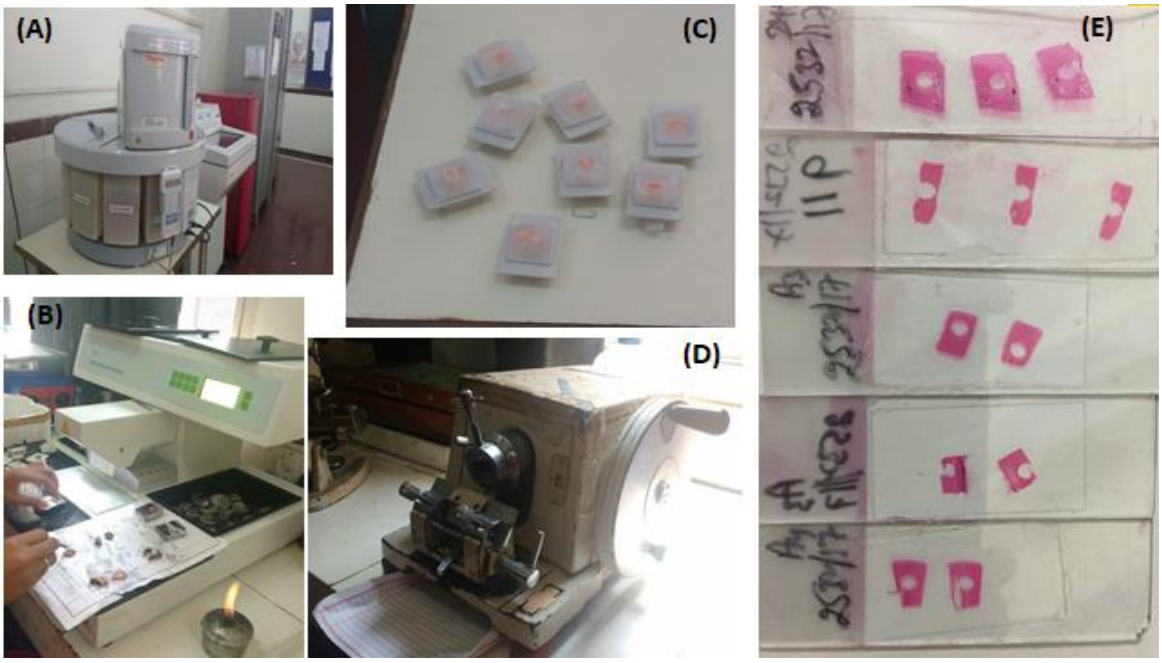

Figure 3.11: Preparing microscopic enabled images from bone samples: (A) chemical processing of bone; (B) preparing wax beds; (c) solidify wax bed specimens; (D) cutting thin films from wax beds; (E) prepared slides for microscopic examination

3.10 AXIAL PULLOUT OF BONE SCREW JOINT

Drilled holes in bones are subjected to analyze the axial pullout strength of bone-screw joint. For a sustainable orthopedic surgery, better axial pullout force of bone–screw joints is recommendable. Instability of a bone screw joint occurs when a high axial load applied on the joint. Low mechanical resistance of the joint, cracks in the drilled walls increases the chances of failures of joints. However, the chances of implant failure are reported 6-10 % only but still it is much more painful for a patient and treated as secondary injury to the patient. Although, the axial pullout force of bone screw joint depends on many factors i.e. location of joint, design of screw, and hole quality. The later one should be controlled during the bone drilling. Thus, delaminated and damaged hole definitely affects the axial pullout force of bone screw joint. To get the axial pullout of bone screw joint, the hole quality factor is assumed to be responsible while trying to keep other factors constant. The detailed process of axial pullout of bone is shown in figure 3.12.

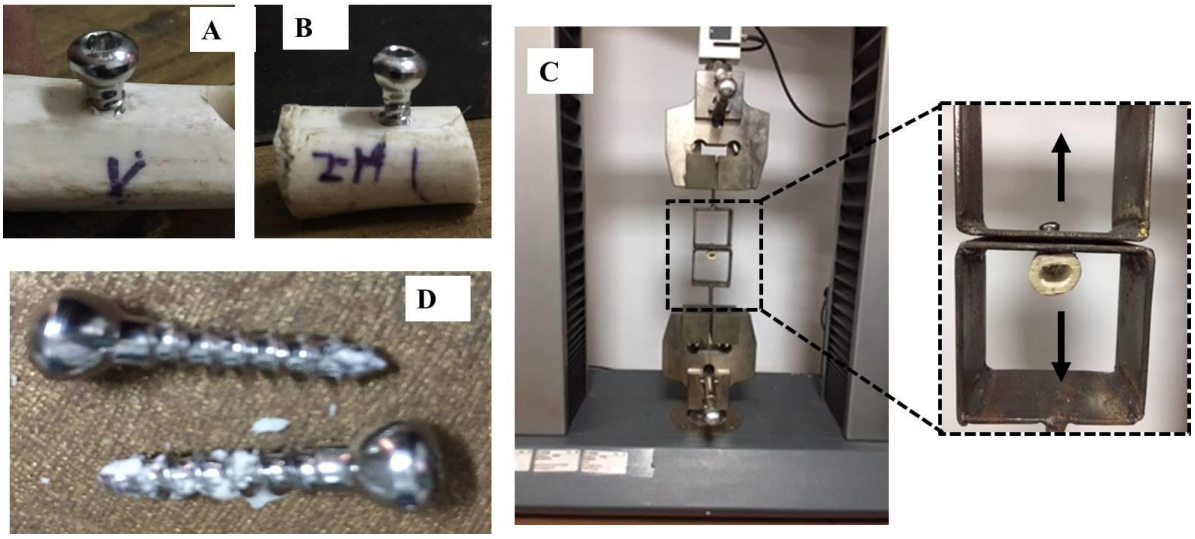

Figure 3.12: follow-up of axial pullout force for bone screw joint; (A&B) cortical screws tighten to the drilled holes; (C) pullout testing on UTM using fixture ;(D) pull out screws

3.11 EXPERIMENTAL DESIGN

3.11.1 Selection of parameters

In order to study the bone drilling damages to the bone experimentally, the drilling parameters is to be selected. Machine parameters, rotational speed and feed rate of tool are the most contributing factors that were studied by different researchers already. The effect of these machine parameters is very important to be study under the effect of ultrasonic vibrations. Drill specifications are the drilling parameters that directly influence the level of damage in bone during drilling. Drill point angle and helix angle are the factors needed to be explored for the thermal and mechanical damage. A wide range of these parameters is to be selected for the experimentation. Within the selected range, five different levels have been selected for experimental investigation. It is found to be difficult to maintain both drill specifications in a single action and studied with machine parameters because of complexity in the drill bit structure. Thus, two different experimental run was performed and shown in table 3.3. The level of parameters is decided on the basis of literature available and with consultant to some senior orthopedic surgeons. From literature, the rotational speed is used in between the range of 100-20,000 rpm [3,24,53,66,87]. However, majority of the researchers recommended the lower rotational speed because higher rotational speed always associated with higher heat generation [27,30,43-45,47-48,51,53]. From the segment of lower rotational speed i.e. 100 rpm to 5000 rpm, the behavior of heat generation with respect to rotational speed is some unpredictable and need to be studied dedicatedly. The feed rate of drill bit is also studied numerously with in the wide range(0.6-150 mm/min) and suggested a lower feed rate for control over mechanical damage[61,65,70,77-82]. However, low feed rate prolong the contact time of drill bit with bone and heat transfer will be increased. Thus, an optimized level of feed rate is to be selected with

respect to the condition of bone and depth of drilling. In view of all these conditions, some specialized orthopedic surgeons were consulted and with their experience the parameters range and levels were selected for the experimental procedure for both trails is shown in table 3.3. Parameters related to ultrasonic transducer are kept constant as described in table 3.3 as fixed parameters.

Table 3.3: Experimental parameters with levels

Parameters	**Units**	**Level 1**	**Level 2**	**Level 3**	**Level 4**	**Level 5**
For first set of experimentation						
Rotational speed (R)	rpm	600	1200	1800	2400	3000
Feed rate (F)	mm/min	10	20	30	40	50
Drill Point angle (P)	Degree	60	80	100	120	140
For Second set of experimentation						
Rotational speed (R)	rpm	600	1200	1800	2400	3000
Feed rate (F)	mm/min	10	20	30	40	50
Drill Helix angle (H)	Degree	12	18	24	30	36
Fixed Parameters						
Frequency	20kHz					
Amplitude	16µm					

3.11.2 Orthogonal Array

The selected drilling parameters described in table 3.3 were studied with the orthogonal array design of experimental approach. Orthogonal array suggested a combinational of parameters to perform the drilling operation on cortical bone. The orthogonal array is a method of selecting design matrix with least number of experiments and attains high efficiency in Taguchi

experimental approach. Orthogonal array is a modified form of the full factorial design matrix approach using mathematical algorithms. The term originality in this technique shows with the equal representation of each level in each column, each level within one column, and each level within any other column will occurs on equal number of times as well in the design matrix. By doing so, the each parameter and their respective levels shows equal representation in the design matrix and design is called orthogonal [143-144]. Orthogonal arrays design matrix can be suggested with a wide range of parameters and levels. Each column is in relation to other because of orthogonally attachment with other column. The outs comes are also interlinked and effect of parameters directly depend upon all outcome with respect to every column. Any change observed in a single column may affect the result outputs. Thus, the following qualities make the taguchi a robust design method for optimization.

1. It shows uniformity in experimental design and further analysis.
2. With minimum number of execution of experiments it is cost effective.
3. Taguchi shows it robustness with performance neglecting the noise factors in the design.

3.11.3 Orthogonal array selection conditions

The specified orthogonal array for a problem is selected on the basis of:

1. No of input parameters (factors) and there interactions of interest.
2. The levels decided for the each respective parameter (factors)

Experimental design in taguchi orthogonal array is a least experiment method to solve an optimization problem. Thus, many experimental parameters can be studied in a single study as compared to the full factorial method.

On the basis of number input parameters and levels, L25 orthogonal array is selected for the both set of experimentation. The design matrix for L25 orthogonal array is shown in table 3.4.

Table 3.4: L25 Design matrix for experiment execution

Experiment No.	**Parameter (A)**	**Parameter (B)**	**Parameter (C)**
1	1	1	1
2	1	2	2
3	1	3	3
4	1	4	4
5	1	5	5
6	2	1	2
7	2	2	3
8	2	3	4
9	2	4	5
10	2	5	1
11	3	1	3
12	3	2	4
13	3	3	5
14	3	4	1
15	3	5	2
16	4	1	4
17	4	2	5
18	4	3	1

19	4	4	2
20	4	5	3
21	5	1	5
21	5	2	1
23	5	3	2
24	5	4	3
25	5	5	4

3.11.4 Degree of freedom

The degree of freedom is the number of terms that can make change in the output. It includes the each factor with their levels selected for the experimentation. In another terms, DOF defined as the no of independent coordinates that can define the position of a system. In taguchi technique, the number of levels reduced by one is the degree of freedom for that specified factor. (K-1) Here K is the number of level for that factor. Total degree of freedom (DOF) of the system is the arithmetic sum of all degree of freedom (DOF) of the involve parameters.

3.11.5 Objective Function

Objective function is the desired output for the experimentation is to be executed. In the present study, the following outputs are considered as the objective function.

- Delamination in hole diameter
- Heat generation
- Thrust forces developed
- Axial Pullout force of bone screw joint

From the above said objective function, there is aim to minimize the delamination in diameter, temperature raised and forced developed and maximize the axial Pullout force of bone screw joint. For the above said objective function the parameters and their levels to be studied is shown in table 3.3 and experiment design matrix subjected to the objective functions is shown in table 3.4.

3.11.6 Execution of experiments

Total 25 interactions of parameters, suggested with the L25 orthogonal array is incorporated with the parameters and their levels. The experimental run formed with this is shown in table 3.5. Two set of experiments performed differently with different tool specifications. In first order, variation in point angle is to be studied and second one is targeting the helix angle of tool while other drill specification kept constant. Along with this, a comparison with the conventional and ultrasonic-assisted drilling is made with the same design matrix. The developed design for the both set of experiments is shown in table 3.5 and 3.6.

Table 3.5: Execution of experiments for first set (point angle group) of experiments with 25 combinations

Experiment No.	Rotational Speed(R) (rpm)	Feed Rate(F) (mm/min)	Drill Point Angle(A) (degree)
1	600	10	60
2	600	20	80
3	600	30	100
4	600	40	120
5	600	50	140
6	1200	10	80
7	1200	20	100
8	1200	30	120

9	1200	40	140
10	1200	50	60
11	1800	10	100
12	1800	20	120
13	1800	30	140
14	1800	40	60
15	1800	50	80
16	2400	10	120
17	2400	20	140
18	2400	30	60
19	2400	40	80
20	2400	50	100
21	3000	10	140
21	3000	20	60
23	3000	30	80
24	3000	40	100
25	3000	50	120

Table 3.6: Execution of experiments for second set (helix angle group) of experiments with 25 combinations

Experiment No.	**Rotational Speed(R) (rpm)**	**Feed Rate(F) (mm/min)**	**Drill Helix Angle(H) (degree)**
1	600	10	12
2	600	20	18
3	600	30	24
4	600	40	30
5	600	50	36
6	1200	10	18

7	1200	20	24
8	1200	30	30
9	1200	40	36
10	1200	50	12
11	1800	10	24
12	1800	20	30
13	1800	30	36
14	1800	40	12
15	1800	50	18
16	2400	10	30
17	2400	20	36
18	2400	30	12
19	2400	40	18
20	2400	50	24
21	3000	10	36
21	3000	20	12
23	3000	30	18
24	3000	40	24
25	3000	50	30

3.11.7 Analysis of objective function

Signal –to-noise ratio

According to taguchi optimization technique, there are two kinds of parameters affecting the response of experimental results i.e. controllable and un-controllable parameters. Controllable parameters are the design parameters, which can be adjusted or decided by the designer itself. Un-controllable parameters are the sources of variation which are not in control of designer and associated with operational condition and environment. The influence

of control factor is high as compared to uncontrolled factors and the best set of parameters combination can be determined through the response output of individual trials. There can be two conditions to specify the output conditions used in this study. i.e. larger- the-better, smaller-the-better,. For each condition S/N ration is calculated as follows in equation 3.1 and 3.2:

For larger-the-better conditions:

$$\mathrm{S/N} = -10log_{10}\left(\sum(1/Y^2)/\mathrm{n}\right)$$

eq. 3.1

For smaller-the-better conditions:

$$\mathrm{S/N} = -10log_{10}\left(\sum(Y^2)/\mathrm{n}\right)$$

eq 3.2

Y is the observation on respective set of combination of parameters and n is the no of observation taken on that particular combination.

Analysis of Variance (ANOVA):

The final output of the experimental results is also influenced by the parameters and their range. To justify the significance of individual parameter in terms of its percentage contribution for the result output ANOVA is used. During this analysis sum of square (SS), variance, Degree of freedom (DOF) F-Ratio, P-Value and percentage contribution of individual parameter is calculated. Sum of square (SS) is calculated using the formula given in equation (3.3) below.

$$SS_A = \left[\sum_{i=1}^{k_A}\left(\frac{A_i^2}{n_{Ai}}\right)\right] - \frac{T^2}{N}$$

eq. *3.3*

Where, average of all observation under A_i level = $\frac{A_i}{n_{Ai}}$

Sum of all observations = T

Average of all observation = T/N

N_{Ai} =Number of observations under A_i level

Error Sum of Squares (SS e) - Squared deviations of observations from parameter (A) averages

3.11.8 Results validation

Estimated Value:

The suggested set of combination of parameters is to be tested for the validation of results. The signal-to-noise ratio for the desired set of combination is predicted using equation 3.4.

$$\boldsymbol{\mu_P} = \eta_m + \sum^{k}_{i=1}(\eta_{oi} - \eta_m) \qquad \textit{eq. 3.4}$$

μ_P is the estimated value of response output, η_m is the total mean response output of all experimental combinations, η_{oi} is the mean value of response output at the optimal levels of each parameter, value taking from response table, k is the number of parameters involved in optimization. The best coordination of results estimation and experimental value of response output shows the success of Taguchi optimization technique.

Confidence Interval (CI):

Confidence interval is a range around the estimated value suggested by Taguchi optimization and within this range the experimental value on the suggested combination of parameters will be accepted. The confidence interval is calculated as follows in equation 3.5:

$$CI = \pm \sqrt{\frac{F_{\alpha(v1:v2)}\, V_e}{\psi_{eff.}}}$$

eq. 3.5

$F_{\alpha(v1:v2)}$ is the F-ratio at the confidence level of (1-α) against degrees of freedom (DOF) equal to 1 and error DOF (f_e). V_e = *SS value of Error / DOF for Error*, and $\psi_{eff.}$ = no of experimental trails/ (1+ Total DOF- Error DOF).

Thus, the optimal value should be place in between the range: $\mu_P + CI < \boldsymbol{\mu_P} < \mu_P - CI$.

3.12 SUMMARY

The developed experimental setup for bone drilling process with its technical specifications and physical design has been described in this chapter. The experimental procedures followed to get the observations in terms of desired outputs are also described. Technique used for post-operative measurements of hole accuracy and pullout force of bone screw joint is pronounced. Experimental process is designed with respect to the number of involved parameters and respective number of levels. L25 design experiment with all possible set of parametric combination to achieve the objective functions with statistical operations, like Signal-to-noise ratio, ANOVA finally validation for the results is explained in this chapter.

CHAPTER 4: EXPERIMENTAL RESULTS

In order to observe the results during experimentation, heat generation and drilling forces were measured during the experimentation by the means of RTD sensor and dynamometer respectively (as described in section 3.5 and 3.6). Further analysis has been done for delamination in diameter measured by coordinate measuring machine (CMM). In microscopic characterization of drilled holes, scanning electron microscopy (SEM) was used to estimate the results of forces on cracks initiations in drilled hole walls. Histopathology of bone specimens was carried out to understand the effect of temperature on drilled hole specimens and thereafter, a comparative analysis has been done to understand the effect of ultrasonic-assisted drilling in bone drilling. Experimental observations were carried out according to the L25 orthogonal array experimental trials. Each trial was repeated up to three times to reduce the chances of errors during execution or observation of results. For both (point angle group and helix angle group) set of experiments, within the selected range of parameters, different levels of rotational speeds, feed rates and drill specifications (point angle/helix angle) were the parameters for optimization of minimum drilling temperature, thrust forces, diameter delamination and maximum axial pullout force of bone-screw joint. Data observed during the experimentation were used to conduct the ANOVA test and help to calculate the effect of individual parameters on outputs. The significance of parameters during each individual parametric study is also calculated using the P value. The results observations were categorized according to experimental group i.e 1^{st} set of experimentation (point angle group) and second set of experimentation (helix angle group)

4.1 OBSERVATION AND ANALYSIS FOR 1ST SET (POINT ANGLE GROUP) OF EXPERIMENTATION

4.1.1 Heat generation

Signal-to noise ratio

The heat generation during drilling is indicated in terms of temperature raised and measured using RTD sensor as described in section 3.6. The temperature rise should be minimum for better results in case of bone drilling. Thus, smaller-the-better condition (eq 3.2) applied for calculating the signal-to-noise ratio and results are as follows in table 4.1:

Table 4.1: Heat generation and S/N ratio for ultrasonic-assisted bone drilling during 1st group of experimentation

Sr No	Rotational Speed (R) (rpm)	Feed Rate (F) (mm/min)	Drill Point Angle (P) (degree)	Max. Temperature Recorded				S/N Ratio
				T1 (°C)	T2 (°C)	T3 (°C)	Avg. Temp. (°C)	
1	600	10	60	42.6	42.7	42.4	42.6	-32.57
2	600	20	80	44.7	44.6	44.7	44.7	-33.00
3	600	30	100	46.2	45.8	45.9	46.0	-33.25
4	600	40	120	48.7	48.9	48.7	48.8	-33.76
5	600	50	140	50.8	51.1	51.0	51.0	-34.14
6	1200	10	80	47.8	48.1	47.8	47.9	-33.60
7	1200	20	100	49.8	48.9	51.0	49.9	-33.95
8	1200	30	120	54.8	55.1	54.7	54.9	-34.78
9	1200	40	140	58.6	58.2	59.1	58.8	-35.38
10	1200	50	60	56.3	55.5	55.6	55.8	-34.93
11	1800	10	100	56.7	56.5	56.9	56.7	-35.07

12	1800	20	120	58.8	59.1	58.8	58.9	-35.40
13	1800	30	140	62.9	62.6	62.5	62.7	-35.93
14	1800	40	60	57.0	57.5	57.2	57.2	-35.14
15	1800	50	80	61.0	60.4	60.1	60.5	-35.63
16	2400	10	120	58.2	58.2	58.0	58.1	-35.28
17	2400	20	140	62.6	62.5	62.1	62.4	-35.90
18	2400	30	60	59.9	59.6	59.8	59.8	-35.53
19	2400	40	80	60.3	60.2	60.1	60.2	-35.59
20	2400	50	100	61.8	62.0	61.6	61.8	-35.81
21	3000	10	140	60.8	60.6	60.4	60.6	-35.64
22	3000	20	60	58.5	58.7	59.2	58.8	-35.38
23	3000	30	80	62.2	62.5	62.9	62.5	-35.91
24	3000	40	100	63.7	62.9	63.9	63.5	-36.05
25	3000	50	120	67.1	67.1	68.0	67.4	-36.57

The heat generation in terms of temperature observed during the experimentation was solved for the optimization of parameters. The response table for signal-to- noise ratio and mean data respective to the individual parameters is shown in table 4.2. On the basis of these values response curves is plotted shown in figure 4.1.

Table 4.2: Response table for S/N ratio and mean values corresponding to individual parameters for heat generation in 1st set of experimentation

Parameters	**Response values of S/N ratio**					**Response values of Mean data**				
	L 1	**L 2**	**L 3**	**L 4**	**L 5**	**L1**	**L2**	**L3**	**L4**	**L5**

R	-33.35	-34.53	-35.44	-35.63	-35.92	46.59	53.45	59.19	60.46	62.56
F	-34.44	-34.73	-35.09	-35.19	-35.42	53.17	54.93	57.16	57.69	59.30
P	-34.72	-34.75	-34.83	-35.16	-35.40	54.83	55.15	55.57	57.61	59.08

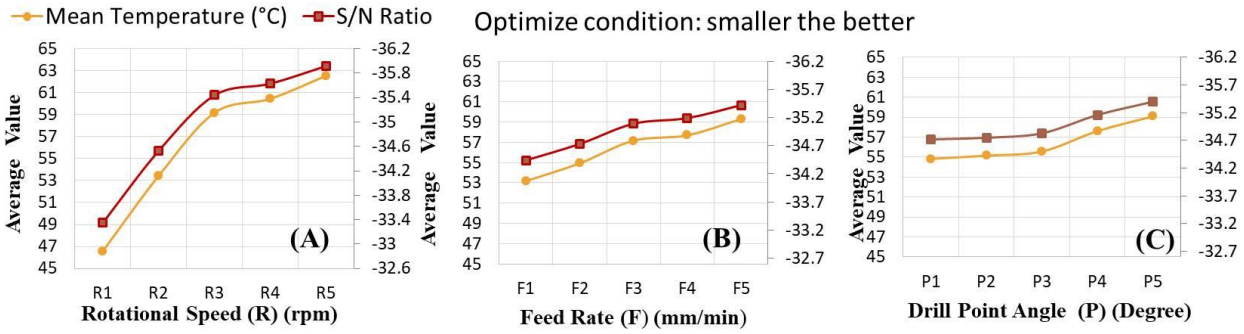

Figure 4.1: Response curves subjected to individual parameters; (A) For rotational speed(R); (B) For Feed rate (F); (C) For drill point angle (P) for heat generation in 1st group of experimentation

Analysis of variance (ANOVA)

Further, the mean data has been analyzed for the analysis of variance (ANOVA). The data obtained with calculation of equation (3.3) is shown in table 4.3. From ANOVA table 4.3, the rotational speed(R) shows the maximum contribution (80.53%) in heat generation during the experimentation process and all parameters affects significantly ($P \leq 0.05$).

Table 4.3: ANOVA table for heat generation during 1st group of experimentation

Source	**SS**	**DOF**	**Variance**	**F-ratio**	**P-value**	**Percentage Contribution**
Rotational Speed (R)	835.54	4	208.885	132.07	0.000	80.53
Feed Rate (F)	116.15	4	29.037	18.36	0.000	11.19
Drill Point Angle (P)	66.83	4	16.708	10.56	0.001	6.44

Residual Error	18.98	12				1.82

Estimation for Optimum Value:

To estimate the results suggested by Taguchi optimization i.e. R1F1A1 (rotational speed: 600 rpm, feed rate:10 mm/min, drill point angle: 60º). The equation (3.4) is used to predict the response value as per suggestion of Taguchi.

$$\boldsymbol{\mu_{TP1}} = \eta_m + \sum_{i=1}^{k}(\eta_{oi} - \eta_m)$$

$\boldsymbol{\mu_{TP1}}$ = 56.448+ {(46.59) – (56.448)} + {(53.17) – (56.448)} + {(54.83) – (56.448)}

$\boldsymbol{\mu_{TP1}}$ = 56.448+ {(– 9.858)} + {(– 3.278)} + {(– 1.618)}

$\boldsymbol{\mu_{TP1}}$ = (41.694)

Further, confidence interval (CI) has been measured using equation 3.5. The interval gives a range of temperature in between the experimental result for optimal combination of parameters should be placed.

$$CI = \pm \sqrt{\frac{F_{\alpha(v1:v2)}\, V_e}{\psi_{eff.}}}$$

$F_{\alpha(v1:v2)}$ is the F-ratio at the confidence level of (1-α) against degrees of freedom (DOF) equal to 1 and error DOF (f_e). V_e = SS value of Error / DOF for Error, and $\psi_{eff.}$ = (no of experimental trails) / (1+ Total DOF – Error DOF).

$F_{\alpha(v1:v2)} = F_{0.05(1:12)} = 4.75$ (this value obtained from the F table with 95% confidence level)

V_e = SS value of Error / DOF for Error

= 18.98/12 = 1.582

ψ_{eff} = (no. of experimental trails) / (1+ Total DOF– Error DOF).

= 25/ (1+24- 12) = 1.923

Using these values in equation 3.5, CI $= \pm$ 1.976

Thus, the estimated temperature value is: $\mu_{TP1} + CI < \boldsymbol{\mu_{TP1}} < \mu_{TP1} - CI$.

The experimental value for optimal temperature should be in between: 39.72 < $\boldsymbol{\mu_{TP1}}$ < 43.67 and compared it with the experimental value in table 4.4.

Table 4.4: Results validation for heat generation during 1st group of experimentation

	Optimized process parameters	
	Predicted Range	Experimental Value
Optimal combination	R1F1P1	R1F1P1
Temperature (°C)	39.72 < μ_{TP1} < 43.67	42.6°C

Comparative statement of heat generation with conventional bone drilling

The same experiments have been performed with conventional process also with the same experimental conditions, parameters selection and measurement of output parameters. The measured temperature during conventional drilling is compared with the temperature measured with the ultrasonic-assisted bone drilling experiments as shown in figure 4.2. From the figure 4.2, it is clearly evident that ultrasonic-assisted drilling technique helps to control the heat generation at every level of experimentation.

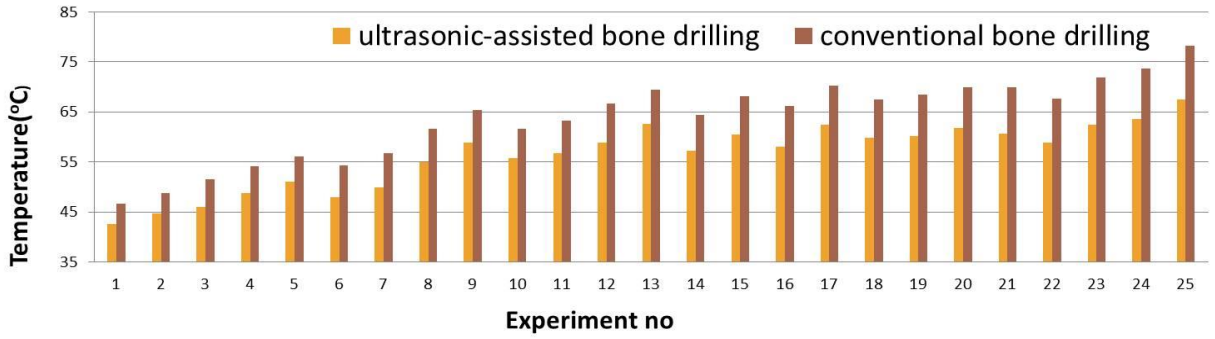

Figure 4.2: Comparative statement for heat generation in conventional and ultrasonic-assisted bone drilling for 1st group of experimentation

4.1.2 Thrust force

Signal-to noise ratio

Thrust forces developed during drilling of bone were measured using dynamometer as described in section 3.5 and shown in table 4.5. The forces should be minimum for better result output and causes less mechanical damage. Thus, smaller-the- better optimization condition (eq. 3.2) used and signal-to noise ratio calculated is listed in table 4.5.

Table 4.5: Thrust forces and S/N ratio for ultrasonic-assisted bone drilling during 1st group of experimentation

Sr No	Rotational Speed (R) (rpm)	Feed Rate (F) (mm/min)	Drill Point Angle (P) (degree)	Thrust forces				S/N Ratio
				T1 (N)	T2 (N)	T3 (N)	Avg. Th force (N)	
1	600	10	60	8.98	9.2	9.25	9.14	-19.22
2	600	20	80	9.83	9.69	9.49	9.67	-19.71
3	600	30	100	9.98	10.91	8.96	9.95	-19.96
4	600	40	120	11.3	9.25	10.98	10.51	-20.43
5	600	50	140	10.9	11.89	11.83	11.54	-21.24
6	1200	10	80	8.17	8.11	8.2	8.16	-18.23

7	1200	20	100	8.58	8.73	8.73	8.68	-18.77
8	1200	30	120	8.89	9.31	9.29	9.16	-19.24
9	1200	40	140	10.3	9.67	9.39	9.78	-19.81
10	1200	50	60	9.79	9.12	9.56	9.49	-19.55
11	1800	10	100	8.1	7.71	7.2	7.67	-17.70
12	1800	20	120	8.11	7.99	8.36	8.15	-18.22
13	1800	30	140	8.41	8.71	8.92	8.68	-18.77
14	1800	40	60	8.12	8.34	8.11	8.19	-18.27
15	1800	50	80	8.38	8.52	8.78	8.56	-18.65
16	2400	10	120	7.39	7.56	7.49	7.48	-17.48
17	2400	20	140	7.59	7.8	8.32	7.9	-17.95
18	2400	30	60	7.64	7.53	7.79	7.68	-17.71
19	2400	40	80	8.02	8.14	8.02	8.06	-18.13
20	2400	50	100	8.27	8.18	8.36	8.27	-18.35
21	3000	10	140	7.42	7.3	7.66	7.46	-17.45
22	3000	20	60	7.09	7.25	7.24	7.19	-17.13
23	3000	30	80	7.52	7.34	7.55	7.47	-17.47
24	3000	40	100	7.75	7.78	7.54	7.69	-17.72
25	3000	50	120	8.1	8.2	7.71	8.00	-18.06

Thrust forces developed during the experimentation were solved for the optimization of parameters. The response table for signal-to- noise ratio and mean data respective to the individual set of parameters is shown in table 4.6. On the basis of these values response curves is plotted shown in figure 4.3.

Table 4.6: Response table for S/N ratio and mean values corresponding to individual parameters for thrust forces in 1st group of experimentation

Parameters	Response values of S/N ratio					Response values of Mean data				
	L 1	L 2	L 3	L 4	L 5	L1	L2	L3	L4	L5
R	-20.11	-19.12	-18.32	-17.92	-17.57	10.16	9.05	8.25	7.87	7.56
F	-18.02	-18.36	-18.63	-18.87	-19.17	7.98	8.31	8.58	8.84	9.17
P	-18.37	-18.44	-18.50	-18.69	-19.05	8.33	8.38	8.45	8.66	9.07

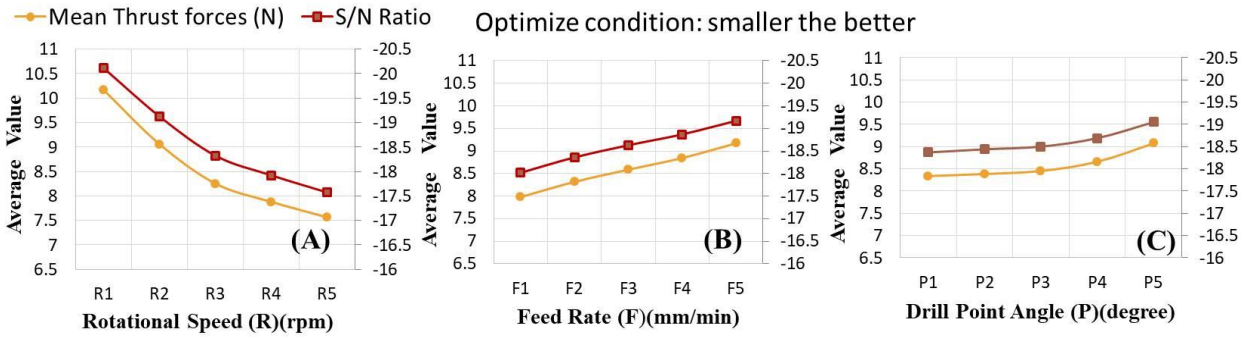

Figure 4.3: Response curves respective to the input parameters; (A) for rotational speed; (B) for feed rate; (C) for drill point angle for thrust forces in 1st group of experimentation

Analysis of variance (ANOVA)

Further, the mean data of thrust forces has been analyzed for the analysis of variance (ANOVA). The data obtained with calculation of equation (3.3) is shown in table 4.7. From ANOVA table 4.7, the rotational speed(R) shows the maximum contribution (77.32%) in heat generation during the experimentation process and all parameters affects significantly ($P \leq 0.05$).

Table 4.7: ANOVA table for thrust force observed during 1st group of experimentation

Source	SS	DOF	Variance	F-ratio	P-value	Percentage Contribution
Rotational Speed (R)	21.827	4	5.456	185.17	0.000	77.32
Feed Rate (F)	4.237	4	1.059	35.95	0.000	15.01
Drill Point Angle (P)	1.809	4	0.452	15.35	0.000	6.40
Residual Error	0.353	12				1.25

Estimation for Optimum Value:

To validate the results suggested by Taguchi optimization i.e. R5F1P1 (rotational speed: 3000 rpm, feed rate: 10 mm/min, drill point angle: 60º). The equation (3.4) is used to predict the response value as per suggestion of Taguchi.

$$\boldsymbol{\mu_{FP1}} = \eta_m + \sum_{i=1}^{k}(\eta_{oi} - \eta_m)$$

$\boldsymbol{\mu_{FP1}}$ = 8.581+ {(–1.019)} + {(–0.599)} + {(–0.243)}

$\boldsymbol{\mu_{FP1}}$ = (6.72)

Further, confidence interval (CI) has been measured using equation 3.5. The interval gives a range of thrust force in between the experimental result for optimal combination of parameters should be placed.

$$CI = \pm \sqrt{\frac{F_{\alpha(v1:v2)}\, V_e}{\psi_{eff.}}}$$

$F_{\alpha(v1:v2)}$ is the F-ratio at the confidence level of (1-α) against degrees of freedom (DOF) equal to 1 and error DOF (f_e). V_e = SS value of Error / DOF for Error, and $\psi_{eff.}$ = (no of experimental trails) / (1+ Total DOF – Error DOF).

$F_{\alpha(v1:v2)} = F_{0.05(1:12)} = 4.75$ (this value obtained from the F table with 95% confidence level)

V_e = SS value of Error / DOF for Error

= 0.353/12 = 0.029

ψ_{eff} = (no. of experimental trails) / (1+ Total DOF– Error DOF).

= 25/ (1+24- 12) = 1.923

Using these values in equation 5, $CI = \pm 0.269$

Thus, the estimated thrust force value is: $\mu_{FP1} + CI < \boldsymbol{\mu_{FP1}} < \mu_{FP1} - CI$.

The experimental value for optimal thrust force should be in between: $6.45 < \mu_{FP1} < 6.98$ and compared it with the experimental value in table 4.8.

Table 4.8: Result validation for thrust force for 1st group of experimentation

	Optimized process parameters	
	Predicted Range	Experimental value
Optimal combination	R5F1P1	R5F1P1
Thrust forces (N)	$6.45 < \mu_{FP1} < 6.989$	6.90 N

Comparative statement for thrust force with conventional bone drilling

In order to ensure the benefits of ultrasonic-assisted bone drilling process, the same experiments has been performed with the conventional drilling process and thrust forces measured using the same experimental setup. The measured values of thrust forces during conventional drilling process compared with the values obtained from ultrasonic-assisted and shown in figure 4.4. From the comparative statement, the effectiveness of ultrasonic-assisted bone drilling process in terms of bone drilling can be clearly visible for low thrust forces. The continuous effect of ultrasonic assisted bone drilling is observed for all experimental combination.

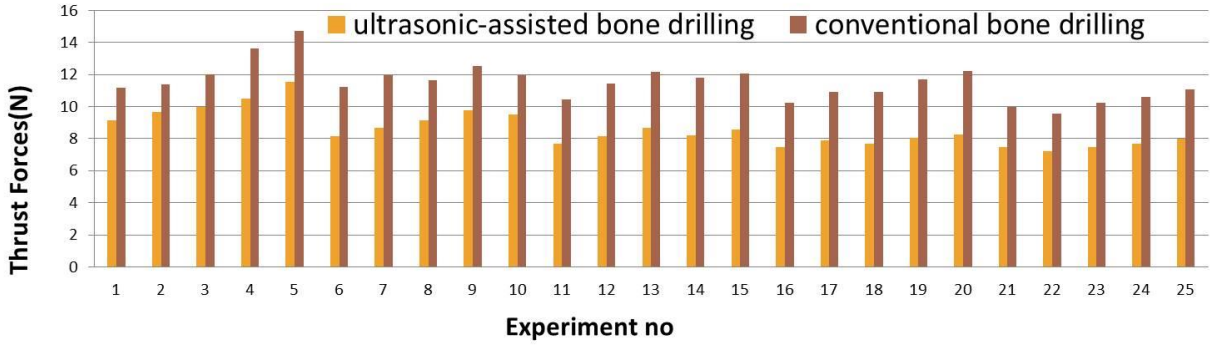

Figure 4.4: Comparative statement for thrust forces in conventional and ultrasonic-assisted bone drilling for 1st group of experimentation

4.1.3 Axial pullout force

Signal-to-Noise

Drilled holes in bones were subjected to fix the implants by the means of cortical screws. To justify the reason, fixation of screw to the drilled holes and tested for maximum axial pullout force up to which bone screw joint can withstand before failure. (as described in section 3.10). The values recorded in newton and listed in table 4.9. The axial force of bone screw joint should be maximum. Thus, the optimize condition used to calculate the S/N ratio is larger-the-better i.e. equation 3.1 in section 3.11.7.

Table 4.9: Maximum axial pullout force and S/N ratio for ultrasonic-assisted bone drilling during 1st group of experimentation

Sr No	Rotational Speed (R) (rpm)	Feed Rate (F) (mm/min)	Drill Point Angle (A) (degree)	Maximum axial pullout force (N)	S/N Ratio
1	600	10	60	780	57.8419
2	600	20	80	767	57.6959
3	600	30	100	727	57.2307
4	600	40	120	716	57.0983
5	600	50	140	670	56.5215
6	1200	10	80	817	58.2444
7	1200	20	100	786	57.9085
8	1200	30	120	749	57.4896
9	1200	40	140	710	57.0252
10	1200	50	60	768	57.7072
11	1800	10	100	927	59.3416
12	1800	20	120	826	58.3396
13	1800	30	140	770	57.7298
14	1800	40	60	819	58.2657
15	1800	50	80	815	58.2232
16	2400	10	120	948	59.5362
17	2400	20	140	890	58.9878
18	2400	30	60	941	59.4718
19	2400	40	80	868	58.7704
20	2400	50	100	806	58.1267
21	3000	10	140	990	59.9127
22	3000	20	60	1094	60.7803
23	3000	30	80	995	59.9565
24	3000	40	100	906	59.1426

25	3000	50	120	848	58.5679

The mean value of maximum axial pullout force respective to each level of parameter is described as response values with respect to the each level and parameters shown in response table 4.10 for axial pullout force. The values from table 4.10 are used to plot the response curves respective to the each level of experimental parameters shown in figure 4.5.

Table 4.10: Response table for axial pullout force for 1st group of experimentation

Parameters	**Response values of S/N ratio**					**Response values of Mean data**				
	L 1	**L 2**	**L 3**	**L 4**	**L 5**	**L1**	**L2**	**L3**	**L4**	**L5**
R	57.28	57.67	58.38	58.98	59.67	732.0	766.0	831.4	890.6	966.6
F	58.98	58.74	58.38	58.06	57.83	892.4	872.6	836.4	803.8	781.4
P	58.81	58.58	58.35	58.21	58.04	880.4	852.4	830.4	817.4	806.0

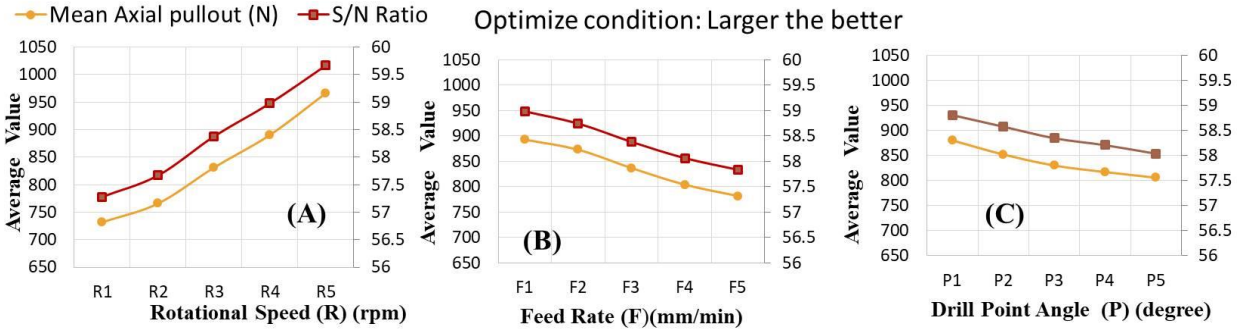

Figure 4.5: Response curves respective to each level for maximum pullout force; (A) for rotational speed, (B) for feed rate, (C) for 1st group of experimentation

Analysis of variance (ANOVA)

Further, the mean data of maximum axial pullout force has been analyzed for the analysis of variance (ANOVA). The data obtained with calculation of equation (3.3) is shown in table 4.11. From ANOVA table 4.11, the rotational speed(R) shows the maximum contribution (70.10%) for maximum axial pullout force during the pullout testing of bone-screw joint and all parameters affects significantly (P≤0.05).

Table 4.11: ANOVA table for maximum axial pullout force for bone-screw joint for 1st set of experimentation

Source	**SS**	**DOF**	**Variance**	**F ratio**	**P value**	**Percentage Contribution**
Rotational Speed (R)	178830	4	44707	33.37	0.000	70.10
Feed Rate (F)	42650	4	10662	7.96	0.002	16.71
Drill Point Angle (P)	17545	4	4386	3.27	0.049	6.877
Residual Error	16077	12				6.30

Estimation for Optimum Value:

To validate the results suggested by Taguchi optimization i.e. R5F1P1 (rotational speed: 3000 rpm, feed rate: 10 mm/min, drill point angle: 60º). The equation 3.4 is used to predict the response value as per suggestion of Taguchi.

$$\boldsymbol{\mu_{AP1}} = \eta_m + \sum_{i=1}^{k}(\eta_{oi} - \eta_m)$$

$\boldsymbol{\mu_{AP1}}$ = 837.32+ {(966.6)-(837.32} + {(892.4)-(837.32)} + {(880.4)-(837.32)}

$\boldsymbol{\mu_{AP1}}$ = 837.32+ {(129.28)} + {(55.08)} + {(43.08)}

$\boldsymbol{\mu_{AP1}}$ = (1064.76)

Further, confidence interval (CI) has been measured using equation 3.5. The interval gives a range of axial pullout force in between the experimental result for optimal combination of parameters should be placed.

$$CI = \pm \sqrt{\frac{F_{\alpha(v1:v2)}\, V_e}{\psi_{eff.}}}$$

$F_{\alpha(v1:v2)}$ is the F-ratio at the confidence level of (1-α) against degrees of freedom (DOF) equal to 1 and error DOF (f_e). V_e = SS value of Error / DOF for Error, and $\psi_{eff.}$ = (no of experimental trails) / (1+ Total DOF – Error DOF).

$F_{\alpha(v1:v2)} = F_{0.05(1:12)} =$ 4.75 (this value obtained from the F table with 95% confidence level)

V_e = SS value of Error / DOF for Error

= 16077/12 = 1339.75

ψ_{eff} = (no. of experimental trails) / (1+ Total DOF– Error DOF).

= 25/ (1+24- 12) = 1.923

Using these values in equation 3.5, $CI = \pm$ 57.52

Thus, the estimated thrust force value is: $\mu_{AP1} + CI < \boldsymbol{\mu_{Ap1}} < \mu_{Ap1} - CI$.

The experimental value for optimal force should be in between: 1007.24 < $\boldsymbol{\mu_{Ap1}}$ < 1122.28 and compared it with the experimental value in table 4.12.

Table 4.12: Result validation for axial pullout force of bone screw joint for 1st group of experimentation

	Optimized process parameters	
	Predicted Range	Experimental value
Optimal combination	R5F1A1	R5F1A1
Axial Pullout Force (N)	$1007.24 < \mu_{Ap1} < 1122.28$	1110 N

Comparative statement for axial pullout force of bone screw joint with conventional bone drilling

The axial pullout force of bone screw joint is also measured for the conventionally drilled holes. Five experimental conditions have been selected in which holes are drilled with five different rotational speeds and compared for maximum axial pullout force as shown in figure 4.6. from the comparison it is observed that holes drilled with ultrasonic assisted technique give better anchorage strength.

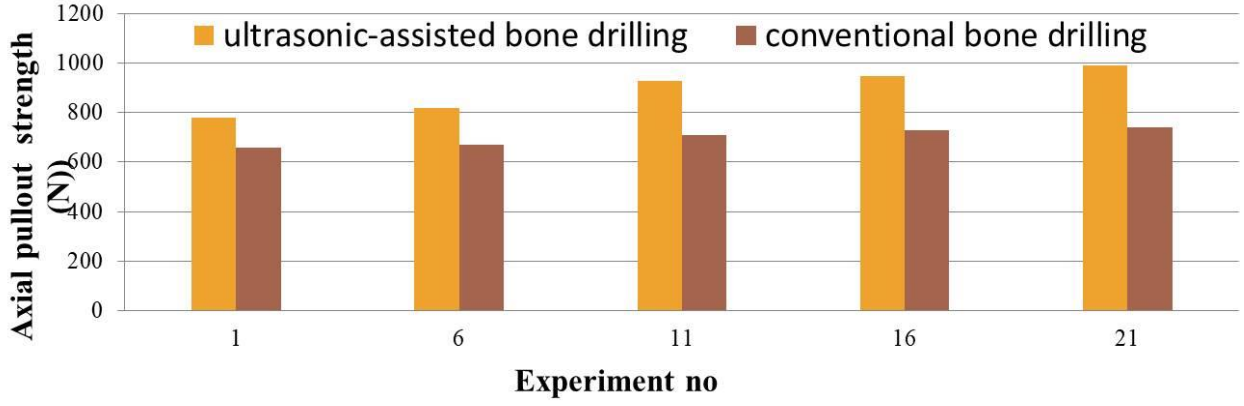

Figure 4.6: Comparative statement for axial pullout force of bone screw joint for conventional and ultrasonic-assisted drilled hole for 1st group of experimentation

4.1.4 Drilled hole diameter delamination

The delamination in drilled holes observed during drilling of bone is caused due to interlinked fibrous structure of bone and somehow, irrelevant combination of drilling parameters increases the chance of drilled hole delamination. Delamination in drilled holes gives an irregular shape holes, weak edges and uneven matching to the screws. Thus, results in the form of loose anchorage strength to the screw. The effect of drilling parameters has been measured on delamination of drilled holes, examined using CMM machine as described in section 3.7. The values observed in terms of percentage delamination are shown in table 4.13 respective to the individual set of parametric combination.

Table 4.13: Delamination of diameter and S/N ratio observed in drilled holes for 1st group of experimentation

Sr No	Rotational Speed (R) (rpm)	Feed Rate (F) (mm/min)	Drill Point Angle (P) (degree)	Diameter Delamination (% age)	S/N Ratio
1	600	10	60	3.438	-10.7249
2	600	20	80	3.750	-11.4806
3	600	30	100	4.569	-13.1959
4	600	40	120	5.525	-14.8466
5	600	50	140	5.706	-15.1270
6	1200	10	80	3.506	-10.8969
7	1200	20	100	4.947	-13.8866
8	1200	30	120	5.016	-14.0065
9	1200	40	140	6.912	-16.7927
10	1200	50	60	6.856	-16.7217

11	1800	10	100	3.953	-11.9388
12	1800	20	120	6.500	-16.2583
13	1800	30	140	7.237	-17.1918
14	1800	40	60	5.828	-15.3106
15	1800	50	80	6.634	-16.4360
16	2400	10	120	4.516	-13.0944
17	2400	20	140	6.925	-16.8084
18	2400	30	60	6.453	-16.1954
19	2400	40	80	6.609	-16.4032
20	2400	50	100	7.063	-16.9792
21	3000	10	140	4.375	-12.8196
22	3000	20	60	4.625	-13.3022
23	3000	30	80	7.331	-17.3036
24	3000	40	100	8.266	-18.3455
25	3000	50	120	8.544	-18.6330

The mean value of percentage delamination in drilled holes respective to each level of parameter is described as response values with respect to the each level and parameters shown in response table 4.14. The values from table 4.14 are used to plot the response curves respective to the each level of experimental parameters shown in figure 4.7.

Table 4.14: Response table for diametric delamination of drilled holes in 1st group of experimentation

Parameters	**Response values of S/N ratio**					**Response values of Mean data**				
	L 1	**L 2**	**L 3**	**L 4**	**L 5**	**L1**	**L2**	**L3**	**L4**	**L5**

R	-13.08	-14.46	-15.43	-15.90	-16.08	4.597	5.447	6.031	6.313	6.628
F	-11.89	-14.35	-15.58	-16.34	-16.78	3.957	5.349	6.121	6.628	6.961
P	-14.45	-14.50	-14.87	-15.37	-15.75	5.440	5.566	5.759	6.020	6.231

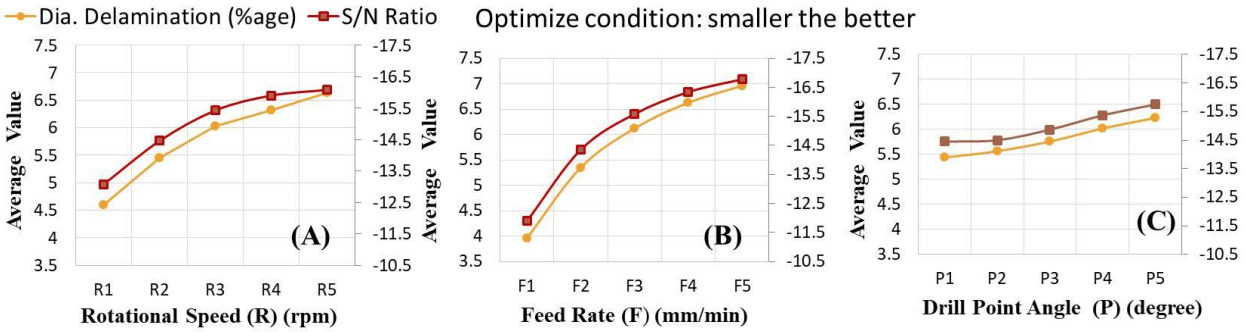

Figure 4.7: Response curves respective to each level for diametric delamination in drilled holes; (A) for rotational speed, (B) for feed rate, (C) for drill point angle for 1st group of experimentation

Analysis of variance (ANOVA)

Further, the percentage delamination of diameter has been analyzed for the analysis of variance (ANOVA). The data obtained with calculation of equation (3.3) is shown in table 4.15. From ANOVA table 4.15, the feed rate (F) shows the maximum contribution (55.175%) for maximum axial pullout force during the pullout testing of bone-screw joint. From the parameters, rotational speed (R) and feed rate (F) affects significantly ($P \leq 0.05$). Change in drill point angle (P) shows its effect on delamination but does not affect the results significantly.

Table 4.15: ANOVA table for maximum axial pullout force of bone-screw joint for 1st group of experimentation

Source	**SS**	**DOF**	**Variance**	**F ratio**	**P value**	**Percentage Contribution**

Rotational Speed (R)	12.862	4	3.2156	4.63	0.017	24.75
Feed Rate (F)	28.669	4	7.1673	10.33	0.001	55.175
Drill Point Angle (P)	2.101	4	0.5253	0.76	0.573*	4.043
Residual Error	8.328	12				16.02

* Parameter does not affect significantly

Estimation for Optimum Value:

To validate the results suggested by Taguchi optimization i.e. R1F1P1 (rotational speed: 600 rpm, feed rate: 10 mm/min, drill point angle: 60º). The equation (3.4) is used to predict the response value as per suggestion of Taguchi.

$$\boldsymbol{\mu_{DP1}} = \eta_m + \sum_{i=1}^{k}(\eta_{oi} - \eta_m)$$

$$\boldsymbol{\mu_{DP1}} = 5.803 + \{(4.597) - (5.803)\} + \{(3.957) - (5.803)\} + \{(5.440) - (5.803)\}$$

$$\boldsymbol{\mu_{DP1}} = 5.803 + \{(-1.206)\} + \{(-1.846)\} + \{(-0.363)\}$$

$$\boldsymbol{\mu_{DP1}} = (2.388)$$

Further, confidence interval (CI) has been measured using equation 3.5. The interval gives a range of percentage delamination of diameter in between the experimental result for optimal combination of parameters should be placed.

$$CI = \pm \sqrt{\frac{F_{\alpha(v1:v2)}\, V_e}{\psi_{eff.}}}$$

$F_{\alpha(v1:v2)}$ is the F-ratio at the confidence level of (1-α) against degrees of freedom (DOF) equal to 1 and error DOF (f_e). V_e = SS value of Error / DOF for Error, and $\psi_{eff.}$ = (no of experimental trails) / (1+ Total DOF – Error DOF).

$F_{\alpha(v1:v2)} = F_{0.05(1:12)} = 4.75$ (this value obtained from the F table with 95% confidence level)

V_e = SS value of Error / DOF for Error

= 8.328/12 = 0.694

ψ_{eff} = (no. of experimental trails) / (1+ Total DOF– Error DOF).

= 25/ (1+24 – 12) = 1.923

Using these values in equation 3.5, $CI = \pm 1.309$

Thus, the estimated thrust force value is: $\mu_{DP1} + CI < \boldsymbol{\mu_{DP1}} < \mu_{DP1} - CI$.

The experimental value for optimal force should be in between: $1.079 < \mu_{DP1} < 3.697$ and compared it with the experimental value in table 4.16.

Table 4.16: Result validation for percentage delamination in diameter for 1st group of experimentation

	Optimized process parameters	
	Predicted Range	Experimental Value
Optimal Combination	R1F1P1	R1F1P1
Dia Delamination (%age)	$1.079 < \mu_{DP1} < 3.697$	3.43

Comparative statement of diameter delamination with conventional bone drilling

The delamination in diameter for conventional drilled holes has been measured under the CMM and compares it with the delamination observed in case of holes drilled with ultrasonic assisted bone drilling technique. The comparative statement for all experimental combinations is shown in figure 4.8.

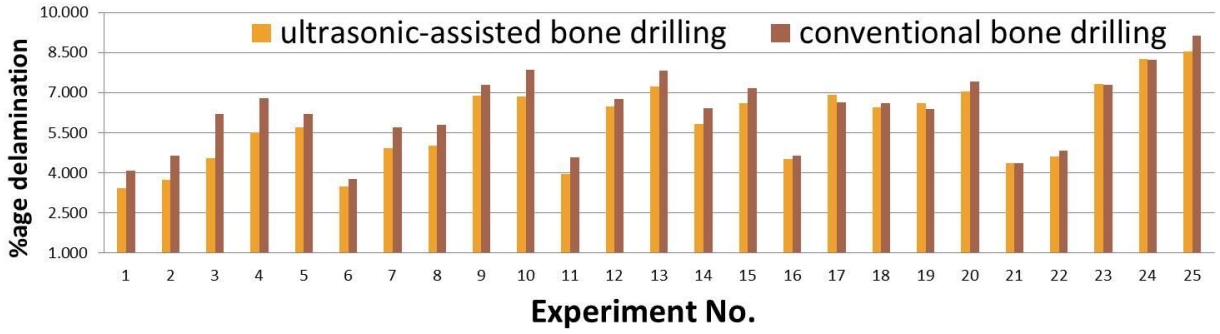

Figure 4.8: Comparative statement for delamination in diameter of conventional and ultrasonic-assisted bone drilling for 1st group of experimentation

4.2 OBSERVATION AND ANALYSIS FOR 2ND SET (HELIX ANGLE GROUP) OF EXPERIMENTATION

4.2.1 Heat generation

Heat generation during experimentation has been measured in terms of temperature rise during drilling. The drilling parameters involved in this experimentation are rotational speed, feed rate and drill helix angle. The temperature values should be minimum during drilling for better result output. Thus, smaller the better condition applicable for calculating S/N ratio (eqn 3.2). The measured temperature values and calculated S/N ratio with available L25 experimental combinations and listed in table 4.17.

Table 4.17: Heat generation and S/N ratio for ultrasonic-assisted bone drilling during 2nd group of experimentation

Sr No	Rotational Speed (R) (rpm)	Feed Rate (F) (mm/min)	Drill Helix Angle (H) (degree)	Max. Temperature Recorded				S/N Ratio
				T1 (°C)	T2 (°C)	T3 (°C)	Avg. Temp. (°C)	
1	600	10	12	52.4	52.0	52.2	52.2	-34.353
2	600	20	18	49.6	49.4	50.1	49.7	-33.927
3	600	30	24	47.2	48.5	47.7	47.8	-33.588
4	600	40	30	47.3	47.0	48.8	47.7	-33.570
5	600	50	36	46.1	46.3	46.0	46.1	-33.274
6	1200	10	18	54.8	54.0	54.7	54.5	-34.727
7	1200	20	24	52.0	52.7	52.8	52.5	-34.403
8	1200	30	30	52.4	52.9	51.0	52.1	-34.336
9	1200	40	36	56.7	57.1	56.4	56.7	-35.077
10	1200	50	12	59.8	60.3	59.8	60.0	-35.558
11	1800	10	24	53.0	53.9	54.8	53.9	-34.626
12	1800	20	30	55.3	55.0	55.5	55.3	-34.852
13	1800	30	36	59.4	59.9	59.0	59.4	-35.480
14	1800	40	12	64.3	63.8	63.8	64.0	-36.116
15	1800	50	18	61.6	61.0	61.4	61.3	-35.754
16	2400	10	30	56.3	56.3	56.3	56.3	-35.005
17	2400	20	36	57.6	57.0	57.4	57.7	-35.226
18	2400	30	12	64.9	64.7	65.0	64.9	-36.239
19	2400	40	18	62.1	63.0	62.0	62.4	-35.898

20	2400	50	24	65.9	65.6	65.3	65.6	-36.338
21	3000	10	36	52.5	52.0	53.0	52.5	-34.403
22	3000	20	12	62.0	61.6	61.8	61.8	-35.819
23	3000	30	18	64.6	64.8	64.2	64.5	-36.191
24	3000	40	24	66.0	66.2	66.7	66.3	-36.430
25	3000	50	30	67.3	67.6	67.2	67.4	-36.566

The mean value of temperature in drilling of bones, respective to each level of parameter is described as response values with respect to the each level and parameters shown in response table 4.18. The values from table 4.18 are used to plot the response curves respective to the each level of experimental parameters shown in figure 4.9.

Table 4.18: Response table for heat generation in 2nd group of experimentation

Parameters	**Response values of S/N ratio**					**Response values of Mean data**				
	L 1	**L 2**	**L 3**	**L 4**	**L 5**	**L1**	**L2**	**L3**	**L4**	**L5**
R	-33.74	-34.82	-35.37	-35.74	-35.88	48.70	55.16	58.78	61.36	62.49
F	-34.62	-34.85	-35.17	-35.42	-35.50	53.87	55.40	57.74	59.41	60.07
H	-35.62	-35.30	-35.08	-34.87	-34.69	60.56	58.48	57.21	55.74	54.50

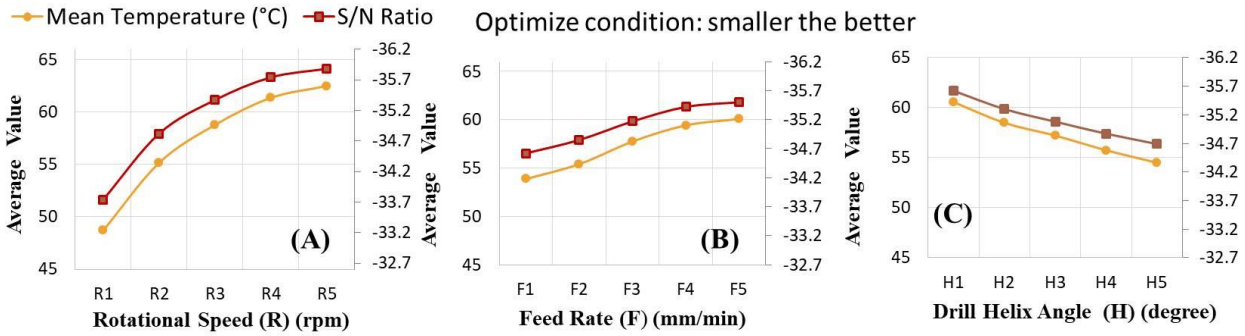

Figure 4.9: Response curves for heat generation during helix angle group of experimentation; (A) for rotational speed, (B) for feed rate, (C) for drill helix angle for 2nd set of experimentation

Analysis of variance (ANOVA)

Further, the mean values of temperature observed have been analyzed for the analysis of variance (ANOVA). The data obtained with calculation of equation (3.3) is shown in table 4.19. From ANOVA table 4.19, the rotational speed (R) shows the maximum contribution (64.132%) for heat generation duration the experimentation process. From the parameters, rotational speed (R) and feed rate (F) and drill helix angle (H) affects significantly ($P \leq 0.05$).

Table 4.19: ANOVA table for heat generation during 2nd group of experimentation

Source	**SS**	**DOF**	**Variance**	**F ratio**	**P value**	**Percentage Contribution**
Rotational Speed (R)	620.73	4	155.182	19.16	0.000	64.132
Feed Rate (F)	138.54	4	34.636	4.28	0.022	14.313
Drill Helix Angle (H)	111.40	4	27.850	3.44	0.043	11.509
Residual Error	97.21	12				10.04

Estimation for Optimum Value:

To validate the results suggested by Taguchi optimization i.e. R1F1H5 (rotational speed: 600rpm, feed rate: 10mm/min, drill helix angle: 36º). The equation (3.4) is used to predict the response value as per suggestion of Taguchi.

$$\boldsymbol{\mu_{TP2}} = \eta_m + \sum_{i=1}^{k}(\eta_{oi} - \eta_m)$$

$$\boldsymbol{\mu_{TP2}} = 57.298 + \{(48.70) - (57.298)\} + \{(53.87) - (56.448)\} + \{(54.50) - (56.448)\}$$

$$\boldsymbol{\mu_{TP2}} = 57.298 + \{(-8.598)\} + \{(-2.578)\} + \{(-1.948)\}$$

$$\boldsymbol{\mu_{TP2}} = (44.174)$$

Further, confidence interval (CI) has been measured using equation 3.5. The interval gives a range of temperature in between the experimental result for optimal combination of parameters should be placed.

$$CI = \pm \sqrt{\frac{F_{\alpha(v1:v2)}\, V_e}{\psi_{eff.}}}$$

$F_{\alpha(v1:v2)}$ is the F-ratio at the confidence level of (1-α) against degrees of freedom (DOF) equal to 1 and error DOF (f_e). V_e = SS value of Error / DOF for Error, and $\psi_{eff.}$ = (no of experimental trails) / (1+ Total DOF – Error DOF).

$F_{\alpha(v1:v2)} = F_{0.05(1:12)} = 4.75$ (this value obtained from the F table with 95% confidence level)

V_e = SS value of Error / DOF for Error

= 97.21/12 = 8.10

ψ_{eff} = (no. of experimental trails) / (1+ Total DOF– Error DOF).

= 25/ (1+24- 12) = 1.923

Using these values in equation 3.5, CI = $\pm$ 4.473

Thus, the estimated temperature value is: $\mu_{TP2} + CI < \boldsymbol{\mu_{TP2}} < \mu_{TP2} - CI$.

The experimental value for optimal temperature should be in between: 39.70 < $\boldsymbol{\mu_{TP2}}$ < 48.65 and compared it with the experimental value in table 4.20.

Table 4.20: Results validation for heat generation during 2nd group of experimentation

	Optimized process parameters	
	Predicted Range	Experimental Value
Optimal Combination	R1F1H5	R1F1H5
Temperature (°C)	39.70 < μ_{TP2} < 48.65	41.20 **°C**

Comparative statement of heat generation with conventional bone drilling

To justify the use of ultrasonic- assisted drilling in case of bone drilling process a comparative statement is developed with the conventional drilling process of bone drilling. From the comparison it is observed that the use of ultrasonic assisted drilling technique is an efficient way to control the temperature during bone drilling process. The comparative statement is shown in figure 4.10.

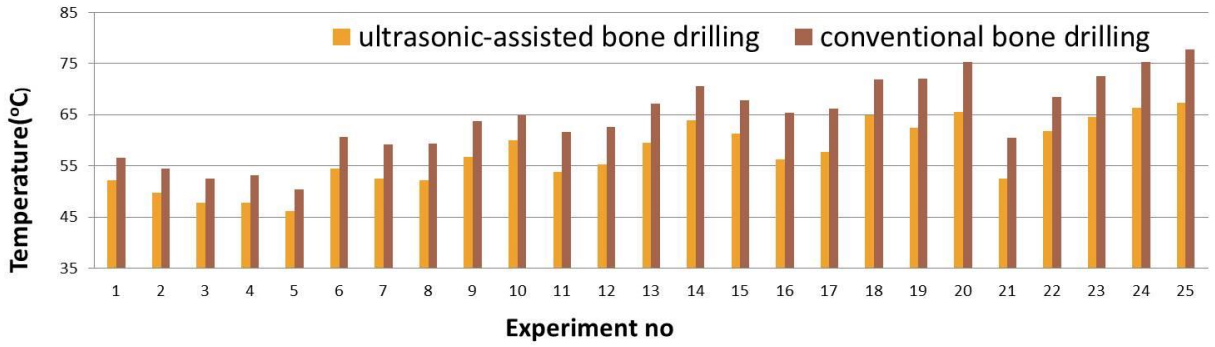

Figure 4.10: Comparative statement for heat generation during conventional and ultrasonic-assisted bone drilling for 2nd group of experimentation

4.2.2 Thrust force

Signal-to noise ratio

Thrust forces developed during drilling of bone were measured using dynamometer as described in section 3.5. Thrust forces developed during the experimentation were solved for the optimization of parameters. The forces should be minimum for better result output and causes less mechanical damage. Thus, smaller-the- better optimization condition (eqn 3. 2) used and signal-to noise ratio calculated is listed in table 4.21.

Table 4.21: Thrust forces and S/N ratio for ultrasonic-assisted bone drilling during 2nd group of experimentation

Sr No	Rotational Speed (R) (rpm)	Feed Rate (F) (mm/min)	Drill Helix Angle (H) (degree)	Thrust forces				S/N Ratio
				T1 (N)	T2 (N)	T3 (N)	Avg. Th Force (N)	
1	600	10	12	10.62	10.85	9.86	10.44	-20.37
2	600	20	18	10.12	10.39	10.24	10.25	-20.21
3	600	30	24	9.64	10.36	9.89	9.96	-19.96
4	600	40	30	9.2	8.77	9.43	9.1	-19.18

5	600	50	36	9.28	8.99	9.64	9.3	-19.36
6	1200	10	18	7.86	7.82	7.66	7.78	-17.81
7	1200	20	24	8.48	9.1	8.43	8.67	-18.76
8	1200	30	30	8.52	8.4	8.9	8.6	-18.69
9	1200	40	36	9.03	9.16	10.13	9.44	-19.49
10	1200	50	12	10.19	11.13	10.29	10.54	-20.45
11	1800	10	24	7.73	7.99	7.83	7.85	-17.89
12	1800	20	30	7.88	7.69	8.28	7.95	-18.00
13	1800	30	36	7.86	7.46	7.31	7.54	-17.54
14	1800	40	12	10.47	9.69	9.79	9.98	-19.98
15	1800	50	18	9.88	10.76	9.81	10.15	-20.12
16	2400	10	30	7.35	7.65	7.59	7.53	-17.53
17	2400	20	36	7.87	7.61	7.2	7.56	-17.57
18	2400	30	12	8.38	9.2	8.64	8.74	-18.83
19	2400	40	18	8.1	8.1	7.9	8.05	-18.11
20	2400	50	24	9.01	8.91	8.93	8.95	-19.03
21	3000	10	36	6.81	7.18	6.89	6.96	-16.85
22	3000	20	12	7.37	7.4	7.52	7.43	-17.41
23	3000	30	18	7.94	8.1	7.83	7.96	-18.01
24	3000	40	24	7.69	7.76	7.5	7.65	-17.67
25	3000	50	30	8.21	8.14	8.4	8.25	-18.32

The response table for signal-to-noise ratio and mean data respective to the individual set of parameters is shown in table 4.22. On the basis of these values response curves is plotted shown in figure 4.11.

Table 4.22: Response table for S/N ratio and mean values corresponding to individual parameters for thrust forces

Parameters	Response values of S/N ratio					Response values of Mean data				
	L 1	L 2	L 3	L 4	L 5	L1	L2	L3	L4	L5
R	-19.82	-19.05	-18.71	-18.22	-17.66	10.16	9.81	9.00	8.69	8.16
F	-18.10	-18.39	-18.61	-18.89	-19.46	8.11	8.37	8.56	8.84	9.43
H	-19.41	-18.86	-18.67	-18.35	-18.17	9.42	8.83	8.61	8.28	8.16

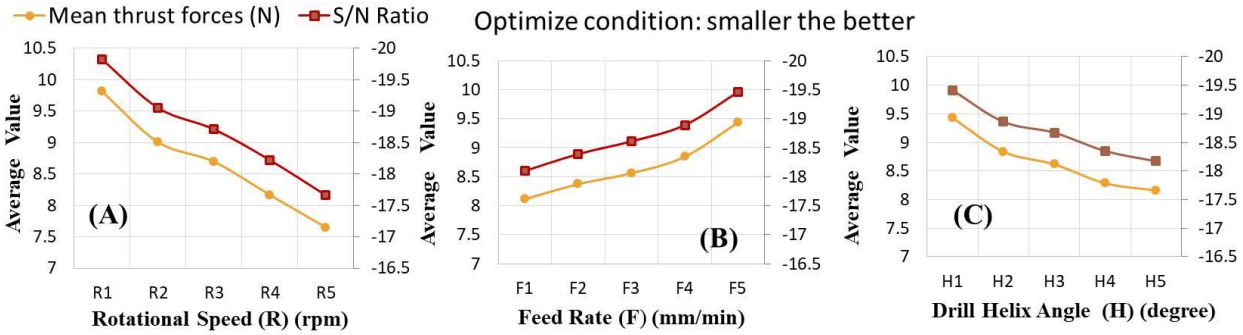

Figure 4.11: Response curves respective to the input parameters for thrust forces; (A) for rotational speed; (B) for feed rate; (C) for drill helix angle for 2nd group of experimentation

Analysis of variance (ANOVA)

Further, the mean data of thrust forces has been analyzed for the analysis of variance (ANOVA). The data obtained with calculation of equation (3.3) is shown in table 4.23. From ANOVA table

4.23, the rotational speed(R) shows the maximum contribution (64.13%) in thrust forces during the experimentation process and all parameters affects significantly (P≤0.05).

Table 4.23: ANOVA table for thrust force during 2nd group of experimentation

Source	SS	DOF	Variance	F-ratio	P-value	Percentage Contribution
Rotational Speed (R)	13.53	4	3.384	8.89	0.001	47.78
Feed Rate (F)	5.16	4	1.290	3.39	0.045	18.22
Drill Helix Angle (H)	5.05	4	1.262	3.32	0.048	17.83
Residual Error	4.56	12				16.05

Estimation for Optimum Value:

To validate the results suggested by Taguchi optimization i.e. R5F1H5 (rotational speed: 3000rpm, feed rate: 10mm/min, drill helix angle: 36º). The equation (3.4) is used to predict the response value as per suggestion of Taguchi and compared it with the result observed experimentally in table 4.24.

$$\boldsymbol{\mu_{FP2}} = \eta_m + \sum_{i=1}^{k}(\eta_{oi} - \eta_m)$$

$$\boldsymbol{\mu_{FP2}} = 8.662 + \{(7.650) - (8.662\} + \{(8.112) - (8.662)\} + \{(8.160) - (8.662\}$$

$$\boldsymbol{\mu_{FP2}} = 8.662 + \{(-1.012)\} + \{(-0.55)\} + \{(-0.502)\}$$

$$\boldsymbol{\mu_{FP2}} = (6.598)$$

Further, confidence interval (CI) has been measured using equation 3.5. The interval gives a range of thrust force in between the experimental result for optimal combination of parameters should be placed.

$$CI = \pm \sqrt{\frac{F_{\alpha(v1:v2)}\, V_e}{\psi_{eff.}}}$$

$F_{\alpha(v1:v2)}$ is the F-ratio at the confidence level of (1-α) against degrees of freedom (DOF) equal to 1 and error DOF (f_e). V_e = SS value of Error / DOF for Error, and $\psi_{eff.}$ = (no of experimental trails) / (1+ Total DOF – Error DOF).

$F_{\alpha(v1:v2)} = F_{0.05(1:12)} = 4.75$ (this value obtained from the F table with 95% confidence level)

V_e = SS value of Error / DOF for Error

= 4.56/12 = 0.38

ψ_{eff} = (no. of experimental trails) / (1+ Total DOF– Error DOF).

= 25/ (1+24- 12) = 1.923

Using these values in equation 3.5, $CI = \pm 0.968$

Thus, the estimated thrust force value is: $\mu_{FP2} + CI < \boldsymbol{\mu_{FP2}} < \mu_{FP2} - CI$.

The experimental value for optimal force should be in between: $5.63 < \boldsymbol{\mu_{FP2}} < 7.56$ and compared it with the experimental value in table 4.24.

Table 4.24: Result validation for thrust force for 2nd group of experimentation

	Optimized process parameters	
	Predicted Range	Experimental Value
Optimal combination	R5F1H5	R5F1H5

Thrust forces (N)	$5.63 < \mu_{FP2} < 7.56$	6.96 N

Comparative statement for thrust forces with conventional bone drilling

Thrust forces during bone drilling should be lower to maintain the lower mechanical damage to the drilled hole surrounding. Ultrasonic assisted bone drilling shows its remarkable effectiveness in order to control the thrust forces during drilling. While comparing it with the forces developed during the conventional drilling process a significant difference is recorded and benefits of ultrasonic assisted bone drilling process is illustrated. A comparative statement is shown in figure 4.12.

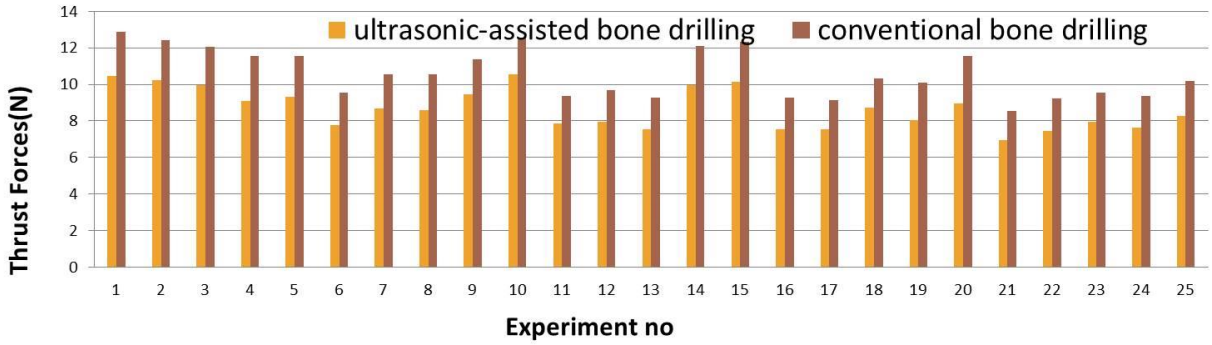

Figure 4.12: Comparative statement for thrust forces during conventional and ultrasonic-assisted bone drilling for 2nd group of experimentation

4.2.3 Axial pullout force

Signal-to-Noise

Drilled holes in bones were subjected to fix the implants by the means of cortical screws. To justify the reason, fixation of screw to the drilled holes and tested for maximum axial pullout force up to which bone screw joint can withstand before failure. (as described in section 3.10). The values recorded in newton (N) and listed in table 4.25. The axial pullout force of bone screw

joint should be maximum. Thus, the optimize condition used to calculate the S/N ratio is larger-the-better i.e. equation 3.1 in section 3.11.7.

Table 4.25: Maximum axial pullout force and S/N ratio for ultrasonic-assisted bone drilling during 2nd group of experimentation

Sr No	Rotational Speed (R) (rpm)	Feed Rate (F) (mm/min)	Drill Helix Angle (H) (degree)	Maximum axial pullout force (N)	S/N Ratio
1	600	10	12	730	57.2665
2	600	20	18	740	57.3846
3	600	30	24	775	57.7860
4	600	40	30	795	58.0073
5	600	50	36	782	57.8641
6	1200	10	18	934	59.4069
7	1200	20	24	835	58.4337
8	1200	30	30	860	58.6900
9	1200	40	36	778	57.8196
10	1200	50	12	686	56.7265
11	1800	10	24	940	59.4626
12	1800	20	30	910	59.1808
13	1800	30	36	1015	60.1293
14	1800	40	12	735	57.3257
15	1800	50	18	745	57.4431
16	2400	10	30	1025	60.2145
17	2400	20	36	998	59.9826

18	2400	30	12	795	58.0073
19	2400	40	18	854	58.6292
20	2400	50	24	796	58.0183
21	3000	10	36	1054	60.4568
22	3000	20	12	1014	60.1208
23	3000	30	18	865	58.7403
24	3000	40	24	895	59.0365
25	3000	50	30	867	58.7604

The mean value of maximum axial pullout force respective to each level of parameter is described as response values with respect to the each level and parameters shown in response table 4.26 for axial pullout force. The values from table 4.26 are used to plot the response curves respective to the each level of experimental parameters shown in figure 4.13.

Table 4.26: Response table for axial pullout force measured for 2nd group experimentation

Parameters	**Response values of S/N ratio**					**Response values of Mean data**				
	L 1	**L 2**	**L 3**	**L 4**	**L 5**	**L1**	**L2**	**L3**	**L4**	**L5**
R	57.66	58.22	58.71	58.97	59.42	764.4	818.6	869.0	893.6	939.0
F	58.36	59.02	58.67	58.16	57.76	936.6	899.4	862.0	811.4	775.2
H	57.89	58.32	58.55	58.97	58.25	792.0	827.6	848.2	891.4	925.4

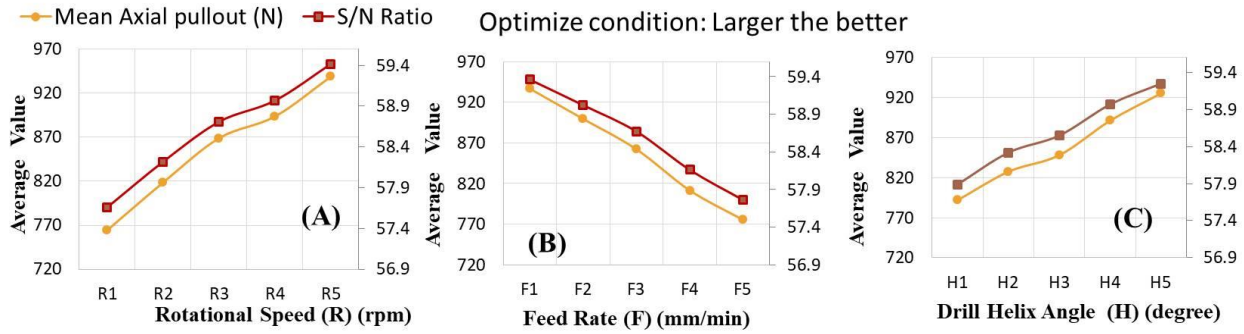

Figure 4.13: Response curves respective to each level for axial pullout force; (A) for rotational speed, (B) for feed rate, (C) for drill helix angle for 2nd group of experimentation

Analysis of variance (ANOVA)

Further, the mean data of axial pullout force has been analyzed for the analysis of variance (ANOVA). The data obtained with calculation of equation (3.3) is shown in table 4.27. From ANOVA table 4.27, the rotational speed(R) shows the maximum contribution (70.10%) for maximum axial pullout force during the pullout testing of bone-screw joint and all parameters affects significantly ($P \leq 0.05$).

Table 4.27: ANOVA table for maximum axial pullout force of bone-screw joint for 2nd group of experiment

Source	SS	DOF	Variance	F ratio	P value	Percentage Contribution
Rotational Speed (R)	91284	4	22821	6.90	0.004	33.71
Feed Rate (F)	84647	4	21162	6.40	0.005	31.26
Drill Helix Angle (H)	55143	4	13786	4.17	0.024	20.36
Residual Error	39675	12				14.65

Estimation for Optimum Value:

To validate the results suggested by Taguchi optimization i.e. R5F1H5 (rotational speed: 3000rpm, feed rate: 10mm/min, drill helix angle: 36º). The equation (3.4) is used to predict the response value as per suggestion of Taguchi and compared it with the result observed experimentally in table 4.28.

$$\boldsymbol{\mu_{Ap2}} = \eta_m + \sum_{i=1}^{k}(\eta_{oi} - \eta_m)$$

$$\boldsymbol{\mu_{Ap2}} = 856.92 + \{(939.0) - (856.92)\} + \{(936.6) - (856.92)\} + \{(925.4) - (856.92\}$$

$$\boldsymbol{\mu_{Ap2}} = 856.92 + \{(82.08)\} + \{(79.68)\} + \{(68.48)\}$$

$$\boldsymbol{\mu_{Ap2}} = (1087.16)$$

Further, confidence interval (CI) has been measured using equation 3.5. The interval gives a range of axial pullout force in between the experimental result for optimal combination of parameters should be placed.

$$CI = \pm \sqrt{\frac{F_{\alpha(v1:v2)}\, V_e}{\psi_{eff.}}}$$

$F_{\alpha(v1:v2)}$ is the F-ratio at the confidence level of (1-α) against degrees of freedom (DOF) equal to 1 and error DOF (f_e). V_e = SS value of Error / DOF for Error, and $\psi_{eff.}$ = (no of experimental trails) / (1+ Total DOF – Error DOF).

$F_{\alpha(v1:v2)} = F_{0.05(1:12)} = 4.75$ (this value obtained from the F table with 95% confidence level)

V_e = SS value of Error / DOF for Error

= 39675/12 = 3306.25

ψ_{eff} = (no. of experimental trails) / (1+ Total DOF– Error DOF).

= 25/ (1+24- 12) = 1.923

Using these values in equation 3.5, $CI = \pm 90.37$

Thus, the estimated thrust force value is: $\mu_{AP2} + CI < \boldsymbol{\mu_{AP2}} < \mu_{AP2} - CI$.

The experimental value for optimal force should be in between: 996.79 < $\boldsymbol{\mu_{AP2}}$ < 1177.53 and compared it with the experimental value in table 4.28.

Table 4.28: Result validation for axial pullout of bone screw joint for 2nd group of experimentation

	Optimized process parameters	
	Predicted Value	Experimental Value
Optimal combination	R5F1H5	R5F1H5
Axial Pullout Force (N)	996.79 < μ_{Ap2} < 1177.53	1054 N

Comparative statement for axial pullout force with conventional bone drilling

The drilled use to fix the cortical screws and the anchorage force of screws fixed in them is measured as axial pullout force of bone screw joint. The force of conventionally drilled holes is compared with the ultrasonic assisted drilled holes screw joint and observed that the drilled holes with ultrasonic assisted drilling technique has more axial pullout force as compared to conventional drilled bone screw joints. For comparison, five specimens has been selected having

different feed rate and a significant difference has been observed for axial pullout force of bone screw joint shown in figure 4.14.

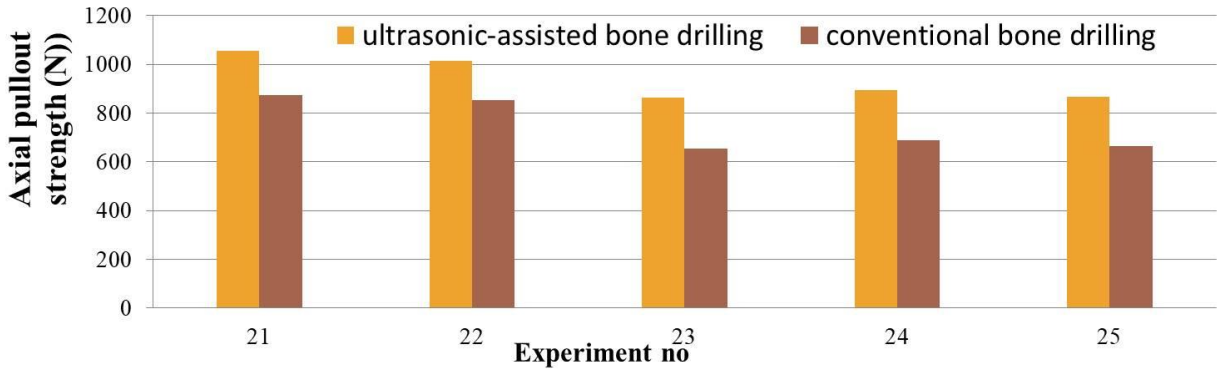

Figure 4.14: Comparative statement for axial pullout force for conventional and ultrasonic-assisted bone drilling for 2nd group of experimentation

4.2.4 Drilled hole diameter delamination

Signal-to-noise

The delamination in drilled holes under the 2nd group of experimentation (Helix angle group) is measured under CMM and observations listed in the table 4.29. The delamination should be minimum to maintain the required symmetry. Thus, smaller-the-better (eqn 3.2) condition applied for calculating the signal-to-noise ratio. The calculated values respective to the experimental condition is listed in table 4.29.

Table 4.29: Delamination of diameter observed and S/N ratio for drilled holes for 2nd group of experiments

Sr No	Rotational Speed (R) (rpm)	Feed Rate (F) (mm/min)	Drill Helix Angle (H) (degree)	Diametric Delamination (%age)	S/N Ratio
1	600	10	12	4.3812	-12.8320

2	600	20	18	4.9437	-13.8811
3	600	30	24	5.6344	-15.0169
4	600	40	30	5.0719	-14.1034
5	600	50	36	7.0000	-16.9020
6	1200	10	18	5.4531	-14.7329
7	1200	20	24	5.8844	-15.3940
8	1200	30	30	5.6625	-15.0602
9	1200	40	36	7.5719	-17.5841
10	1200	50	12	10.1031	-20.0891
11	1800	10	24	6.1781	-15.8171
12	1800	20	30	7.7594	-17.7965
13	1800	30	36	8.2594	-18.3389
14	1800	40	12	10.1031	-20.0891
15	1800	50	18	10.4875	-20.4134
16	2400	10	30	7.8063	-17.8488
17	2400	20	36	6.8125	-16.6661
18	2400	30	12	10.7937	-20.6634
19	2400	40	18	11.9125	-21.5201
20	2400	50	24	12.3469	-21.8311
21	3000	10	36	7.2812	-17.2441
22	3000	20	12	11.8562	-21.4789
23	3000	30	18	11.9719	-21.5632
24	3000	40	24	12.2594	-21.7694
25	3000	50	30	12.3219	-21.8135

The mean value of diameter delamination respective to each level of parameter is described as response values with respect to the each level and parameters shown in response table 4.30. The values from table 4.30 are used to plot the response curves respective to the each level of experimental parameters shown in figure 4.15.

Table 4.30: Response table for diameter delamination observed in 2nd group of experimentation

Parameters	Response values of S/N ratio					Response values of Mean data				
	L 1	L 2	L 3	L 4	L 5	L1	L2	L3	L4	L5
R	-14.55	-16.57	-18.49	-19.71	-20.77	5.406	6.935	8.557	9.934	11.138
F	-15.69	-17.04	-18.13	-19.01	-20.21	6.220	7.451	8.464	9.384	10.452
H	-19.03	-18.42	-17.97	-17.32	-17.35	9.447	8.954	8.561	7.724	7.385

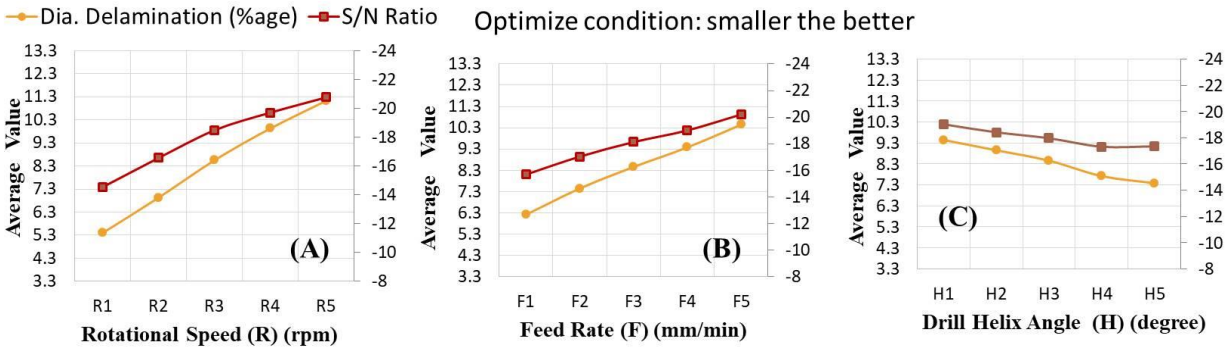

Figure 4.15: Response curves respective to each level for diameter delamination; (A) for rotational speed, (B) for feed rate, (C) for drill helix angle for 2nd group of experimentation

Analysis of variance (ANOVA)

Further, the mean data of percentage delamination of diameter has been analyzed for the analysis of variance (ANOVA). The data obtained with calculation of equation (3.3) is shown in table

4.31. From ANOVA table 4.31, the rotational speed(R) shows the maximum contribution (70.10%) for delamination in drilled hole during the bone drilling experiment and all parameters affects significantly (P≤0.05).

Table 4.31: ANOVA table for delamination in diameter for 2nd group of experimentation

Source	**SS**	**DOF**	**Variance**	**F ratio**	**P value**	**Percentage Contribution**
Rotational Speed (R)	104.92	4	26.23	47.12	0.000	58.211
Feed Rate (F)	54.17	4	13.54	24.33	0.000	30.05
Drill Helix Angle (H)	14.47	4	3.61	6.50	0.005	8.02
Residual Error	6.68	12				3.70

Estimation for Optimum Value:

To validate the results suggested by Taguchi optimization i.e. R1F1H5 (rotational speed: 3000rpm, feed rate: 10mm/min, drill helix angle: 36º) equation (3.4) is used to predict the response value as per suggestion of Taguchi and compared it with the result observed experimentally in table 4.32.

$$\Psi_p = \eta_m + \sum_{i=1}^{k} (\eta_{oi} - \eta_m)$$

$$\Psi p = 8.394 + \{(5.406) - (8.394)\} + \{(6.220) - (8.394)\} + \{(7.385) - (8.394)\}$$

$$\Psi p = 8.394 + \{(-2.988)\} + \{(-2.1742)\} + \{(-1.0092)\}$$

$$\Psi p = (2.222)$$

Further, confidence interval (CI) has been measured using equation 3.5. The interval gives a range of percentage delamination of diameter in between the experimental result for optimal combination of parameters should be placed.

$$CI = \pm \sqrt{\frac{F_{\alpha(v1:v2)}\, V_e}{\psi_{eff.}}}$$

$F_{\alpha(v1:v2)}$ is the F-ratio at the confidence level of (1-α) against degrees of freedom (DOF) equal to 1 and error DOF (f_e). V_e = SS value of Error / DOF for Error, and $\psi_{eff.}$ = (no of experimental trails) / (1+ Total DOF – Error DOF).

$F_{\alpha(v1:v2)} = F_{0.05(1:12)} =$ 4.75 (this value obtained from the F table with 95% confidence level)

V_e = SS value of Error / DOF for Error

= 6.68/12 = 0.556

ψ_{eff} = (no. of experimental trails) / (1+ Total DOF– Error DOF).

= 25/ (1+24 – 12) = 1.923

Using these values in equation 3.5, $CI = \pm$ 1.172

Thus, the estimated thrust force value is: $\mu_{DP2} + CI < \boldsymbol{\mu_{DP2}} < \mu_{DP2} - CI$.

The experimental value for optimal force should be in between: 1.05 < $\boldsymbol{\mu_{DP2}}$ < 3.39 and compared it with the experimental value in table 4.32.

Table 4.32: Result validation for diameter delamination of 2nd group of experimentation

	Optimized process parameters	
	Predicted Range	Experimental Value
Optimal combination	R1F1H5	R1F1H5
Dia delamination (%age)	$1.05 < \mu_{DP2} < 3.39$	3.21

Comparative statement for diameter delamination with conventional bone drilling

Delamination in diameter using conventional bone drilling is observed and compared with the delamination caused in ultrasonic assisted bone drilling process. From comparison, the effect of ultrasonic assisted bone drilling technique in terms of minimizing the delamination of diameter is observed. The comparison of delamination is shown in figure 4.16.

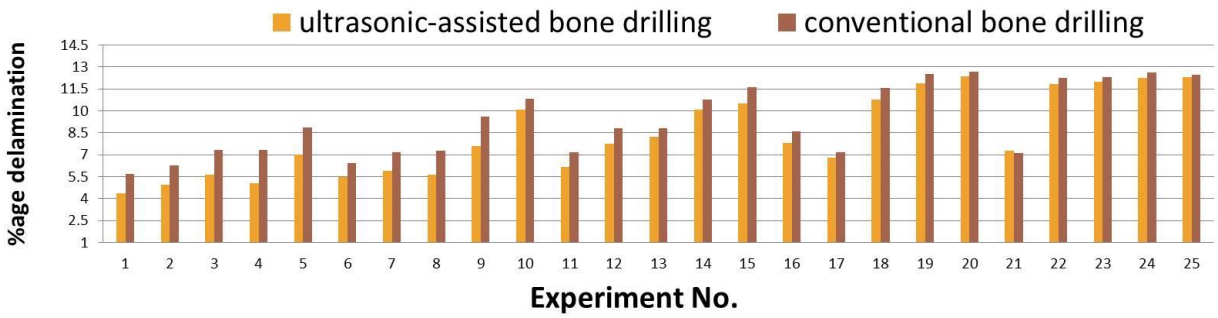

Figure 4.16: Comparative statement for delamination in diameter for conventional and ultrasonic-assisted bone drilling for 2nd group of experimentation

4.3 HISTOPATHOLOGY STUDY

In order to understand the behavior of bone cells under the effect of heat generation the histopathology of bone specimens were carried out as described in section 3.9. The bone specimens sliced and follow the declination process. Prepared specimens observed under the microscopic study and behavior of cells observed in terms of lacunas conditions with the

osteocytes. In first attempt the behavior of temperature has been studied by selecting the five different specimens exposed to different temperature range during the experimentation.

4.3.1 Effect of temperature on morphology of bone

The selected specimen from helix angle group as described in table 4.33.

Table 4.33: Specimens selected for histopathology

Experimental Trial no.	Temperature Recorded (ºC)
5	46.1 ºC
8	52.1 ºC
16	56.27 ºC
22	61.8 ºC
25	67.35 ºC

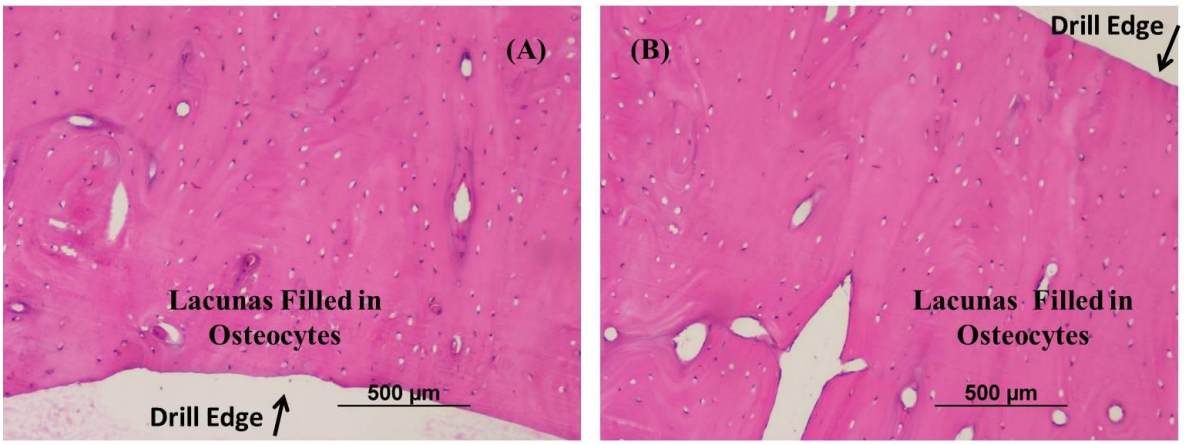

Figure 4.17(A&B): Histogram of sample 5; temperature during drilling recorded: 46.1ºC

Figure 4.17(A&B), show the histogram of bone sample drilled with drilling condition 5. The temperature recorded during drilling was lowest among the all drilling conditions (T= 46.1ºC).

The histogram images were taking around the drill site and found that at this temperature elevation lacunae found filled near the drill site as well as far away from the drill site. There is no damage recorded at this temperature osteocytes were found filled in the both images. Images also justify that the threshold temperature limit for osteonecrosis is below 47 ºC in cortical bones.

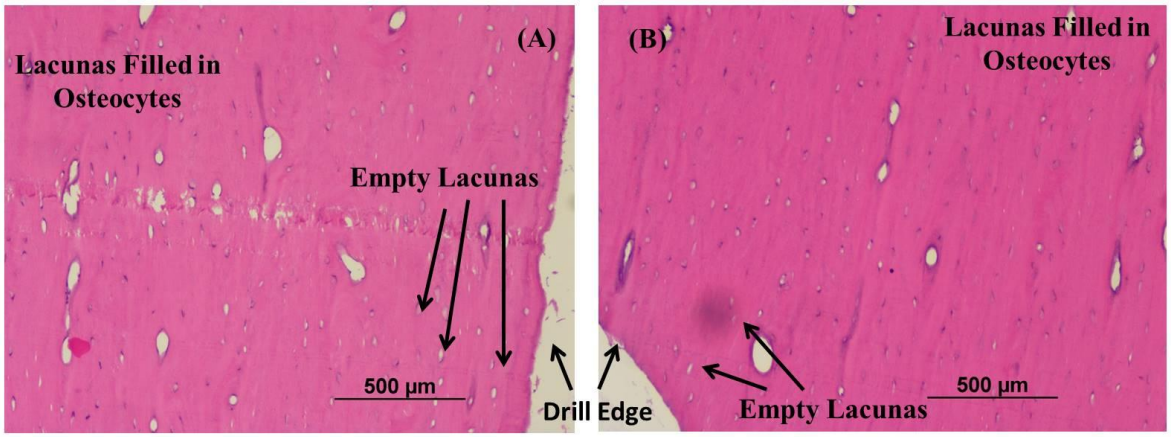

Figure 4.18(A&B): Histogram of sample 8; temperature during drilling recorded: 52.1ºC

Figure 4.18 (A&B) show the histogram of drilled sample no 8. The maximum temperature recorded during this experiment was 52.1ºC i.e. just exceeding the threshold limit of osteonecrosis. The morphology of bone in this specimen shows that there are few lacunas which get evaporated near the drill site. Histogram of bone on both sides of drill shows that around 400-500µm distance was affected in this experiment. Some lacunas in this region were found in transition stage while the lacunas present outside this range are unaffected.

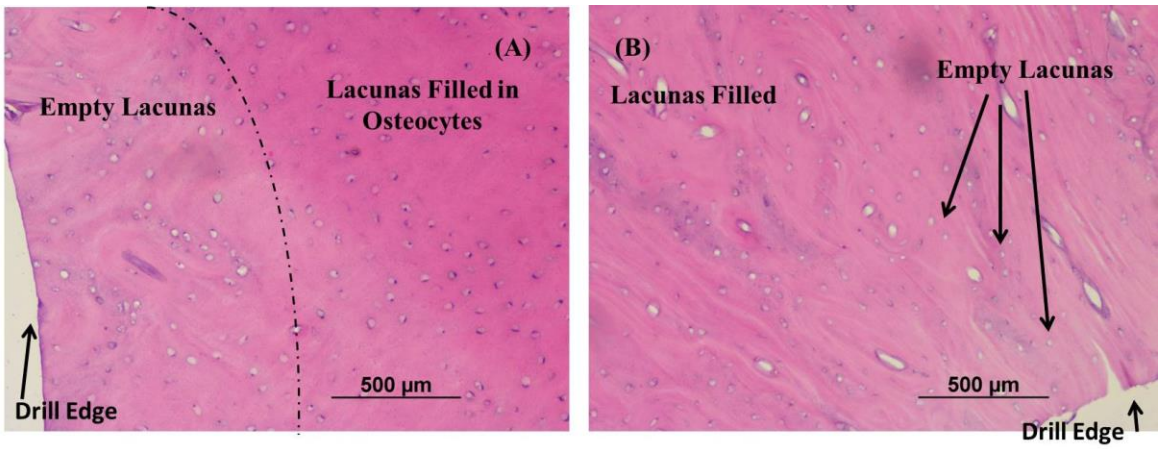

Figure 4.19 (A&B): Histogram of sample 16; temperature during drilling recorded: 56.3ºC

Figure 4.19 (A&B) shows the morphology of drilled sample no 16, having maximum temperature rised during drilling was 56.27ºC. Morphology of this sample was analyzed around the drill site and found that the damage in this sample is more than the previous one (in figure 4.19 (A&B). The damage observed in this sample is due to excessive heat generation i.e. 56.3ºC. The damage in this site illustrated with a margin line in figure 4.19A. Within this region, the damage is done due to heat absorption and lacunas found empty. Outside this region most of the lacunas are partially filled which shows that the damage range in this sample is higher. Very few lacunas away from the drill site were found live in this case.

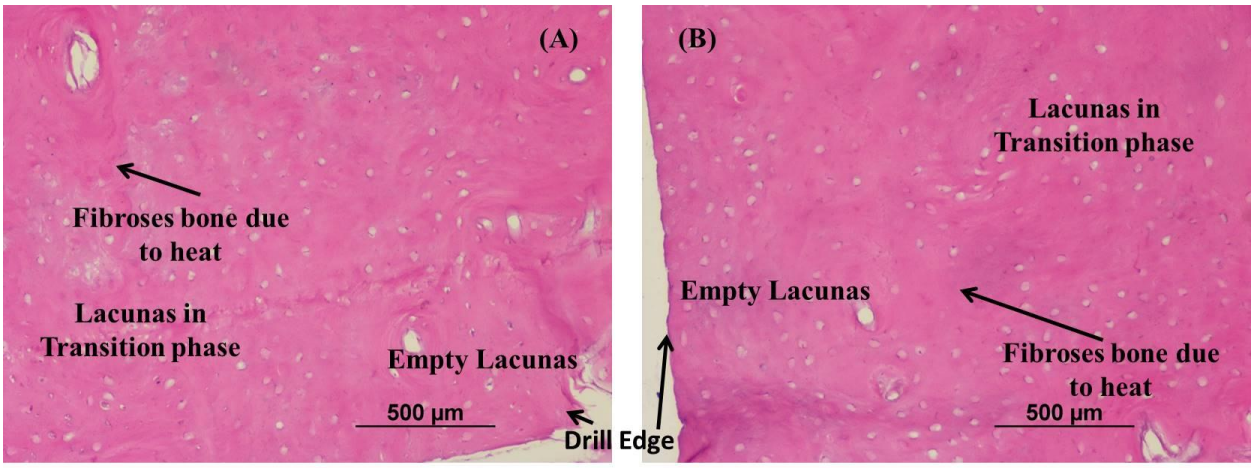

Figure 4.20(A&B): Histogram of sample 22; temperature during drilling recorded: 61.8ºC

Figure 4.20 (A&B) shows the morphology observation of drilled sample no.22 where maximum temperature recorded during drilling was 61.8ºC. The morphology of this specimen clearly evident the effect of heat absorption and most of the lacunas were observed empty. Some section of bone was observed like fibroses i.e. permanent damage to tissues. Few lacunas away from the drill site are partially filled, but 90 % damage has been already done which is unrecoverable in terms of tissue lose.

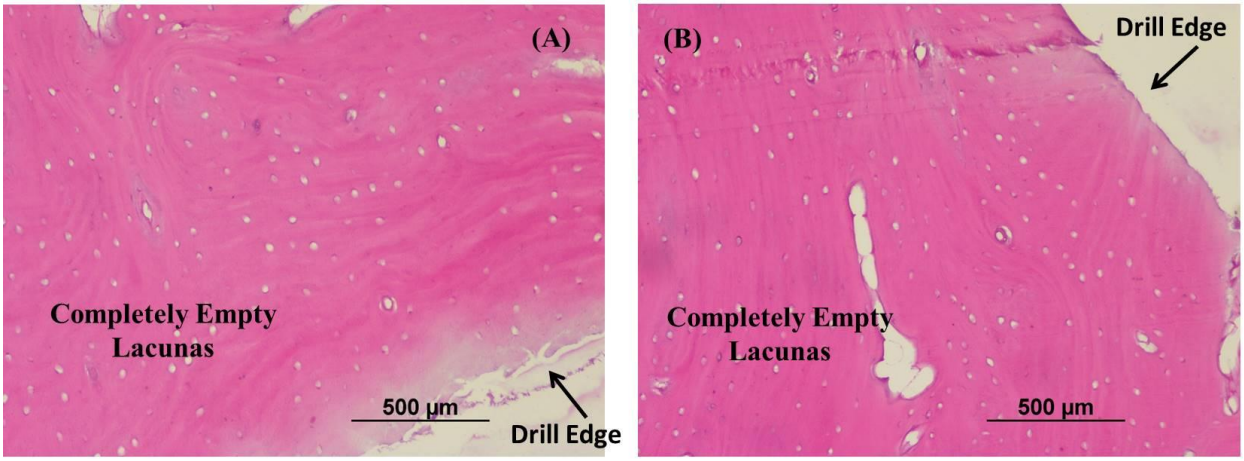

Figure 4.21(A&B): Histogram of sample 25; temperature during drilling recorded: 67.3ºC

Figure 4.21(A&B) shows the histogram images of drilled sample 25 and temperature recorded in this drilling experimentation was 67.35ºC. Images A &B in this figure show either sides of the drilled specimen. From images it was observed that around the drill site all lacunas were empty in images it is clearly evident that this high temperature elevation will leads to the maximum damage to the drill site and bone will get complete osteonecrosis.

4.3.2 Comparative histopathology

In order to observe the effect of ultrasonic-assisted bone drilling(UABD) process over the conventional bone drilling (CBD) process comparative histopathology of bones specimens has been made. Five experimental specimens were selected for histopathology one from each

category of rotational speed. Experiment 1, 6, 11, 16 and 25 has been selected for the histopathology which shows the wide range of heat generation for ultrasonic-assisted and conventional drilling of bone experimental process.

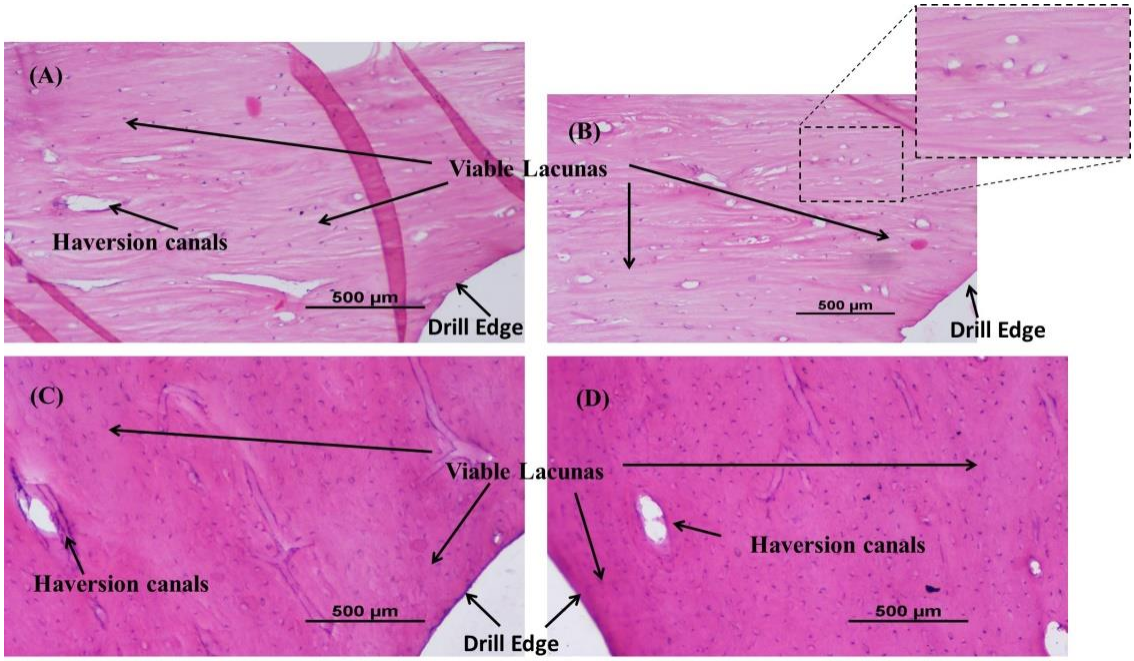

Figure 4.22(A, B, C&D): Histopathology of UAB drilling (A&B)(Temp: 42.5ºC) and conventional drilling(C&D)(Temp: 46.7ºC) of specimens from Experiment 1 : Point angle group

Figure 4.22 shows the morphology of specimens collected from experiment 1 having parameters at this experimental level are rotational speed 600 rpm, feed rate 10 mm/min and drill point angle is 60 degree. All biopsy images in figure 4.22 are at 100X magnification. From morphological image, it is clear that bony trabaculae having almost all viable lacunae near as well as far from the drill site. From figure 4.22, Images A &B are biopsy images of ultrasonic-assisted drilling specimen and images C & D are biopsy images received from conventional drilled specimens. From these images, it is observed that there is no osteonecrosis at this experimental level in both

of cases. The experimental results also shows maximum temperature is less than 47º C, which indicated that at this temperature osteocytes does not get damaged.

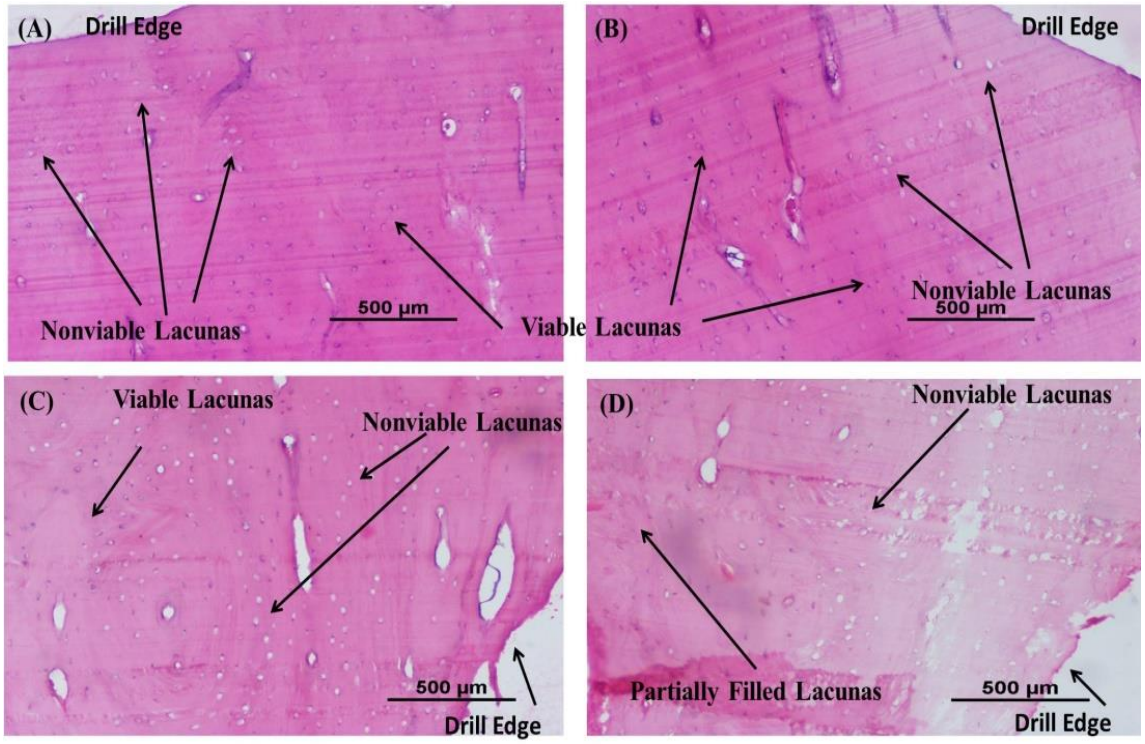

Figure 4.23(A,B,C & D): Histopathology of UAB drilling(A&B) (Temp: 49.9ºC) and conventional drilling(C&D)(Temp: 54.3ºC) of specimens from Experiment 6: point angle group

Figure 4.23 shows the morphology of specimens from experiment no 6 (Point angle group), drilling with rotational speed 1200 rpm, feed rate 10 mm/min and 80º drill point angle. Image A & B are the biopsy images received from the ultrasonic-assisted drilling specimen and images C&D are the images received from conventional drilling specimen. While comparing these images, the effect of ultrasonic-assisted drilling is clearly visible. Image A & B shows less damage as compared to the damage in image C & D. In image A & B we can see the osteonecrosis around drill site up to distance of 500-700µm beyond this most of lacunae are viable. While in case of conventional drilling, image C & D of figure 4.23 shows more damage

and very few lacunas are found viable. A few lacunas are partially viable which are around more than 1000µm from the drill site. This comparative statement shows the importance of Ultrasonic-assisted drilling at this experimental condition.

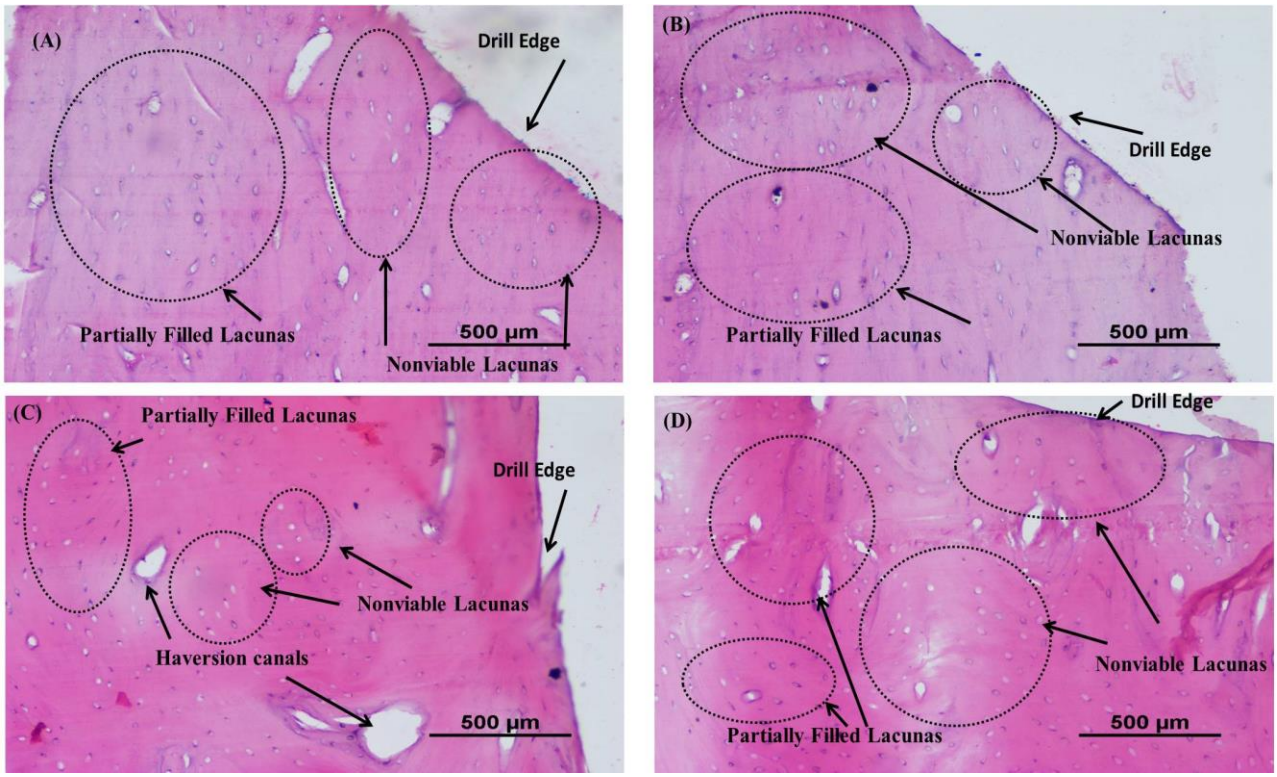

Figure 4.24(A,B,C & D): Histopathology of UAB drilling(A&B) (Temp: 56.7ºC) and conventional drilling(C&D) (Temp : 63.2ºC)of specimens from Experiment 11: Point angle group

In next comparison, figure 4.24 shows the morphology of experiment 11, drilling with rotational speed 1800 rpm, feed rate 10mm/min and 100 º drill point angle. In figure 4.15, Image A & B shows the biopsy images of ultrasonic-assisted drilling. It shows more damaged area in the images as compared to the images of experiment 6. Moreover, it is also evident that there is more necrosis observed in conventional drilling(C&D) as compared to ultrasonic-assisted

drilling(A&B). In case of ultrasonic-assisted drilling(image A&B) it is seen that after 700µm some space is having partially viable lacunas, While in case of conventional drilling very few lacunas are found viable. From experimental results, it is also clear that the temperature rise in case of ultrasonic-assisted drilling is less as compared to conventional drilling.

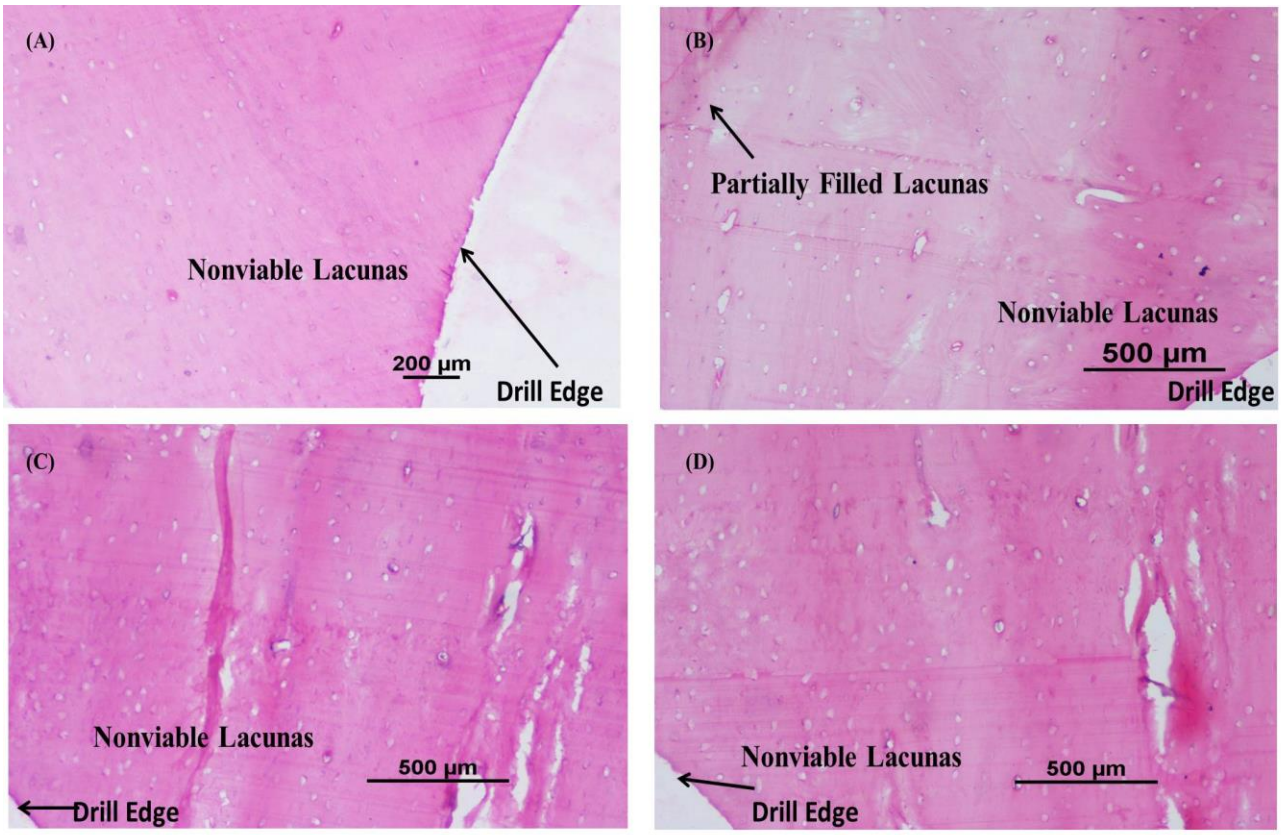

Figure 4.25(A,B,C & D): Histopathology of UAB drilling(A&B) (Temp: 58.1ºC) and conventional drilling(C&D)(Temp : 66.1ºC) of specimens from Experiment 16: point angle group

Figure 4.25 shows the morphology of experiment 16, drilling with rotational speed 2400rpm, 10mm/min and 120º drill point angle. It shows extensively damaged area in biopsy images of ultrasonic-assisted as well as conventional drilling method. For ultrasonic-assisted drilling,

image (B) shows very few lacunas are found partially viable which are very less as compared to biopsies received from experiment no 11. In image (C&D), the amount of partially viable lacunas is again less as compared to ultrasonic-assisted drilled specimen of same experiment.

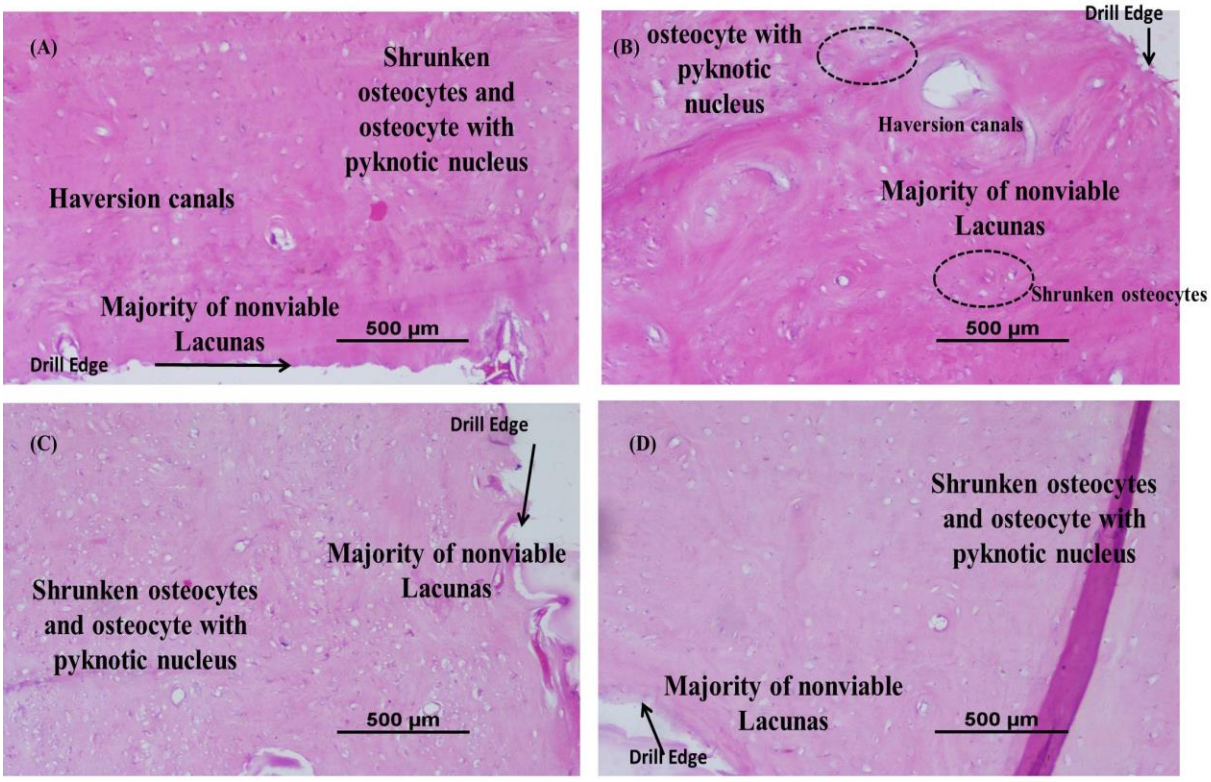

Figure 4.26(A,B,C&D): Histopathology of UAB drilling(A&B) (Temp:67.4ºC) and conventional drilling(C&D)(Temp : 78.2 ºC) of specimens from Experiment 25: Point angle group

Figure 4.26(A,B,C &D) shows the morphology of experiment 25, biopsy images show that there is massive thermal loss in this experimental combination of parameters i.e. rotational speed 3000 rpm, feed rate 50 mm/min and 120º drill point angle. The temperature at this combination of parameters is 67.4ºC for ultrasonic-assisted drilling and 78.2ºC for conventional drilling, which is very high from the threshold limit. From biopsy examination, it is evident that all lacunas get evaporated due to high temperature. The experimental results also verified that at this temperature the thermal damage in term of necrosis is very high.

4.4 SCANNING ELECTRON MICROSCOPY (SEM)

The behavior of cutting forces on surface of drilled holes has been studied with the help of surface topography of drilled hole specimens observed under scanning electron microscopy (SEM). The surface chosen for scanning electron microscopy of the bone specimens are the inner surface of the drilled hole which is shown in figure 3.10 a schematic representation of the surface taken for SEM is shown in figure 4.27. The effect of forces on surface of drilled hole walls is clearly evident in the form of cracks and voids. Specimens exerted different thrust forces during experimental process are selected for SEM analysis the selected specimens are listed in table 4.34 increasing order of thrust forces.

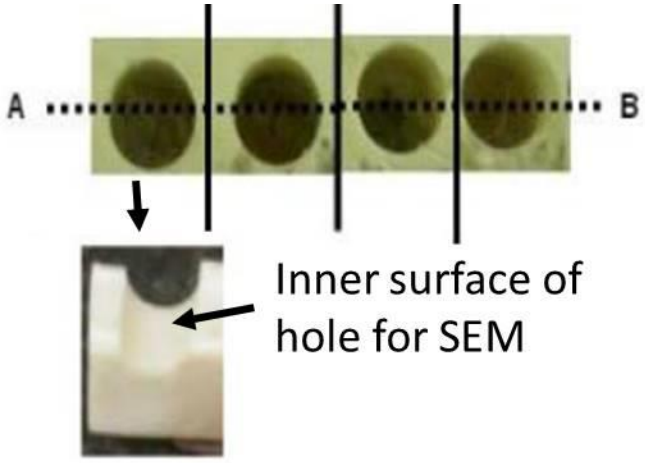

Figure 4.27: Schematic representation of bone samples taking for SEM

Table 4.34: Specimens selected for SEM analysis on the basis of thrust forces during drilling

Exp. no.		**Thrust forces (N)**
22 (Helix angle group)	UABD	6.96
	CBD	8.55
21 (Point angle group)	UABD	7.46
	CBD	9.97
12 (Helix angle group)	UABD	7.95
	CBD	9.67

15 (Point angle group)	UABD	8.56
	CBD	12.08
4 (Helix angle group)	UABD	9.1
	CBD	11.54
9 (Point angle group)	UABD	9.78
	CBD	12.55
15 (Helix angle group)	UABD	10.15
	CBD	12.35
10 (Helix angle group)	UABD	10.54
	CBD	12.55
5 (Point angle group)	UABD	11.54
	CBD	14.75

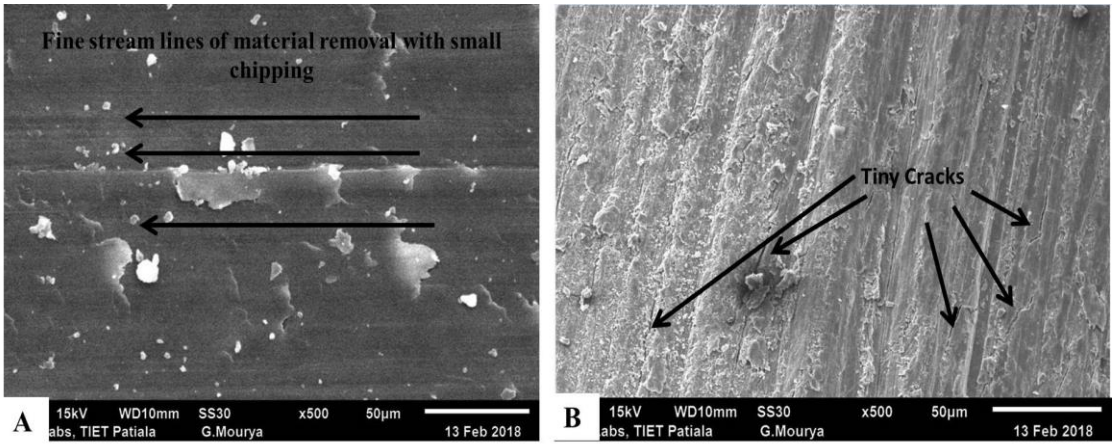

Figure 4.28: SEM observation of Exp 22 (helix angle group); Thrust forces {(A):UABD: 6.96 N; (B): CBD: 8.55 N}

Figure 4.28 shows the scanning electron microscopy (SEM) of drilled hole samples at 500X. The forces exerted during this process are lowest as recorded among the all experimental combinations (UABD: 6.96N, CBD:8.55N). From microscopic images, it is visible that there is fine streamlining as sign of material removal. There are no visible micro cracks in SEM image of

UABD. While comparing the image A and B, heavy streamlining is visible with tiny cracks along the streamlining.

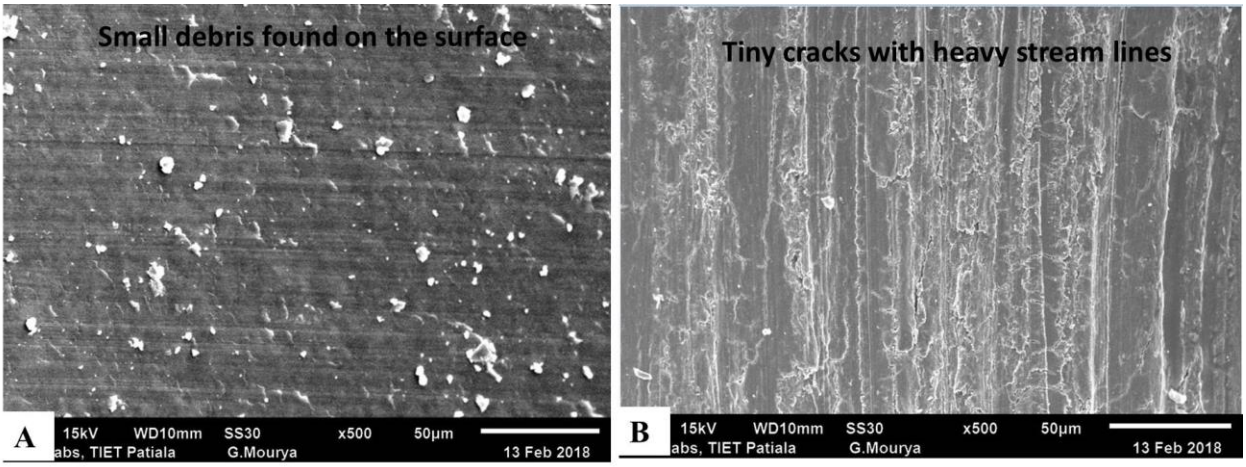

Figure 4.29: SEM observation of Exp 21 (Point angle group); Thrust forces: {(A): UABD: 7.46 N; (B): CBD: 9.97N}

In the next observation of SEM images shown in Figure 4.29, experiment no 21 from point angle group is selected. The thrust forces observed in this experiment is 7.46N for UNBD and 9.97 for CBD. From image A, i.e. UABD, it is observed that small debris sticks on the surface of drilled bone walls. However the surface is free from any cracks or any major destruction. Debris observed on surface may be result of continuous striking of tool at ultrasonic frequency during drilling. While comparing it with conventional drilled specimen at the same experimental combinations, heavy streamlining was observed with microcracks on the surface.

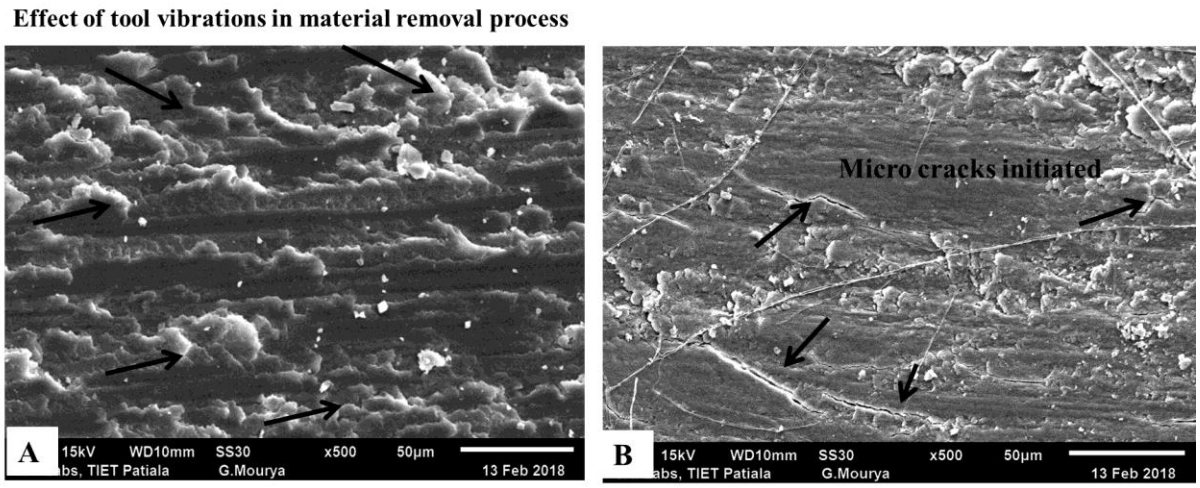

Figure 4.30: SEM observation of Exp 12 (Helix angle group); Thrust forces: {(A): UABD: 7.95 N; (B): CBD: 9.67N}

Further, next specimen from helix angle group exp no 12 having UABD: 7.95N & CBD: 9.67N forces. From Figure 4.30, it is evident that increasing thrust forces during drilling causes damage in the bone specimens. Uneven chipping of material removal is observed in case of ultrasonic assisted drilling process. In image B, SEM of conventional bone drilling is shown. From image, there are microcarcks all over the image and surface is damaged with cracks, chips and uneven material shearing.

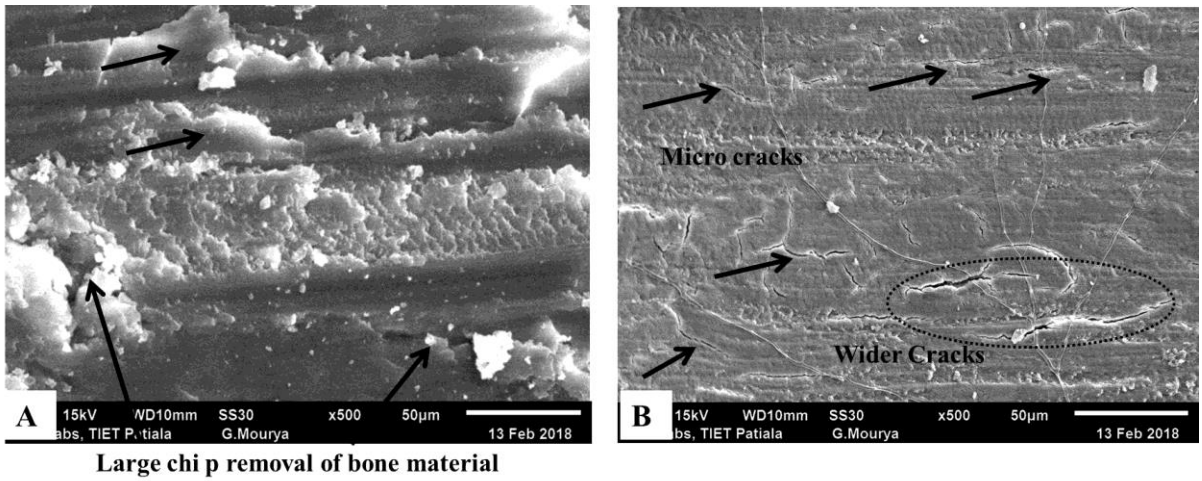

Figure 4.31: SEM observation of Exp 15 (Point angle group); Thrust forces {(A):UABD: 8.56 N; (B): CBD: 12.08N}

From Figure 4.31, the forces observed are 8.56 N in UABD & 12.08 N in case of CBD. From images shown in figure 4.31, the material removal mechanism in form of peeling of chips and hammering effect of tool can also be observed. Material removed in the form of large but thin chips or irregular thickness of chips can be observed. On the other hand, conventional drilled specimen shows a clear surface due to conventional material removing mechanism. But the formation of cracks on the surface is clearly evident and sign of heavy shearing can be seen in the form of wider cracks.

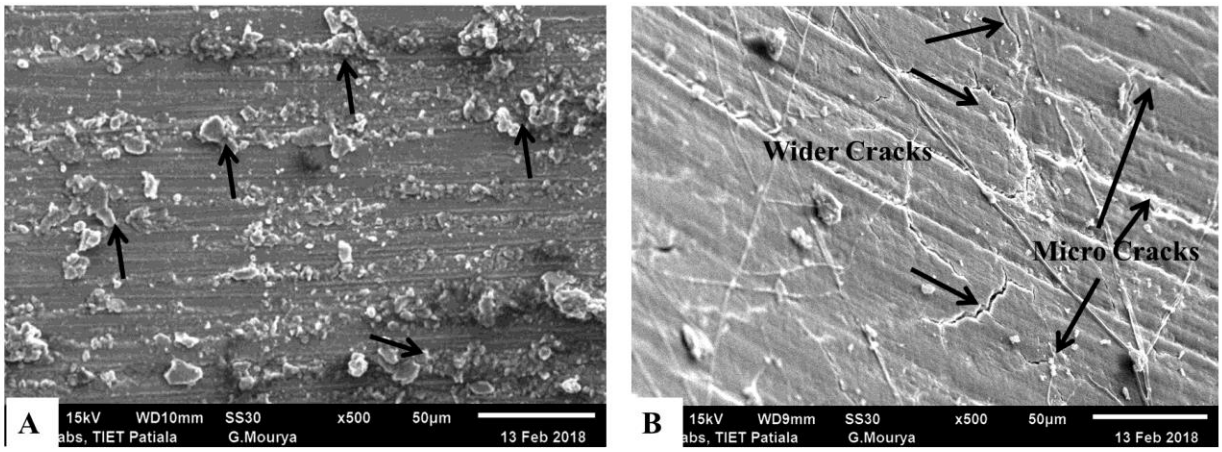

Figure 4.32: SEM observation of Exp 15 (Point angle group); Thrust forces {(A): UABD: 8.56 N; (B): CBD: 12.08N}

Next observation of SEM analysis is done for the exp 4 from helix angle group. The observation is reported in figure 4.32. The experimental values of thrust forces in this experiment were observed high from the previous studied experimental group i.e. 9.1N for UABD and 11.54 N for CBD. Surface was found with heavy debris and sign of left chips particles in the drilled holes. However, the surface is intact from the cracks and voids. In comparison with conventional drilled hole of same category the surface is somewhere free from debris and chips, but having deep streamlines of movement of tool with micro cracks and somewhere wider cracks also.

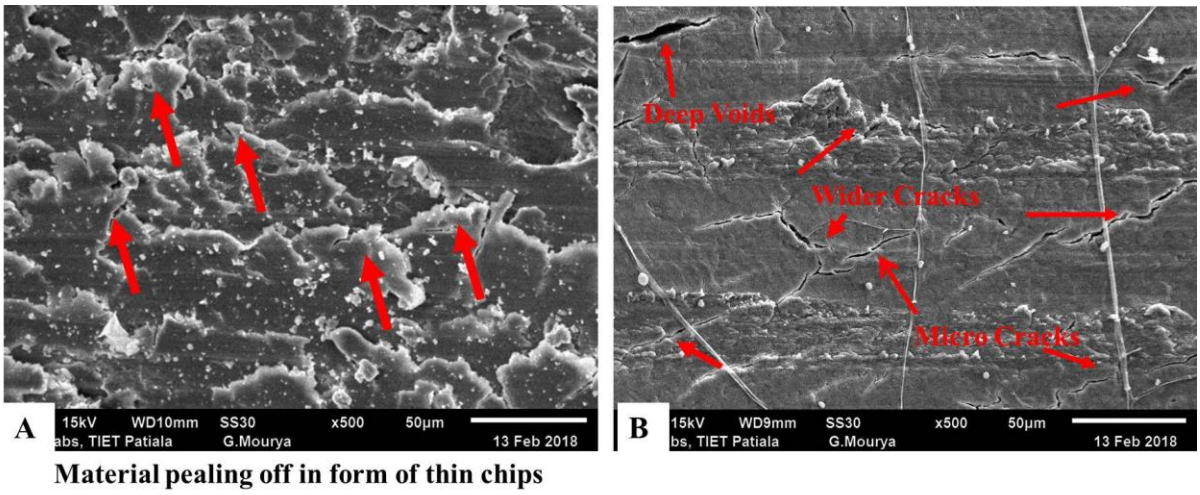

Figure 4.33: SEM observation of Exp 9 (Point angle group); Thrust forces {(A): UABD: 9.78 N; (B): CBD: 12.55N}

Further increase in thrust forces results in the form of more damaged as shown in figure 4.33. The specimen drilled with ultrasonic assisted technique is still free from cracks but the material chipping is very thin and wide in shape. Very irregular thickness of chipping is observed as compared to the conventional drilling. Whereas, SEM image of conventional drilling shows deep and wide voids on the surface with higher number of microcracks in the specimen. These deep voids and cracks on the surface is a result of high shearing energy during material cutting.

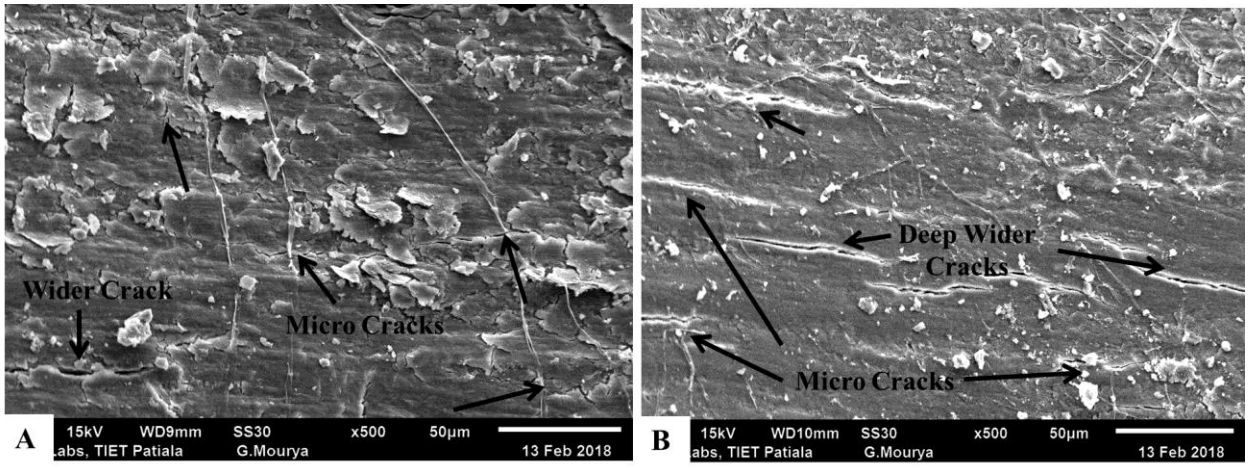

Figure 4.34: SEM observation of Exp 15 (Helix angle group); Thrust forces {(A): UABD: 10.15 N; (B): CBD: 12.35N}

In experiment 15 of helix angle group, the thrust forces observed as 10.15N for UABD and 12.35N for CBD shown in figure 4.34. The effect of increasing thrust forces and results in terms of damage is continuous with this observation at this level of forces few micro cracks are visible on the surface of UABD specimen. The mechanism of material removing is same and fine chipping is observed. While comparing it with CBD specimen, it was observed that deep wider cracks are visible on the surface with some fine debris dispersed over the drilled wall.

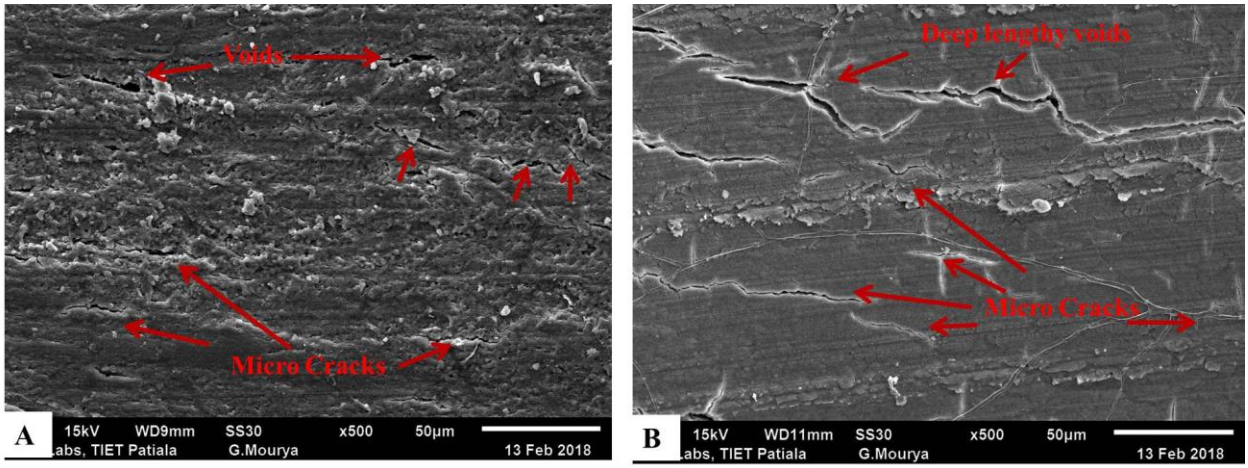

Figure 4.35: SEM observation of Exp 10 (Helix angle group); Thrust forces ((A): UABD: 10.54 N; (B): CBD: 12.55N)

The number of cracks and their length are found to be increasing in the next observation shown in figure 4.35. Few short voids are visible with micro cracks on the surface of UADB specimen. On the other side, CDB specimen shows heavy damaged area in the form of deep wide cracks along the full length of image. Some micro cracks in CDB specimen are also observed.

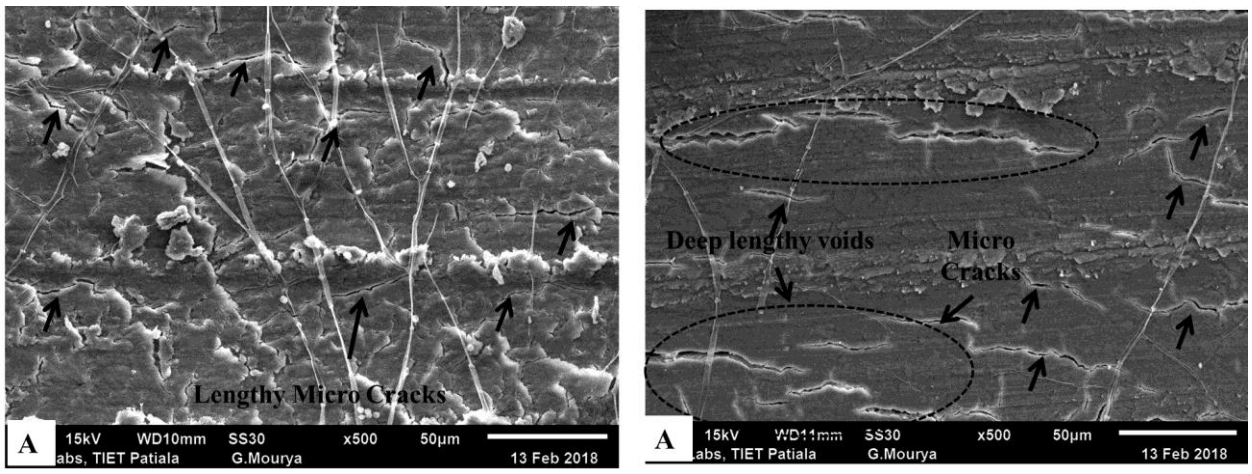

Figure 4.36: SEM observation of Exp 5 (Point angle group); Thrust forces {(A):UABD: 11.54 N; (B):CBD: 14.75N}

For the highest observed thrust forces during bone drilling observed under SEM and illustrated in figure 4.36. From image, it is observed that there are more lengthy cracks in case of UABD specimen as compared to the previous one. Cracks are observed over the complete surface of the specimen. In conventional drilled specimen, of the same experimental combination there is much more damaged area consisting of lengthy wider cracks with microcracks spread over the surface of specimen.

4.5 COMPARATIVE CHIPPING MECHANISM

The mechanism of material removal is completely different in both kind of drilling process. To understand the material removal process surface topography has been studied of different drilled specimens under Scanning electron mechanism. There is a discontinuous contact of tool with the workpiece in ultrasonic assisted bone drilling process. The tool leaves the workpiece and get connected again very rapidly at 20kHz frequency. While in conventional drilling process there is a continuous contact of drill bit with the bone results in the form of high shearing force

developed at the interface. Due to all this, there is a difference in material removal mechanism for both of the technique shown in figure 4.37 and 4.38. From figure 4.37, the material removal in form of half peeled off chips is clearly visible that is results of discontinuous contact and hammering effect of tool on workpiece. While studying the conventional drilled specimen, the surface is much smoother in terms of chips and debris but the surface consist of heavy damage in form of cracks and voids due to continuous contact of tool with the workpiece.

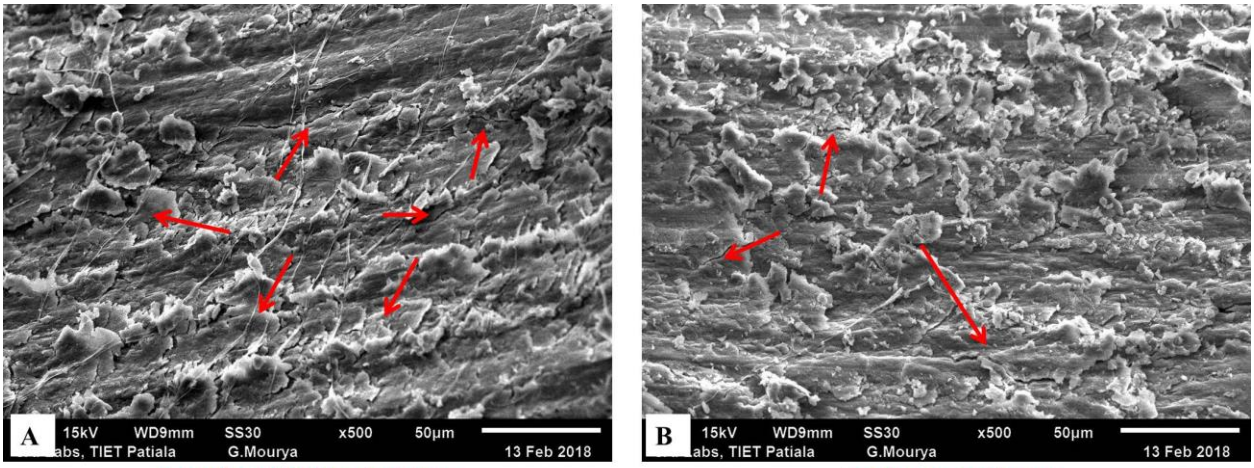

Figure 4.37: Surface topography of ultrasonic assisted drilling on bone (UABD)

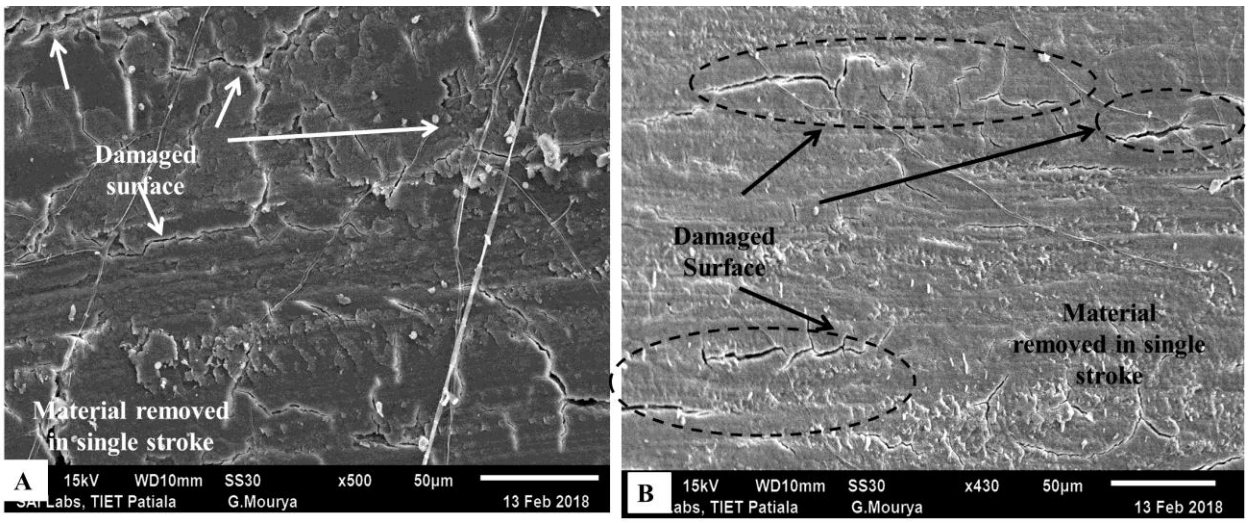

Figure 4.38: Surface topography of conventional drilling on bone (CBD)

4.6 SUMMARY

The chapter explores the experimental observation of bone drilling process using desired set of drilling parameters suggested by L25 orthogonal array. The experimental observation i.e. heat generation and thrust forces developed during drilling further, delamination of hole diameter and axial pullout force of bone screw joint were measured after experimentation. All individual outputs have been evaluated for the optimal combination of parameter from the experimental design using taguchi optimization technique. All desired outputs of experimentation were solved for the analysis of variance (ANOVA) and trends of each parameter respective to the levels are identified using response curves. Percentage contribution of individual parameter on desired output is identified and P-value of respective parameters signifies the effectiveness of parameter in the ANOVA table. In this chapter, effect of temperature on morphology of bone is studied by the means of histopathology. Effect of increasing temperature on structure of bone lacunas is studied and comparative statement is made for conventional drilling and ultrasonic-assisted bone drilling. Effect of thrust forces on surface topography of bone specimens were studied using scanning electron microscopy (SEM). From SEM images it is also detected that the material removal mechanism is also different in both the cases.

CHAPTER 5: RESULTS ANALYSIS & DISCUSSION

The observation from the experimental procedure and their analysis for the specific requirements is discussed in the previous chapter. Behavior of individual output with respect to the change in drilling parameters is demonstrated as response curves. The behavior of parameters with respect to the individual output will be discussed under this chapter.

5.1 DISCUSSION ABOUT PARAMETRIC EFFECT

The observation and analysis for the desired outputs i.e heat generation, thrust forces, axial pullout force and diameter delamination is done and the parametric effectiveness is checked using ANOVA analysis. For the different outputs the response of parameters is different and their behavior is studied as follows:

5.1.1 Heat generation: Effect of Process Parameters

The heat generation measured in terms of temperature rise around the drill site during the two different set (point angle group and helix angle group) of experimentation and behavior of temperature with respect to the change in parameters levels is shown in figure 4.1 and 4.9. From response curves, the prediction of the combination of parameters for minimum temperature value is R1F1P1 and R1F1H5 respectively i.e the value of temperature increases with increase in rotational speed (R), feed rate (F) and drill point angle (P). While the drill helix angle (H) shows reverse effect on temperature rise in bone drilling process. From the optimization process, it is suggested that the lower rotational speed *(R1: 600 rpm)* should be used to maintain the temperature minimum suggested in response curve figure 4.1(A) and 4.9(A). The reason for temperature elevation with rotational speed is directly linked with the frictional energy developed due the frictional forces induced at the rake face of cutting tool and bone material. The developed frictional energy is linearly depend on rotational speed of drill bit and maximum

amount of this energy is converted in to heat, thus the rise in temperature is expected with increasing the rotational speed during bone drilling process. Another obvious reason for generating high temperature at high rotational speed is rapid continuous contact of drill bit with bone, results in transfer of more heat from tool to the bone material. The effect of high rotational speed in term of increasing temperature during drilling is also studied by different previous studies, i.e. *Thompson, (1958); Matthews and Hirsch, (1972); Saha et al., (1982); Matthews et al., (1984); Ohashi et al., (1994); Brisman, (1996); Davidson and James, (2003); Anitua et al., (2007); Augustin et al., (2008); Basiaga et al., (2013); Lee et al., (2011, 2012); Sezek et al., (2012); Xu et al., (2014)* and suggested lower rotational speed for minimum temperature rise [27,50,55,57-60,62-65,66-67,80]. While analyzing the effect of feed rate, the Taguchi optimizing technique suggests the lower feed rate *(F1: 10 mm/min)* for controlling the temperature within the threshold limit. Feed rate in case of drilling model can be described as the thickness of chip to be removed from the workpiece in a single revolution of drill bit. Increasing feed rate in drilling result in a deeper cut per revolution and thickness of chip is increased with further downward movement of tool. This required a high shearing energy for material cutting and thus, the developed energy contributes for the temperature rise in bone drilling. The effect of feed rate on temperature studied by various studies i.e. *Wang et al., (2013); Alam et al., (2011), (2015); Soriano et al., (2012); Lee et al., (2012); Tahmasbi et al., (2017*) and supports the results obtained from the Taguchi optimization technique[48, 70-71,77,85].

In the next attempt, the effect of drill point angle (P) and drill helix angle (H) is analyzed. From the optimization process, it was observed that the drill point angle should be minimum from the selected range (60-140 degree). The point angle of tool directly influences the width of the chip and forces developed at initial phase of the drilling. Small point angle gives an acute tip to the

tool which reduces the chances of the drill wandering from irregular bone surface. Smaller point angle give less contact in the starting and thus starting with the small chips which gradually increases and helps to dissipate the heat within the environment. Further, when full tip comes in contact with the bone surface the smaller point angle gives wider chips because of lengthy cutting edge as compared to the standard drill bit. This will increase the radial forces and reduce the axial forces during drilling (*Lee et al., 2011*)[66]. In addition to all this, higher point angle induced high shear deformation in bone materials thus, reflecting the results in the form of high temperature around the drill site. While optimizing the helix angle group results, it was observed that higher helix angle (36 degree) produces less temperature rise during bone drilling process. The results obtained from experimental and statistical analysis supports the results suggested by *Davidson and James (2003), Lee et al., (2011) Karmani and Lam, (2004)*[27,66,90]. The act justify that in case of bone drilling, where shorter chips produced and due to moist nature of bone these chips clog within the flutes, causing the friction between tool and bone and resulting in the form of high temperature. A high helix angle *(24-36 degree)* of drill bit encouraging the efficient chip removal in case of surgical bone drilling process *(Karmani and Lam, 2004; Natali et al., 1996; Pal and Saha, 1981)*[37,56,90].

The evidence of damaging the bone constituents is also clearly visible in the histopathology of bone specimens (Figure 4.17 to 4.26). From histopathogy examinations, the levels of evaporations of lacuna from the osteocytes are observed to be increased which is directly relate to the increase of heat generation in the bone drilling.

5.1.2 Thrust forces: effect of process parameters

The Thrust forces measured in newton (N) on dynamometer during the two different set of (point angle group and helix angle group) of experimentation and behavior of thrust forces with

respect to the change in parameters levels is shown in figure 4.3 and 4.11. From response curves, the prediction of the combination of parameters for minimum thrust forces is R5F1P1 and R5F1H5 respectively i.e the value of thrust forces increases withincrease in feed rate (F) and drill point angle (P). While the drill rotational speed (R) drill helix angle (H) shows reverse effect on thrust forces in bone drilling process. From the optimization process it is suggested that the higher rotational speed *(R5: 3600 rpm)* should be used to control the thrust forces lower which is desirable for the sustainable bone drilling process. During bone drilling process, the rotational speed of drill bit contributing its major part in the experimental outputs. According to studies conducted by *Alam et al., (2011); Wang et al., (2013); Xu et al., (2014)* the decreasing thrust forces with increases the rotational speed is a factor of friction coefficient[65,70,71]. The chip thickness removed per revolution of drill bit reduces the required shear deformation of material and resulting in the form of reduced thrust forces with increased rotational speed. The next effect of feed rate was studied on thrust forces developed during the drilling process. From the optimization process it is clear that the lower feed rate *(F1:10 mm/min)* helps to maintain the thrust forces minimum. The feed rate of tool in a drilling operation can be understood as thickness of chip to be removed from the material per revolution of the drill bit. Increasing feed rate directly correlate with the increase in chip thickness, this requires high shearing energy which results in the form of high thrust force. The results observed for effect of feed rate in this study supports the experimental observation of *Alam et al., (2011); Soriano et al., (2012); Lee et al., (2012);Wang et al., (2013); Xu et al., (2014); Alam et al., (2015)*[48,65,70-71,77].The mathematical model develop by Lee et al. (2012) also confirms that thrust forces increases withincrease in feed rate[67].

The effect of drill specifications involved in experimental study i.e. drill point angle (P) and drill helix angle (H) shows their impact on the thrust forces. From the response curves shown in figure 4.3(C) and 4.11 (C) the behavior of thrust forces with the change in level of respective parameter is observed and suggested lower drill point angle *(P1: 60 degree)* and higher drill helix angle *(H5: 36 degree)* for minimum thrust forces during bone drilling. The effect of point angle observed significantly in thrust forces and the reason for this change in thrust forces during change in drill point angle is simply depend upon the structure of drill bit. With small point angle *(P1: 60 degree)* the chips width increases gradually which diversify the developed forces and reduces the axial thrust forces. Whereas in case of high point angle full cutting edge comes in contact with the material rapidly induces higher shear deformation that generates high thrust forces and continues throughout the process. The Findings are in-line with the results of other researchers i.e. *Bechtol, (1959); Jacob et al., (1976); Hillery and Shuaib, (1999); Basiaga et al., (2011)* and recommended a range of 70-90 *degree* point angle for surgical drilling operations [26,63,88,89]. While studying the helix angle in 2^{nd} group of experimentation, the results observed from the response curve (4.11(C)) show that the increasing helix angle helps to reduce the thrust forces developed during the bone drilling process. From curve it is evident that higher helix angle *(H5: 36 degree)* is suitable for maintaining the thrust forces minimum. The reason for decreasing the thrust forces with increasing the helix angle is due to factor that high helix angle help to evacuated the drill chips efficiently and reduces the chances of coagulation in between the flutes of drill bit. The coagulated chips increases the frictional forces and resulting in the form of high thrust forces. Thus, a high helix angle *(H5: 36 degree)* is desirable in case of bone drilling as it efficiently clear the chips and reduces the thrust forces. It is also observed from the literature that helix angle of higher range (24-36 *degree)* is recommended by *Albright et al.,*

(1978); Saha et al., (1982); Karmani and Lam, (2004) for better efficiency in surgical bone drilling process [57,90,145]. The mathematical model developed by Lee et al., (2011) also supports the suggestion of taguchi optimization technique of this experimental design in terms of drill bit specification i.e. lower point angle *(P1: 60 degree)* and higher drill helix angle *(H5: 36 degree)*[66].

The thrust forces were observed to be increases with increase of feed rate. Thus, observed that increasing feed rate causes more damage to the inner surface walls of drilled holes in the form of cracks and voids [figure 4.27 to 4.37]. These damages in the surrounding of hole walls makes the bone screw joints less sustainable.

5.1.3 Axial pullout force: effect of process parameters

Drilled hole created in bones are prepared to fix the cortical screws for the purpose of fixing implants to give support to the fractured bone. The better axial pullout force of bone screw joint is desired for good sustainable orthopedic surgery. The axial pullout force is the level of anchorage force of screw to the bone. The anchorage of screw is definitely depending upon the level of damage observed around the drill site during drilling. From the previous sections 5.1.1 and 5.1.2, it is evident that the drilling parameters affect the thermal and mechanical damage of drilled holes while drilling with different combinations of drilling parameters. The damage exerted by the bone around the drill site may undermine the drill site and causes low axial pullout force to the bone screw joint. The observed values for the axial pullout force used to optimize the drilling parameters for maximum axial pullout force. From response curves figure 4.5 and figure 4.13 illustrate the effect of parameters on axial pullout force of bone screw joint. From response curves of both experimental group, it is observed that R5F1P1 and R5F1H5 are the optimize combination for the maximum output. In order to study the behavior of individual

parameter on axial pullout force, the axial pullout force was observed as maximum with increasing the rotational speed (R) and drill helix angle (H), whereas the feed rate (F) and drill point angle (P) shows reverse effect and shows that increasing these parameters shows decrease in axial pullout force. From figure 4.5(A) and 4.13(A), for axial pullout force, the suggested rotational speed (*R5: 3600 rpm*) is the higher value from the experimental design. The concept behind this is, increasing rotational speed generates less thrust forces at the time of drilling causes less damage to the surrounding of bone. This will definitely lead to a crack free drilled holes and strengthen the bone screw joint. From figure 4.5 (B) and 4.13(B), the effect of feed rate is visible and Taguchi technique suggested low feed rate *(F1:10 mm/min)* for better axial pullout force. It was already discussed that (in section 5.1.1 and 5.1.2) increasing feed rate increases the thermal and mechanical damage in bone drilling process. Increasing mechanical damage around the drill site will developed microcarcks and thermal damage causes dead cells in the affected area. These kinds of damages will lead to the loose anchorage to the bone screw joint and result in the form of low axial pullout force.

Drill specifications studied in the experimental study, i.e Drill point angle (P) and Drill helix angle (H) shows there effect on axial pullout force and can be estimated there behavior by the means of figure 4.5(C) and 4.11(C) respectively. Drill Point angle should be lower i.e *(P1:60 degree)* and drill helix angle should be high *(H5: 36 degree).* From response curves, we can see that the pullout force decreased gradually with increases the point angle and same effects are visible with decreasing the drill helix angle. The increased point angle and decreased helix angle during drilling of bone is a reason for increased thrust forces and temperature rise during drilling. Thus, increasing point angle during bone drilling origins destruction to the bone structure which will later on reduced the axial pullout force of bone joint.

5.1.4 Diameter delamination: effect of process parameters

During bone drilling process, diametric delamination is an issue which also needs to be addressed with the behavior of parametric change. Figure 4.8 and 4.16 shows the behavior of delamination in diameter of drilled holes with respect to parametric change. From response curves in figure 4.8 and 4.16, the Taguchi suggestion is R1F1P1 and R1F1H5 respectively. From both the response curves, it is clear that rotational speed and feed rate should be low for minimum delamination. From curves, 4.8(A) and 4.16(A) the effect of rotational speed is noticed and it is observed that increasing rotational speed causes damage in drilled diameter in terms of more delamination and suggested lower rotational speed *(R1: 600 rpm).* Increasing centrifugal forces with increase of rotational speed may be the reason for this increase in delamination. Drilled chips strike the drilled wales before evacuate is complete and erode the surface of walls in between the drill bit and tool interface. Increasing feed rate also showing this effect and from response curves: 4.8(B) and 4.16(B), it is suggested that low feed rate should be used *(F1: 10 mm/min)* to control the delamination in drilled hole. High feed rate damaged the hole mechanically as it produces the high thrust forces and a rapid movement of tool forces the drill bit to cut a thick material per revolution. This action of tool shear off thick chip increases the chances of wander which delaminate the drilled hole in the final result.

Drill point angle (P) and Drill helix angle (H) also showing their effects while analyzing it with Taguchi technique. From curves 4.8 (C) and 4.16 (C) the behavior of point angle and helix angle is observed. While observing point angle, it is observed that increasing point angle lower the delamination in drilled holes *(P1: 60 degree)*. Whereas increasing helix angle lift up the delamination of drilled holes *(H5: 36 degree)*. The reason for these effects may be the concept of increasing thrust forces with increasing the point angle. However, from ANOVA table (Table:

4.15) it is evident that the change in point angle does not affect significantly (P= 0.573). In case of analysis of helix angle, higher helix angle is suggested by the analysis of experimental observation. Higher helix angle evacuate the chips efficiently and reduced the friction in between the drilled walls and drill bit interface surface.

5.2 DISCUSSION ABOUT HISTOPATHOLOGY

5.2.1 Structural changes

Histopathology of bone specimens is a technique used to examine the level of structural and morphological damage observed due to its expose to the heat during drilling. From figure 4.17 to 4.21, the specimens exposed to different level of heat during experimentation were examined and the level of damage is measured in terms of evaporated osteocytes present in the bone cells. Large number of evaporated lacunas from osteocytes is a reason for exposure to more than the threshold temperature during process. From figure 4.17 to 4.21, it is observed that as the experimental temperature increases the level of the damage also increases. At the initial stage, in figure 4.17, where exposed temperature is just below the threshold temperature, There is no damage in terms of evaporated lacunas and maximum numbers of lacunas are found protected in the histopath image. Further, when the experimental temperature increases the level of damage also increases in proportional to the temperature rised in the drilling operation. From figure 4.18 and 4.19 there is gradually increases in the damage with respect to the temperature. Later on, in figure 4.20 and 4.21, a complete damage was observed in the structure of bone. Therefore, from the histopathology examination of bone it is proven that the damage in bone is linearly a dependable factor for temperature rises in orthopedic bone drilling process.

5.2.2 Comparison: UABD and CBD

While comparing the histopathology of ultrasonic-assisted bone drilled (UABD) specimens and conventional bone drilled (CBD) specimens, a significant effect of UABD is observed. From the comparison of temperature the changes in temperature values is already observed in figure 4.2 and figure 4.10 for UABD and CBD. Therefore, the structural changes that are directly depended on temperature in bone drilling process also show significant changes. While comparing the experimental group of having low heat generation, in figure 4.22, the temperature observed by both techniques is lower than the threshold limit. Thus, there is no damage observed in the morphology of bone structure for both specimens. However, there is a difference in maximum temperature observed because the temperature is controlled below the threshold limit as a result same kind of structure is observed. Furthermore, in the figure 4.23 and 4.24 the morphological changes in bone structure are observed in terms of damaged osteocytes around the drill site. From these images, the effect of UABD process is clearly detectable in the form of nonviable lacunas around the drill site and more damaged area was observed in CBD process. The temperature around the drill bit observed in the experimentation process is also having a significant difference. From figure 4.25 and 4.26, the level of damage in the histopathology of bone specimens is increased and non-viable lacunas are dispersed all over the image. These osteocytes are considered as nonviable as they cannot recover from this stage and lead to the osteonecrosis in bone.

In general, On the basis of morphological study of drilled hole specimens, drilled at varying drilling parameters and exposed to different drilling temperature, the level of osteonecrosis or the level of the damage in terms of the situation of osteocytes within lacuna. The damage of lacunas has been established in four stages: (i) normal osteocytes, (ii) shrunken osteocyte, (iii) osteocyte

with pyknotic nucleus,(iv) empty lacuna. However, the shrunken osteocyte, and osteocyte with pyknotic nucleus are also the stages of irreversible death. Thus, consider them under the nonviable lacunas. An approximate estimation of these four stages has been made for all morphological studies shown in table 5.1.

Table 5.1: Status of lacunas in bone morphology at different drilling conditions

Exp. no.		**Osteocyte Condition**
1	UABD	95-98% lacunas are viable
	CBD	95-98% lacunas are viable
6	UABD	40-45 % lacunas are observed viable
	CBD	30-40% lacunas were found viable
11	UABD	20-30% viable lacunas, and around 50% of lacunas are partially damaged
	CBD	15-25% live lacunas within the osteocytes, 30-40% are partially damaged
16	UABD	Only 5-7% found partially live at the far edge of drill site
	CBD	Only 2-3% intact, dispersed around the histopath image
25	UABD	2-3% dispersed randomly in histopath image
	CBD	2-3% dispersed randomly in histopath image

5.3 DISCUSSION ABOUT SCANNING ELECTRON MICROSCOPY (SEM)

Scanning electron microscopy (SEM) is a characterization technique used to study the surface topography of drilled holes walls. Drilled holes walls undergone the shear deformation of material while cutting the material. This deformation of material may damage the drilled hole surface topography and using different drilling parameters the level of damage may get varied. The level of damage in drilled holes is examined by means of cracks and voids developed in drilled holes surrounding. Scanning electron microscopy (SEM) is an influential tool to examine

the level of damage in drilled holes. The level of damage is directly correlated with the thrust forces developed during drilling and specimens are to be examined under the SEM analysis selected on the basis of thrust forces observed. From figure 4.27 to 4.35, different drilled specimens exerted different thrust forces followed to check the surface topography and also make a comparison of UABD specimens with CBD. It is detected that increasing thrust forces during drilling lead to the damage in the drill surrounding. From figure 4.27(A) to 4.32(A), the level of thrust forces is within the range of 6.96 N to 9.78 N for ultrasonic-assisted drilling process (UABD) the surface is crack free and free from any irregularities in the surface. While comparing the same with the conventional drilling method (CBD){figure 4.27(B) to figure 4.32(B)} the surface is irregular and having cracks in the surface. These cracks in the conventional drilling process increases with increase in the thrust forces in the drilling process. Furthermore, from figure 4.33, the damage in UABD specimens shows some cracks initiation in the surface and increasing further thrust forces for UABD process shows much more micro cracks and damaged surface. In comparison with conventional drilled specimens, the damage is leading towards large cracks and deep voids in the surface which increasing the thrust forces up to 14.75 N.

5.4 SUMMARY

The above mentioned discussion about the observation and analysis of bone drilling process give an overview about the benefits expected with the ultrasonic-assisted bone drilling (UABD) process over the conventional bone drilling process. From Taguchi optimization analysis, the effect of different drilling parameters has been analyzed under the effect of ultrasonic vibrations in tool. From these analysis the effect of rotational speed(R), feed rate(F) and drill specifications (Drill Point angle(P), Drill Helix angle(H)) has been studied for different experimental outputs

i.e. heat generation, thrust forces, axial pullout force and diameter delamination. Each parameter shows their effect on the output. The cutting edge impact of ultrasonic assisted bone drilling (UABD) technique is easily visible, which helps to reduce the drilling temperature, thrust forces in the bone drilling process as compared to the conventional bone drilling process. The study of drill specifications i.e drill point angle and helix angle, which are rarely available in the literature, is also studied under the impact of ultrasonic vibrations. This has been analyzed and the reason for their behavior has been discussed in this chapter. Structural characterization techniques i.e histopathology used to examine the morphological changes observed in the bone with effect of temperature and a comparison has also been made for the UABD and CBD technique. Further, scanning electron microscopy (SEM) is employed to understand the effect of thrust forces on the surface topography of drilled hole specimens. From SEM analysis, it is observed that the discontinuous contact of tool and bone reduces the level of cracks and also shows different chipping mechanism from the analysis of sectioned bone specimens.

CHAPTER 6: BONE DRILLING: FINITE ELEMENT ANALYSIS

6.1 FINITE ELEMENT ANALYSIS (FEA): INTRODUCTION

Finite element analysis (FEA) is method of simulation for computational solution of complicated real time problems in easy and convenient manner. In order to solve the present problem, finite element analysis is directly implacable to simulate the process of drilling procedure and significant study of the interaction surface of tool and material. FEA provide detailed and real time data about the forces, stress and temperature during the process and an easy comparison of results for different set of parameters without wasting the actual resources. For modern machining and manufacturing industry, the development of Finite element simulations gave the cutting edge effects and helps to reduce the experimental trials which were used to get the appropriate design for system tool and also helps to get optimum set of parameters within the desired limits. The present study focuses the comparison of conventional bone drilling (CDB) and ultrasonic-assisted bone drilling (UABD) process for thermal damage around the drill site.

6.2 NUMERICAL MODELING FOR FINITE ELEMENT SIMULATION

For simulation of conventional and ultrasonic assisted bone drilling process, A 3D thermo-mechanical finite element model has been developed using FEM code DEFORM 3D v 11.0. The developed model follows the Lagrangian incremental formulation with uninterrupted remeshing for dynamic analysis process. The developed dynamic simulation processed for temperature generation, stress generation, and damage around the drill site. These outcomes of drilling operations are thermally coupled to each other and finally result as temperature raise in drilling process. The developed model directly influenced by the thermal properties i.e. thermal conductivity, specific heat, material density and material flow stress properties. The dynamic simulation process includes remeshing as a key factor as it helps to restore the distorted mesh

continuously within the cutting zone. The complete simulation process is disturbed over the three steps as follows [146]:

i) Pre-processor

ii) Simulator

iii) Post-processor

6.2.1 Pre-processor

The first stage of simulation includes the preparation steps required for the generation of database for the simulation study. These inputs are started with providing data to the model in the form of desired drilling parameters, environment conditions and thermal factors. The input given to the pre-processor in a systematic way as follows:

i) *Defining input process condition with geometric models:* in this step the desired input parameters with ambient conditions and geometry of required dimensions for work piece and tool.

ii) *Meshing:* FEM discrete the complicate problem in to small sections or elements by means of meshing. The meshing size and shape is directly affecting the accuracy of model and its results. The dynamic modeling process incorporate the remeshing option which restore the mesh nodes after every successive cutting step [146].

iii) *Material model:* assigning material to the geometries i.e. workpiece and drilling tool, identify the material behavior i.e rigid, plastic and elasto-plastic) and reference temperature to the individual objects. Furthermore, the Johnson-Cook model properties for the workpiece , mechanical and thermal properties need to be defined in this section.

iv) *Interface conditions:* the machining models required a fixed friction model to process the model with respect to the drilling conditions. Different friction models available are shear friction model, coulomb model, hybrid model and variable model.

v) *Simulation controls:* For an efficient and effective drilling simulation the appropriate simulation steps, time and data saving is managed with simulation controls.

vi) *Boundary conditions:* it decides kinetic and physical conditions and within that limit the model is processed for simulation. In drilling operation, the movement of drill bit and restricted degree of freedom for workpiece. The top surface of workpiece which is to be drill during the process does not get fixed or restricted. Thermal conditions fixed the heat sources, assignment of temperature to the elements and heat transfer constants to the individual surfaces in some cases.

vii) *Generating database:* The developed model, controls and conditions built in a single file for generating a database and save it for further simulation.

The pre-processor and preparation of model is also set up on some assumptions. These assumptions are helpful to make the model and simple and acceptable in all universal conditions. The assumptions taken for the model is as follows:

i) The material is assumed as isotropic and homogenous plastic material i. e. the properties are assumed to be same in all direction.

ii) The cutting tool was assumed as rigid as the stiffness is way higher then bone material.

iii) The thermal conductivity of tool material is taken very high as compared to bone material. Thus, heat is assumed to be flow from tool to bone and temperature profiles in tool are neglected while conducting simulation.

6.2.2 Simulator

The generated model undergone for the solution assigned according to the simulation control. There are different methods for solving the problem with the help of different algorithm used. There are direct iteration, newton-Rapson method, Lagrangian, Arbitrary Lagrangian, and steady state algorithm. During simulation process an observation can be visible for the desired steps in simulation graphics window.

6.2.3 Post-processor

During simulation process the results for each successive step has been stored in the post-processor in a database file (*.DB). Different output responses for which simulation has been done can be studied from this file. Contours at different steps can also be obtained in the post processor file.

6.3 DATABASE GENERATION FOR CBD & UABD

6.3.1 Workpiece-Tool setup

The input process started with the selection of module i.e. drilling from the user interface and followed with the input of desired rotational speed, feed rate and process conditions shown in table 6.1.

Table 6.1: Process conditions input for drilling

Process condition	**Value**
Rotational Speed	600 rpm
Feed rate	50 mm/min / 0.0833 mm/rev
Environment temperature	20°C
Convection coefficient	0.02 N/s/mm/C
Shear-friction factor	0.35

The drill bit of diameter 3.2 mm generated in SOLIDWORKS and saved in STL file imported to the DEFORM 3D in tool setup process and positioned perpendicular to the X- axis and Y- axis and make it co-centric with the Z-axis shown in figure 6.1(A). Workpiece setup enabled the type of workpiece as elastic material and fixed its initial temperature at 37°C. The shape of workpiece generates as cylindrical shape of diameter 8 mm and thickness 3 mm shown in figure 6.1(B).

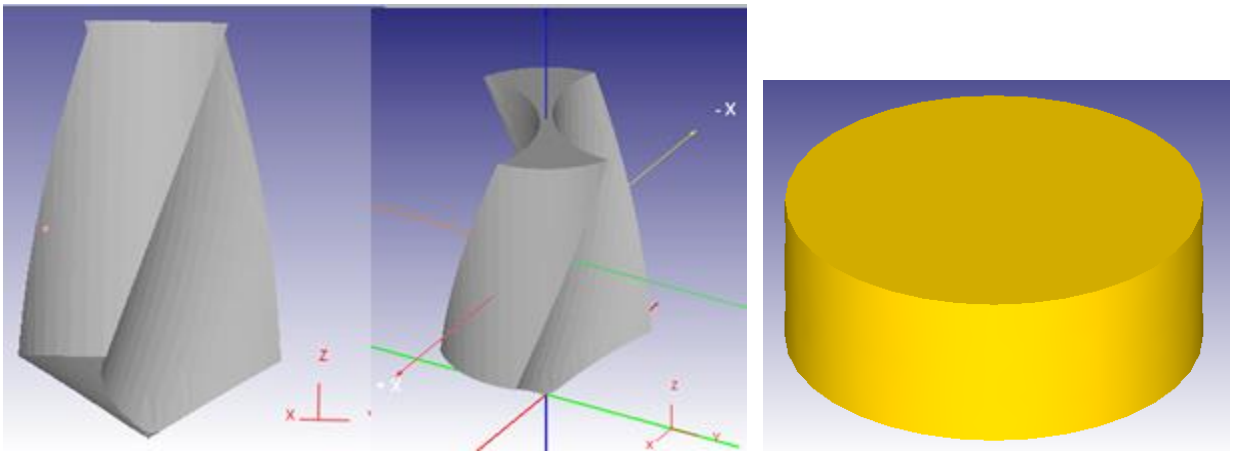

Figure 6.1: Drill bit and Workpiece imported in DEFORM 3D for drilling

6.3.2 Meshing of workpiece and tool

Meshing of the model is doing purposely to make the problem solvable using finite element approach. During meshing, the whole component, model or the elements of the model discretized in to small pieces, each piece represent as an element of the developed model. All discretized available elements are now able to understand the finite element analysis since this process is collecting the solution from the every single element and bunch them together to get the final solution. Thus, the size of element plays a vital role in the approach and solution observed from FEA. In this case, few trails have been made and try to take the observation from them is as shown in table 6.2 below:

Table 6.2: Estimation of grid sensitivity for successful operation of model

Sr No.	Elements in Workpiece	Elements in tool	Results observed
1.	10000	5000	Simulation process terminated after 500 steps. No results observed.
2.	14000	7000	Simulation stop at 500 step again, workpiece get distorted.
3.	17000	10000	Simulation progress further but remeshing of model process aborted the analysis in between and all data lost
4	25000	15000	Simulation process successfully completed but the workpiece material contracted around the drill bit and results were not satisfactory.
5	25000 (0.04 mm in cutting zone)	15000 (0.04 mm tool tip)	Successfully completed with a fine hole created with accurate chipping.

The developed workpiece in the model generation process discretized in to the range of 12000 to 30000 elements numbers of tetrahedral shape. The number of elements is chosen for simulation after grid independency test and it makes sure that further change of mesh numbers dose not affects the results significantly. Finally, the number of elements in workpiece is selected as 25000 and within the cutting zone, the mess size has been reduced up to 0.04 mm as shown in figure 6.2. Drilling tool of diameter 3.2 mm was imported from STL file generated in SOLIDWORKS was considered as rigid body and discretized into 15000 elements and mesh density increased in the cutting edge surface shown in figure 6.2. During chip formation, remeshing of workpiece comes in action when the elements of the mesh get distorted. There are

different methods to implement the regeneration of meshed object based on the triggers available in DEFORM 3D. For the present study, maximum interface depth criterion method is implemented which control the remeshing process with respect to the depth of interface in between workpiece and drill bit.

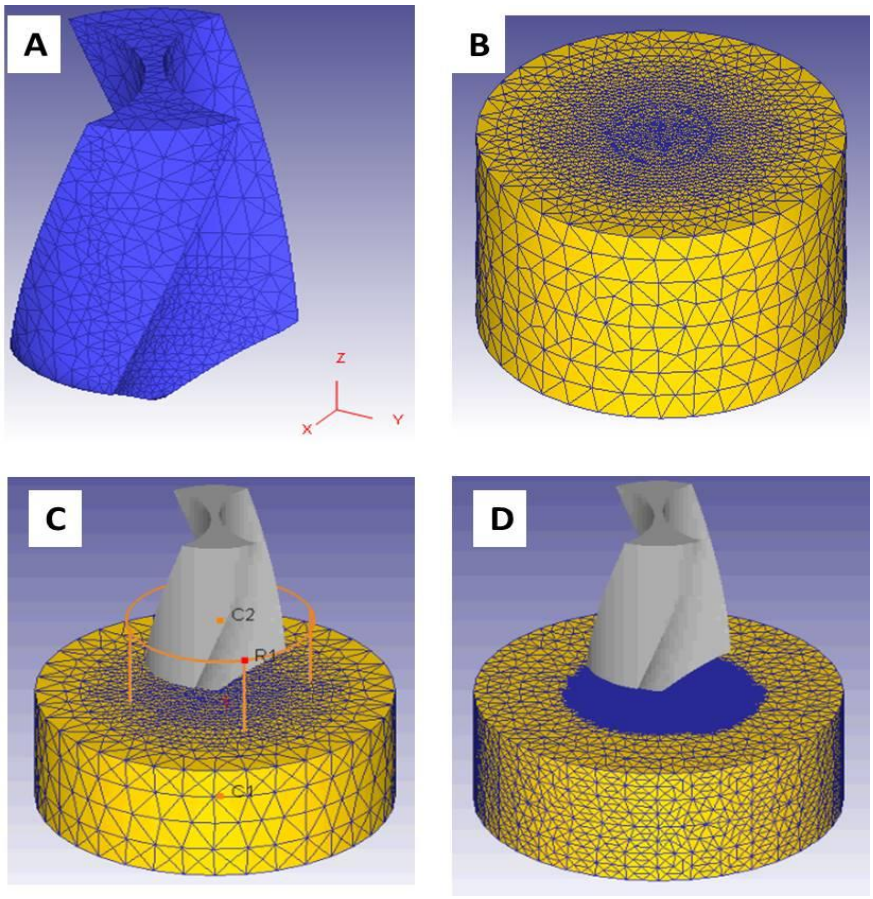

Figure 6.2: Development of meshing elements (A): meshed drill bit; (B): workpiece at 12000 elements; (C): selection of cylindrical surface for dense meshing in cutting area; (D): final meshing of workpiece with 25000 mesh elements and dense meshing in the cutting area

6.3.3 Defining material properties

Drill bit has been considered as rigid material and imported the material properties as HSS to the drill bit from material library. Material properties for workpiece have been incorporated using

non-linear dependency of material under high strain rate and temperature. In order to understand the behavior of bone the flow stress of the workpiece under high strain, strain rate and temperature, conditions has been modeled using generalized Johnson and cook model with equation 6.1. The Johnson-cook (JC) material model proposed and used in machining simulations are as follows and from J-C model the constants represents in table 6.3[147-148].

$$\sigma = [A + B(\varepsilon)^n]\left[1 + Cln\left(\frac{\bar{\varepsilon}}{\bar{\varepsilon}_o}\right)\right]\left[1 - \left\{\frac{T - T_r}{T_m - T_r}\right\}^m\right]$$

eq. 6.1

Table 6.3: Representation of constants, stress and strain notations in JC model

A	Yield strength
B	Hardening modulus
C	Strain rate sensitivity
N	Strain-hardening
M	Thermal softening exponent
$\bar{\varepsilon}_o$	Reference Plastic strain rate
$\bar{\varepsilon}_o$	Plastic strain rate
ε	Equivalent strain
σ	Equivalent flow stress
T_r	Room temperature
T_m	Melting temperature
T	Temperature for flow stress properties

The magnitude of the constants to fit with the Stress –Strain curve of bone is shown in table 6.4 and thermal properties obtained from literature is listed in table 6.5[149-150].

Table 6.4: J-C constants used for simulation in bone drilling

A(MPa)	*B(MPa)*	*C*	*n*	*m*	T_r *(°C)*	T_m *(°C)*
50	101	0.03	0.08	1	20	1665

Table 6.5: Thermal and mechanical properties of bone used in simulation process

Property	**Value**
Elastic modulus (GPa)	20.0 [24,69]
Density (kg/m^3)	2.26× 10^3 [69,151]
Thermal conductivity (W/m K)	0.54 [27,49,69]
Heat capacity (J/m^{3}K)	2.86 × 10^6 [150-151]
Emissivity	0.95 [152]

6.3.4 Friction model

Friction is the main source of temperature rise in cutting simulation models. It acts in between the drill bit and work piece during the shear deformation during the cutting process. As the cutting progress in real time machining, high stresses and high strain rate at the interface of tool and workpiece generated high mechanical power leading to the heat generation. However there is no universal contact law through which a prediction can be made for frictional forces. There are several drilling factors which influence the temperature in drilling. There are two kinds of friction model available i.e coulomb friction model and shear friction model. For the given drilling simulation, simple shear friction model has been implemented in this simulation process in which frictional force directly linked with the friction of equivalent shear stress developed during process($\lambda = \mu_x m$) here $\lambda\ is$ friction force, μ_x is frictional coefficient and m is the shear

yield strength. The frictional stress developed in the model is presented as follows in equation 6.2[24,153]:

$$\sigma_f = \mu_x \left\{\frac{\bar{\sigma}}{\sqrt{3}}\right\}\left(\frac{2}{\pi}\right) sgn(v_r) arctan\left(\frac{v_r}{v_{cr}}\right)$$

eq. 6.2

Where, σ_f is frictional stress, $\bar{\sigma}$ is the equivalent stress, v_r is relative sliding velocity, v_{cr} is critical sliding velocity and μ_x is a friction coefficient.

6.3.5 Heat transfer model

Heat transfer during drilling is result of shear deformation and friction and it is calculated during the simulation process. In present finite element model, heat generated due to mechanical distortion at interface is modeled according to the heat flux volume. Heat flux volume considers both shear deformation and friction factor. The primary heat transfer started with the initiation of cutting process and thermal transfer in drilling covers the following steps [24]:

i) Initiation of heat in the workpiece due to frictional force (frictional heating source) at the interface.
ii) Followed up with contact heat transfer between tool and workpiece.
iii) finally convection heat transfer from outer surfaces to the environment as equation 6.3 [24]:

$$-k\frac{\partial T}{\partial n} = h(T - T_\alpha)$$

eq. 6.3

Where, k is thermal conductivity; h is the connective heat transfer coefficient, n is normal towards out of the surface, T_α is the ambient temperature.

Further, the thermal flux transferring from material chip to the cutting edge of tool is equation 6.4[24]:

$$q = H(T_b - T_t)$$

eq. 6.4

Where, H is constant for heat transfer coefficient, T_b and T_t are the bone and tool surface temperature.

6.3.6 Boundary conditions

In case of conventional drilling simulation process, drill bit is rotating at a fixed rotational speed and feed motion as prescribed in the drill tool setup process. Workpiece is fixed from its nodes in all direction keeping its top surface free for machining i.e. V_X= 0; V_Y= 0; V_Z= 0. Movement from the bottom surface of workpiece is restricted. While in case of ultrasonic assisted bone drilling process, Ultrasonic feed motion superimposed to the tool along with the rotational speed and feed motion given to the workpiece in positive Z direction keeps all other nodes of workpiece constant i.e. V_X= 0; V_Y= 0; V_Z= 0.0833 mm/rev . Drill bit gives linear vibration of 20 kHz with amplitude of 16 µm. The translation position of tool during the ultrasonic addicted drilling process is as follows in equation 6.5 and 6.6[24,154]:

$$X = asin(\omega t) \qquad \textit{eq. 6.5}$$

$$\bar{X} = a\omega cos(\omega t) \qquad \textit{eq.6.6}$$

Where X is the drill bit position, $\bar{X}$ is the drill bit velocity during translation motion of tool. t is time and a is the vibration amplitude, ω is the angular frequency with respect to the vibration frequency i.e. ($\omega = 2\pi F$).

6.4 SIMULATION RESULTS FOR HEAT GENERATION

The heat generation in drilling of bone is calculated during the simulation. The main objective of the simulation process is to compare the conventional bone drilling (CBD) and ultrasonic assisted bone drilling bone (UABD) drilling for temperature rise with all other drilling parameters keeping constant. The interface when come in contact with the workpiece it started cutting process and started generating heat. With passing of specified steps the data has been stored in the post process file (*.DB) and temperature rise has been evaluated for the process. For conventional drilling process, the generated profile for heat generation is shown in figure 6.3 at various steps. The maximum temperature in case of conventional drilling is recorded around 80°C for a depth of 70 mm within the bone specimen shown in figure 6.3.

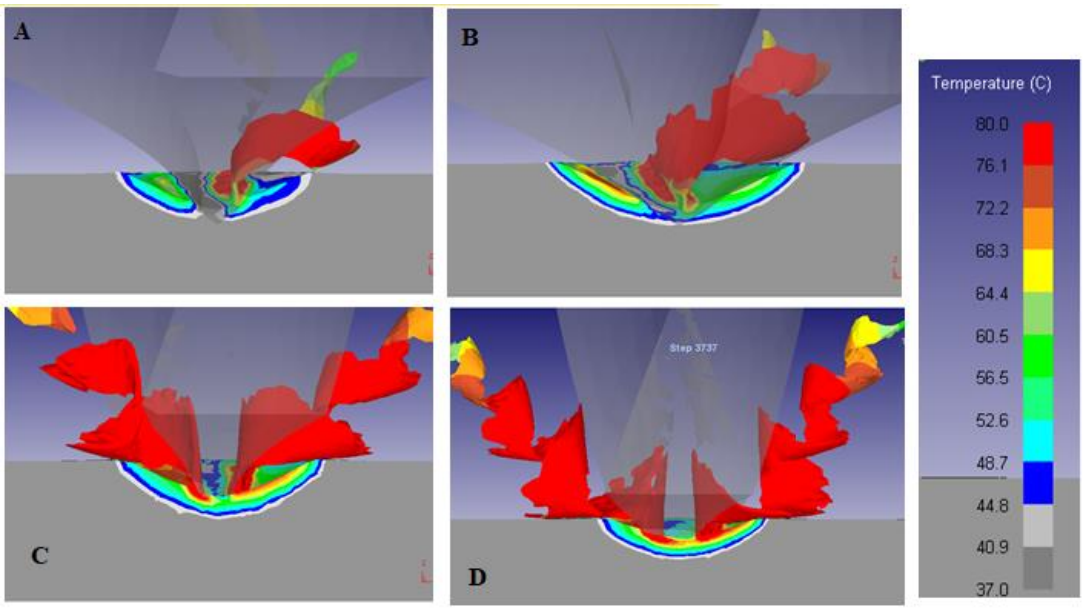

Figure 6.3: Temperature profile generated during simulation conventional bone at various depths (CBD) drilling; (rotational speed: 600 rpm, feed rate: 50mm/min/ 0.0833 mm/rev)

While in simulation of ultrasonic-assisted bone drilling process, the tool vibrates at frequency of 20 kHz with amplitude of 16 µm. keeping other drilling conditions same as conventional drilling

process i.e. rotational speed: 600 rpm; feed rate; 50mm/min / 0.0833mm/rev. The effect of ultrasonic vibrations in drilling give discontinuous contact of tool with the workpiece and its effect on chipping mechanism is evident as short and segmented chips. From simulation results, temperature rise in ultrasonic assisted bone (UABD) drilling is recorded and found lower than the conventional bone drilling (CBD) process. A contour plot for ultrasonic assisted bone drilling process is shown in figure 6.4.

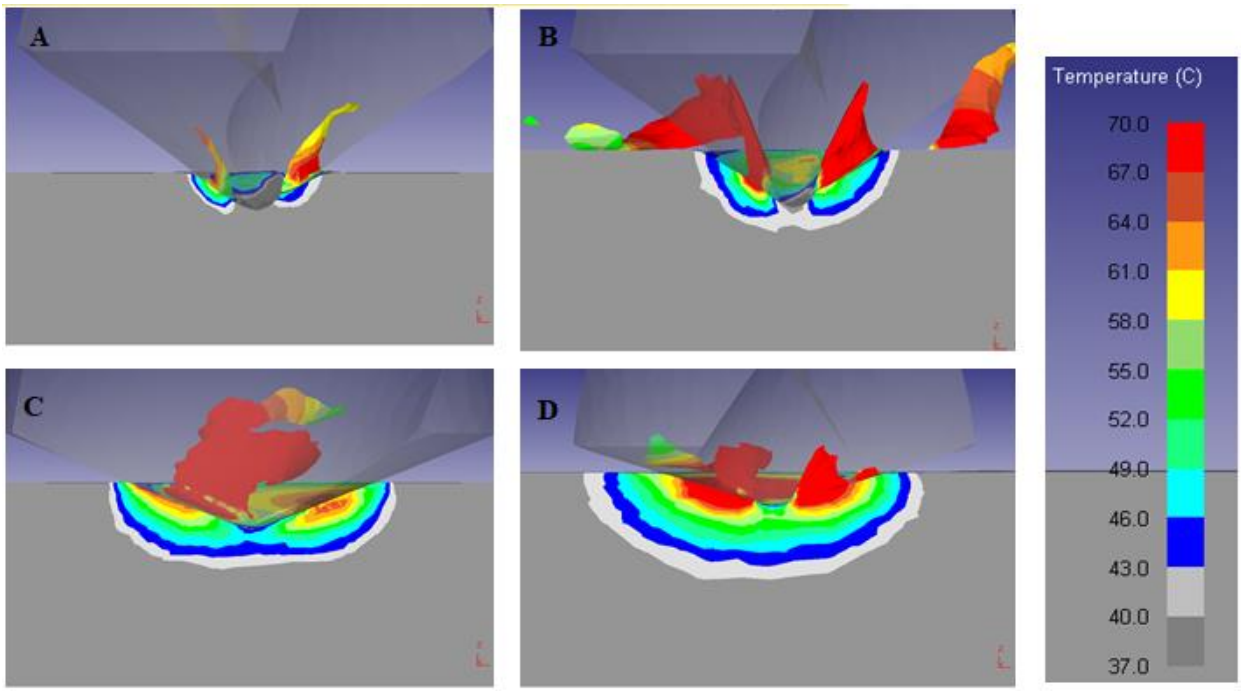

Figure 6.4(A,B,C&D): Temperature profile generated during simulation of ultrasonic assisted bone (UABD) drilling at various depths ; (rotational speed: 600 rpm, feed rate: 50mm/min/ 0.0833mm/rev; frequency: 20 kHz; amplitude: 16 µm)

Further, temperature at different section of time has been recorded for the conventional bone drilling and ultrasonic assisted bone drilling process. From data base file the temperature recorded with respect to the time is compared for both drilling processes and shown in figure 6.5.

From compression, the effect of ultrasonic assisted tooling condition has been justified for minimum thermal damage to the bone.

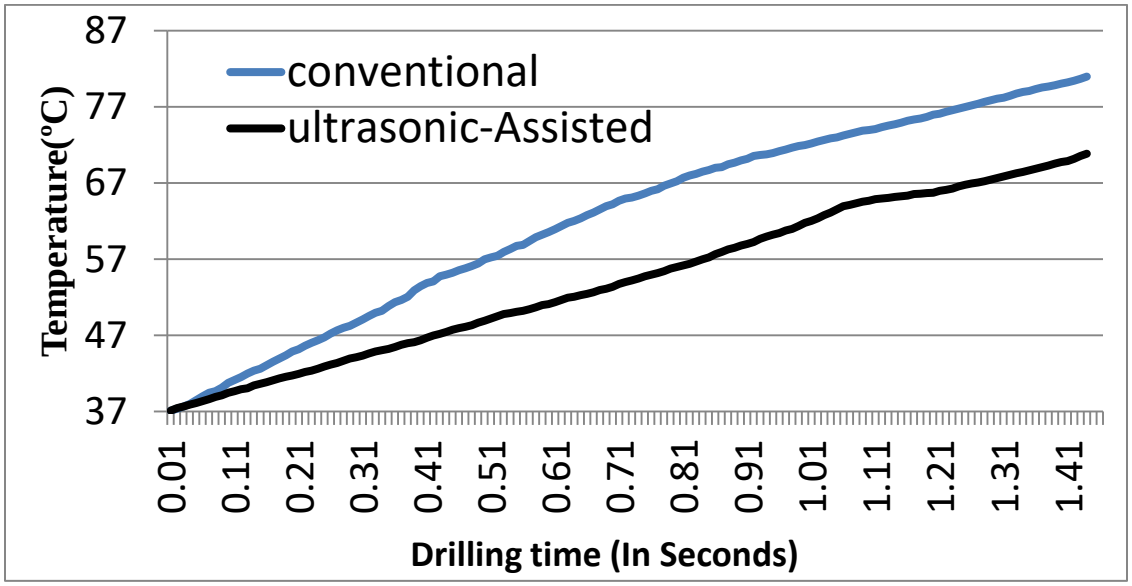

Figure 6.5: Comparison for temperature rise in conventional and ultrasonic assisted bone drilling

6.5 SUMMARY

In this chapter, a finite element analysis (FEA) for the conventional bone drilling and ultrasonic assisted bone drilling process has been studied. The effect of ultrasonic frequency on drilling outcomes is already studied experimentally. The finite element simulation of conventional bone drilling process shows the continuous and large chips while in case of ultrasonic assisted bone drilling simulation shorts and segmental chips are observed. From results, the maximum temperature recorded with ultrasonic assisted tooling condition is reduced up to 10 °C in this specified case. Therefore, from simulation it is very clear that effect of ultrasonic vibration is a key factor to reduce the temperature and the use of thermal model is a helping tool to reduce the risk of thermal and mechanical damage in bone and improve the implant fixture sustainability.

CHAPTER 7: CONCLUSIONS & FUTURE SCOPE

The study was conducted for better understanding of bone drilling outcomes under the effect of ultrasonic vibrations and its comparison with the conventional bone drilling. Discontinuous contact of drilling tool with the bone gives an aerodynamic lubrication effect to the process. That helps to maintain the thermal and mechanical damage as low as possible. The objective framed with respect to the research gaps was explored experimentally and the effect of drilling parameters was studied by Taguchi optimization technique. Along with, a comparison of results were made which showed the effectiveness of ultrasonic- assisted tooling technique over the conventional drilling method for minimizing the thermal and mechanical damage. Further, the following conclusions were made:

7.1 COMPARATIVE CONCLUSIONS FOR CBD AND UABD

Ultrasonic-assisted drilling technique showed its cutting edge effect on the drilling of bone in terms of reduced thermal and mechanical damage and from experimental analysis the following conclusions were made.

- From comparative examination, it was observed that ultrasonic assisted bone drilling help to reduce the heat generation by 5-15 % from the conventional drilling.
- Thrust forces developed during drilling are also controlled by 10-30% from the conventional drilling.
- Delamination in diameter of holes are also affected by the UAD and found 0.2 - 2.2 % less delaminated as compared to conventional drilling process.

- Axial force requited to pullout the bone screw joints of ultrasonic assisted drilled holes are 18-33% better than the conventional drilled holes.

7.2 CONCLUSION FROM TAGUCHI OPTIMIZATION TECHNIQUE

Taguchi optimization is robust method of optimization help to analyze the outcomes with minimum number of possible experimentation. Using Taguchi optimization on desired outcomes the following conclusions were made:

Conclusions From 1st set of experimentation (point angle group):

- For minimum delamination in hole diameter, Slow rotational speed (600 rpm), low feed rate(10 mm/min) and minimum point angle (60 degree) i.e. (R1F1P1) is recommended.
- For minimum thermal invasive to the bone, slow rotational speed (600 rpm), low feed rate (10 mm/min) and minimum point angle (60 degree) i.e. (R1F1P1) is recommended.
- For minimum thrust forces during bone drilling, high rotational speed (3000 rpm), low feed rate (10 mm/min) and minimum point angle (60 degree) i.e. (R5F1P1) is recommended.
- For maximum axial pullout strength, high rotational speed (3000 rpm), low feed rate (10 mm/min) and minimum point angle (60 degree) i.e. (R5F1P1) is recommended.

Conclusions From 2nd set of experimentation (Helix angle group):

- For minimum delamination in hole diameter, Slow rotational speed(600 rpm), low feed rate (10 mm/min) and higher helix angle(36 degree) i.e. (R1F1H5) is recommended.

- For minimum thermal invasive to the bone, Slow rotational speed (600 rpm), low feed rate (10 mm/min) and higher helix angle (36 degree) i.e. (R1F1H5) is recommended.

- For minimum thrust forces during bone drilling, high rotational speed (3000 rpm), low feed rate (10 mm/min) and higher helix angle (36 degree) i.e. (R5F1H5) is recommended.

- For maximum axial pullout strength, high rotational speed (3000 rpm), low feed rate (10 mm/min) and higher helix angle (36 degree) i.e. (R5F1H5) is recommended.

7.3 CONCLUSION FROM ANOVA ANLAYSIS

Conclusions From 1st set of experimentation (point angle group):

- For minimum delamination, feed rate shows the higher percentage contribution for heat generation (55.17%) and parameters expect drill point angle (P), shows their significance with ($p \leq 0.05$) and confirm the result within the range of ± 1.309 %.

- For minimum thermal invasive to the bone, rotational speed shows the higher percentage contribution for heat generation (80.53%) and all involved parameters shows their significance with ($p \leq 0.05$) and confirm the result within the range of ± 1.976°C.

- For minimum thrust forces during bone drilling, rotational speed shows the higher percentage contribution for thrust forces (77.32%) and all involved parameters shows their significance with ($p \leq 0.05$) and confirm the result within the range of ± 0.269 N.

- For maximum axial pullout strength, rotational speed shows the higher percentage contribution for maximum axial pullout (70.10%) and all involved parameters shows their significance with ($p \leq 0.05$) and confirm the result within the range of ± 57.52 N.

Conclusions From 2nd set of experimentation (Helix angle group):

- For minimum delamination, rotational speed shows the higher percentage contribution for delamination (58.21%) and all involved parameters shows their significance with ($p \leq 0.05$) and confirm the result within the range of ± 1.172 %.

- For minimum thermal invasive to the bone, rotational speed shows the higher percentage contribution for heat generation (64.132%) and all involved parameters shows their significance with ($p \leq 0.05$) and confirm the result within the range of ± 4.473 °C.

- For minimum thrust forces during bone drilling, rotational speed shows the higher percentage contribution for thrust forces (64.32%) and all involved parameters shows their significance with ($p \leq 0.05$) and confirm the result within the range of ± 0.968 N.

- For maximum axial pullout strength, rotational speed shows the higher percentage contribution for axial pullout strength (33.71%) and all involved parameters shows their significance with ($p \leq 0.05$) and confirm the result within the range of ± 90.37 N.

7.4 CONCLUSION FROM HISTOPATHOLOGY OF BONE

- The effect of heat generation with respected variation in drilling parameters is verified in terms of structural/cell damage observed in pathology images.

- Increase in heat generation due to machining parameters, increases the osteonecrosis in bone in terms of evaporated lacunas.

- The vibrational effect of tool reduces the thermal damage and help to control the bone up to threshold limit of osteonecrosis.

7.5 CONCLUSION FROM SCANNING ELECTRON MICROSCOPY (SEM)

- In case of UAB drilling the surface is full of half pealed chips shows the effect of vibrations in tool.
- The discontinuous contact of tool and workpiece in case of UAD reduces the thrust forces and thus minimize the crack.
- The level of cracks increased with the rotational speed and feed rate.
- Point angle and helix angle also shows significant effect in generation of cracks.

7.6 CONCLUSION FROM SIMULATION OF BONE DRILLING

- Simulation study shows that there is less temperature generation during Ultrasonic assisted drilling as compare to conventional drilling
- The simulation study is further given an advantage to the orthopedic surgeon to speculate the results in the real time surgery.

7.7 FUTURE SCOPE

- The present study focuses on the estimation of drill point angle and helix angle. Therefore, some other drill specifications i.e. rake angle, chisel edge angle, no of flutes can be the possible reasons for damages. Thus, experimental studies targeting the effect of these drill specifications can be helpful to reduce the thermal and mechanical damages.
- In order to understand the mechanism of material removal in ultrasonic assisted bone drilling, a video study using very high frame rate (10^5 fr/s) camera can be done. This will help to further improve the ultrasonic assisted drilling process and help to develop a FE model based on the segmented chip formation.

- Experiments can be performed to measure the temperature directly at the tool tip by the means of thermography, which will reduce the error of measuring temperature through thermocouple.
- Experiments were performed in vivo experimental conditions. Further, a real time experimental conditions can be generated and check the behavior of drilling techniques and parameters directly to the in-vitro conditions.
- Majority of the fractures observed at the mid-diaphysis section thus, experiments were performed on the mid-diaphysis portion of bone only. some other fractures in the joints parts are also observed where density of the bone is different from the mid diaphysis part where nail insertion is a possible case of rehabilitation throughout the long bone. Experimental study to drill the bone from joint ends can be performed for nail implants.
- Mathematical modeling to predict the thermal and mechanical damage in case of ultrasonic-assisted drilling can be the topic of further study in this field.
- Feasibility and practicality of Micro-drilling to insert the wires during orthopedic surgery.

7.8 SUMMARY

The final conclusions of experimental and numerical simulation study of bone drilling process were observed in this chapter. In broad spectrum, ultrasonic assisted drilling technique is an efficient method to control the mechanical and thermal damage around the drill site in case of orthopedic bone drilling. The effect of discontinuous contact of tool during the bone cutting process shows its impact in terms of less heat generation and less thrust forces developed. Furthermore, this will lead to the less surface damage and minimizing the chances of osteonecrosis in the bone. Parametric optimization of individual outcome of bone drilling process gives estimation for the selection of parameters to avoid the secondary damage during

the drilling of bone. Histopathology of bone specimens shows that the osteonecrosis is a depending factor of temperature only and level of thermal damage with ultrasonic assisted bone drilling process is less as compared to the drilling with conventional process.

REFERENCES

1. Clarke B. Normal Bone Anatomy and Physiology. Clin J Am Soc Nephrol. 2008; 3: 131–139.
2. Rodan GA. Introduction to bone biology. Bone. 1992;13(1):3-6.
3. Pandey RK, Panda SS. Drilling of bone: A comprehensive review. J Clin Orthop Trauma. 2013;4(1):15–30.
4. Odgaard A. Three-dimensional methods for quantification of cancellous bone architecture. Bone. 1997;20(4):315–28.
5. Wall A, Board T. The Compressive Behavior of Bone as a Two-Phase Porous Structure. In: Banaszkiewicz P., Kader D. (eds). Classic Papers in Orthopaedics. Springer, London. 2014.
6. Antonio M, Leali PT. Hard tissues structure and functionality. In: Santin M, Phillips GJ (eds)Biomimetic, Bioresponsive, and Bioactive Materials: An Introduction to Integrating Materials with Tissues. John Wiley & Sons. 2012.
7. Safadi FF et al. Bone Structure, Development and Bone Biology. In: Khurana J. (eds) Bone Pathology. Humana Press. 2009.
8. Gordon CL, Lang TF, Augat P, Genant HK. Image-based assessment of spinal trabecular bone structure from high-resolution CT images. Osteoporosis International 1998;8:317–325.
9. Donnelly E. Methods for assessing bone quality: a review. Clinical orthopaedics and related research. 2011; 469 (8): 2128-2138.
10. Mckibbin B. The biology of fracture healing in long bones. The journal of bone and joint surgery. 1978; 60-B(2); 150-162)

11. Gordon Betts J. DeSaix P, Jhonson E. et al. Anatomy and Physiology. OpenStax Rice University, Houston, Texas (USA). 2013.
12. Weiner S, Traub W, Wagner H D: Lamellar Bone: Structure-function relations. Journal of Structural Biology 1999;126(3):241-255.
13. Rho JY, Kuhn-Spearing L, Zioupos P. Mechanical properties and the hierarchical structure of bone. Medical Engineering & Physics 1998;20(2):92–102.
14. Keaveny T, Wachtel EF, Ford CM, Hayes WC. Differences between the tensile and compressive strengths of bovine tibial trabecular bone depends on modulus. Journal of Biomechanics. 1994; 27: 1137–1146.
15. Piekarski K. Analysis of bone as a composite material. International Journal of Engineering Science 1973;11(6):557–558.
16. Pidaparti RMV, Chandran A, Takano Y, Turner CH. Bone mineral lies mainly outside collagen fibrils: Predictions of a composite model for osteonal bone. Journal of Biomechanics 1996;29(7):909–916.
17. Huang J, Rapoff A J, Haftka RT. Attracting cracks for arrestment in bone-like composites. Materials & Design 2006;27(6):461–469.
18. Guedes R.M, Simões JA, Morais JL. Viscoelastic behaviour and failure of bovine cancellous bone under constant strain rate. Journal of Biomechanics 2006;39:49–60.
19. Gibson LJ, Ashby MF. Cellular solids: structure and properties. Oxford: Pergamon Press, 1998.
20. DePaula CA, Jornson C, Panc Y, Kotha SP, Koike K, Guzelsu N. Changing the structurally effective mineral content of bone within vitro fluoride treatment. Technical note, Journal of Biomechanics 2002;35:355–361.

21. Kotha SP, Guzelsu N. Tensile behavior of cortical bone: Dependence of organic matrix material properties on bone mineral content. Journal of Biomechanics. 2007;40:36–45.
22. Yeh OC, Keaveny TM. Relative roles of microdamage and microfracture in the mechanical behavior of trabecular bone. Journal of Orthopaedic Research. 2001; 19: 1001–1007.
23. Ford CM, Keaveny TM. The dependence of shear failure properties of trabecular bone on apparent density and trabecular orientation. Journal of Biomechanics.1996; 29: 1309–1317.
24. Alam K. Experimental and numerical analysis of conventional and ultrasonically-assisted cutting of bone. PhD thesis. Loughborough University (Institutional Repository). Jan 2009.
25. Karam MD, Willey M, Shurr DG. Total knee replacement in patients with below-knee amputation. Iowa orthopaedic journal. 2010; 30:150-152.
26. Hillery HT, Shuaib I. Temperature effects in drilling of human and bovine bone. Journal of Material Processing Technology. 1999; 92-93: 302-308.
27. Davidson SRH, James DF. Drilling in bone: modeling heat generation and temperature distribution. Journal of Biomechanical Engineering 2003;125:305–314.
28. Olson S, Clinton JM, Working Z, et al. Thermal effects of glenoid reaming during shoulder arthroplasty in vivo. American Journal of Bone Joint Surgery. 2011; 93:11–29.
29. Augustin G, Davila S, Mihoci K, Udiljak T, Vedrina DS, Antabak A. Thermal osteonecrosis and bone drilling parameters revisited. Archives of Orthopaedic Trauma & Surgery. 2007; 128:71–77.

30. Eriksson RA, Albrektsson T. The effect of heat on bone regeneration: an experimental study in the rabbit using bone growth chamber. Journal of Oral & Maxillofacial Surgery. 1984; 42:705-711.

31. Lundskog J. Heat and bone tissue. Scandavian Journal of Plastic & Reconstruction Surgery Suppl. 1972; 9:1-80.

32. Krause WR, Bradbury DW, Kelly JE, Lunceford EM. Temperature elevations in orthopaedic cutting operations. Journal of Biomechanics. 1982; 15: 267–275.

33. Bachus KN, Rondina MT, Hutchinson DT. The effects of drilling force on cortical temperatures and their duration: an in vitro study. Medical Engineering & Physics. 2000; 22:685-691.

34. Iyer S, Weiss C, Mehta A. Effect of drill speed on heat production and the rate and quality of bone formation in dental implant osteotomies. Part I: relationship between drill speed and heat production. International Journal of Prosthodontics. 1997; 10(5):411-414.

35. Iyer S, Weiss C, Mehta A. Effect of drill speed on heat production and the rate and quality of bone formation in dental implant osteotomies. Part II: relationship between drill speed and healing. International Journal of Prosthodontics. 1997; 10(6):536-540.

36. Noble B. Bone microdamage and cell apoptosis. European Cells and Material journal. 2003; 6:46-56.

37. Natali C, Ingle P, Dowell J. Orthopaedic bone drills-can they be improved? Temperature changes near the drilling face. The Journal of bone and joint surgery. British volume. 1996; 78(3):357-362.

38. Moritz AR, Henriques FC. Studies of thermal injury: II. The relative importance of time and surface temperature in the causation of cutaneous burns. Am J Pathol. 1947;23:695-720.
39. Bonfield W, Li CH. The temperature dependence of the deformation of bone. J Biomech. 1968;7(2):323-329.
40. Eriksson RA, Albrektsson T. Temperature threshold levels for heat-induced bone tissue injury: a vital-microscopic study in the rabbit. J Prosthet Dent. 1983;50:101-107.
41. Augustin G, Davila S, Udiljak T, Vedrina DS, Bagatin D. Determination of spatial distribution of increase in bone temperature during drilling by infrared thermography: preliminary report. Arch Orthop Trauma Surg. 2009;129(5):703-709.
42. Eriksson RA, Albrektsson T, Magnusson B. Assessment of bone viability after heat trauma. A histological, histochemical and vital microscopic study in the rabbit. Scand J Plast Reconstr Surg. 1984;18:261-268.
43. Eriksson AR, Albrektsson T, Albrektsson B. Heat caused by drilling cortical bone. Temperature measured in vivo in patients and animals. Acta Orthop Scand. 1984;55(6):629-631.
44. Eriksson RA, Albrektsson T, Grane B, Mcqueen D. Thermal- injury to bone e a vital-microscopic description of heat- effects. Int J Oral Surg. 1982;11(2):115-121.
45. Eriksson RA, Adell R. Temperatures during drilling for the placement of implants using the osseointegration technique. J Oral Maxillofac Surg. 1986;44:4-7.
46. Karaca F, Aksakal B, Kom M. Influence of orthopaedic drilling parameters on temperature and histopathology of bovine tibia: an in vitro study. Medical Engineering & Physics. 2011; 33; 1221-1227.

47. Lee J, Rabin Y, Ozdoganlar OB. A new thermal model for bone drilling with application to orthopaedic surgery. Medical Engineering & Physics; 2011; 33:1234-1244.
48. Lee J, Gozen BA, Ozdoganlar OB. Modeling and experimentation of bone drilling forces. Journal of Biomechanics. 2012; 45: 1076–1083.
49. Davidson SRH, James DF. Measurement of thermal conductivity of bovine cortical bone. Med Eng Phys. 2000;22:741-747.
50. Thompson HC. Effect of drilling into bone. J Oral Surg. 1958;16:22-30.
51. Vaughan RC, Peyton FA. The influence of rotational speed on temperature rise during cavity preparation. J Dent Res. 1951;30(5):737-744.
52. Nam OH, Yu WJ, Choi MY, Kyung HM. Monitoring of bone temperature during osseous preparation for orthodontic micro-screw implants: effect of motor speed and pressure. Key Eng Mater. 2006;321-323:1044-1047.
53. Kalidindi V. Optimization of Drill Design and Coolant Systems During Dental Implant Surgery. MS thesis, University of Kentucky; 2004.
54. Pallan FG. Histological change in bone after insertion of skeletal fixation pins. J Oral Surg Anest Hosp Dent Serv. 1960; 18:400-408.
55. Matthews L S, Hirsch C. Temperatures measured in human cortical bone when drilling. J Bone Joint Surg Am. 1972; 54:297-308.
56. Pal S, Saha S, Effect of cutting speeds on temperature during drilling of bone. Proc. 34th Ann. Conf. on Eng. in Med. & Bio. 1981; 23: 289.
57. Saha S, Pal S, Albright JA. Surgical drilling: design and performance of an improved drill. J Biomech Eng. 1982; 104:245-252.

58. Matthews LS, Green CA, Goldstein SA. The thermal effects of skeletal fixation-pin insertion in bone. J Bone Joint Surg Am. 1984;66:1077-1083
59. Ohashi H, Therin M, Meunier A, Christel P. The effect of drilling parameters on bone. J Mater Sci Mater Med. 1994; 5 (4): 237–241.
60. Brisman DL. The effect of speed, pressure, and time on bone temperature during the drilling of implant sites. Int J Oral Maxillofac Implants. 1996; 11:35-37.
61. Toews A, Bailey J, Townsend H, Barber S. Effect of feed rate and drill speed on temperatures in equine cortical bone. Am J Vet Res. 1999; 60 (8): 942–944.
62. Anitua E, Carda C, Andia I. A novel drilling procedure and subse- quent bone autograft preparation: a technical note. Int J Oral Maxillofac Implants. 2007; 22 (1): 138–145.
63. Basiaga M, Paszenda Z, Szewczenko J, Kaczmarek M. Numerical and experimental analyses of drills used in osteosynthesis. Acta Bioeng Biomech. 2011; 13 (4): 29–36.
64. Sezek S, Aksakal B, Karaca F. Influence of drill parameters on bone temperature and necrosis: a FEM modelling and in vitro experiments. Comput Mater Sci. 2012; 60: 13–18
65. Xu L, Wang C, Jiang M, He H, Song Y, Chen H, Shen J, Zhang J. Drilling force and temperature of bone under dry and physiological drilling conditions. Chin J Mech Eng. 2014; 27 (6): 1240–1248.
66. Lee J E. Modeling and experimentation of forces and temperature distribution for bone drilling with applications to orthopaedic surgery. Ph.D. thesis, Carnegie Mellon University, Pittsburg, PA. 2011.
67. Lee JE, Ozdoganlar OB, Rabin Y. An experimental investigation on thermal exposure during bone drilling. Med Eng Phys 2012; 34 (10): 1510–1520.

68. Alam K, Mitrofanov AV, Silberschmidt V . Thermal analysis of orthogonal cutting of cortical bone using finite element simulations. Int J Exp Comput Biomech. 2010;1(3):236.
69. Alam K, Khan M, Silberschmidt V V. 3D finite-element modelling of drilling cortical bone: Temperature analysis. J Med Biol Eng. 2014; 34(6):618–23.
70. Alam K, Mitrofanov A, Silberschmidt VV. Experimental investigations of forces and torque in conventional and ultrasonically-assisted drilling of cortical bone. Med Eng Phys 2011; 33 (2): 234–239.
71. Wang Y, Cao M, Zhao Y, Zhou G, Liu W, Li D. Experimental investigations on microcracks in vibrational and conventional drilling of cortical bone. J Nanomaterials. 2013;1–5. Article ID 845205.
72. Rafel SS. Temperature changes during high-speed drilling on bone. J Oral Surg Anesth Hosp Dent Serv. 1962; 20: 275–277.
73. Abouzgia MB, James DF. Temperature rise during drilling through bone. Int J Oral Maxillofac Implants. 1997;12(3):342-353.
74. Sharawy M, Misch CE, Weller N, Tehemar S. Heat generation during implant drilling: the significance of the motor speed. J Oral Maxillofac Surg. 2002;60:1160-1169.
75. Pandey RK, Panda SS. Optimization of multiple quality characteristics in bone drilling using grey relational analysis. J Orthop. 2015;12: 39-45.
76. Pandey RK, Panda SS. Multi-performance optimization of bone drilling using Taguchi method based on membership function. Measurement. 2015; 59:9–13.

77. Soriano J, Iriarte L, Eguren J, Aristimuno P, Garay A, Arrazola P. Effects of rotational speed and feed rate on temperature rise, feed force and cutting torque when drilling bovine cortical bone. In: AIP Conference Proceedings. 2012; 1431: 408–416.
78. Alam K, Hassan E, Bahadur I. Experimental measurements of temperatures in ultrasonically assisted drilling of cortical bone. Biotechnology & Biotechnological Equipment. 2015;29(4): 753-757.
79. Krause W. Orthogonal bone cutting: saw design and operating characteristics. J Biomech Eng 1987;109 (3): 263–271.
80. Augustin G, Davila S, Mihoci K, Udiljak T, Vedrina DS, Antabak A. Thermal osteonecrosis and bone drilling parameters revisited. Arch Orthop Trauma Surg. 2008; 128 (1): 71–77.
81. Lughmani WA, Bouazza-Marouf K, Ashcroft I. Finite element modeling and experimentation of bone drilling forces. J Phys Conf Ser 451. 2013:01034.
82. Wang W, Shi Y, Yang N, Yuan X. Experimental analysis of drilling process in cortical bone. Med Eng Phys. 2014;36(2):261–266.
83. Karaca F, Mustafa K, Aksakal B. Structural and histopathologic changes of calf tibial bones subjected to various drilling processes. Kafkas Universitesi Veteriner Fakultesi Dergisi 19 (Supplement A). 2013: A67–A72.
84. Tai BL, Palmisano AC, Belmont B, Irwin TA, Holmes J, Shih AJ. Numerical evaluation of sequential bone drilling strategies based on thermal damage. Med Eng Phys. 2015; 37 (9): 855–861.

85. Alam K, Khan M, Muhammad R, Qamar SZ, Silberschmidt V V. In-vitro experimental analysis and numerical study of temperature in bone drilling. Technol Heal Care. 2015;23(6):775–83.
86. Bertollo N, Walsh WR. Drilling of bone: practicality, limitations and complications associated with surgical drill bits. Biomech Appl; 2011.
87. Lee JE, Chavez CL, Park J. Parameters affecting mechanical and thermal responses in bone drilling: A review. J Biomech. 2018;71:4–21.
88. Bechtol CO, Ferguson AB, Laing PG. Metals and Engineering in Bone and Joint Surgery. Baltimore: Williams and Wilkins; 1959.
89. Jacob CH, Berry JT. A study of the bone machining process-drilling. J Biomech. 1976;9:343-349.
90. Karmani S, Lam F. The design and function of surgical drills and K-wires. Curr Orthop. 2004;18:484-490.
91. Farnworth GH, Burton JA. Optimization of drill geometry for orthopaedic surgery. In: Int Mach Tool Des and Res Conf 15th Proc; 1974:227-233.
92. Sneath RS. The determination of optimum twist drill shape for bone. Biomechanics and related bioengineering topics. In: Proceedings of the Symposium of Glasgow. Oxford: Peragamon Press; 1964.
93. Alam K, Ghodsi M, Al-Shabibi A, Silberschmidt V. Experimental Study on the Effect of Point Angle on Force and Temperature in Ultrasonically Assisted Bone Drilling. J Med Biol Eng. 2018;38(2):236-243.
94. Wiggins KL, Malkin S. Drilling of bone. J Biomech. 1976;9:553-559.

95. Plaskos C, Hodgson A J, Cinquin P. Modelling and optimization of bone-cutting forces in orthopaedic surgery. In: Int Conf Med Image Comput Comput-Assist Interv. Springer, 2003: 2878:254–261.
96. Yeager C, Nazari A, Arola D. Machining of cortical bone: surface texture, surface integrity and cutting forces. Mach Sci Technology. 2008; 12 (1): 100–118.
97. Soriano J, Garay A, Ishii K, Sugita N, Arrazola PJ, Mitsuishi M. A new surgical drill bit concept for bone drilling operations. Mater Manuf Processes. 2013; 28 (10): 1065–1070.
98. Bertollo N, Gothelf TK, Walsh WR. 3-Fluted orthopaedic drills exhibit superior bending stiffness to their two fluted rivals: clinical implications for targeting ability and the incidence of drill bit failure. Injury. 2008;39:734-741.
99. Bertollo N, Milne HRM, Ellis LP, Stephens PC, Gillies RM, Walsh WR. A comparison of thermal properties of 2- and 3- fluted drills and the effect on bone cell viability and screw pull out strength in an ovine model. Clin Biomech. 2010;25:613-617.
100. Jochum RM, Reichart PA. Influence of multiple use of Timedur-titanium cannon drills: thermal response and scanning electron microscopic findings. Clin Oral Implants Res. 2000;11(2):139-143.
101. Allan W, Williams ED, Kerawala CJ. Effects of repeated drill use on temperature of bone during preparation for osteosynthesis self-tapping screws. Br J Oral Maxillofac Surg. 2005;43(4):314-319.
102. Chacon GE, Bower DL, Larsen PE, McGlumphy EA, Beck FM. Heat production by 3 implant drill systems after repeated drilling and sterilization. J Oral Maxillofac Surg. 2006;64(2):265-269.

103. Ercoli C, Funkenbusch PD, Lee HJ, Moss ME, Graser GN. The influence of drill wear on cutting efficiency and heat production during osteotomy preparation for dental implants: a study of drill durability. Int J Oral Maxillofac Implants. 2004;19(3):335-349.
104. Misir AF, Sumer M, Yenisey M, Ergioglu E. Effect of surgical drill guide on heat generated from implant drilling. J Oral Maxillofac Surg. 2009;67(12):2663-2668.
105. Oliveira N, Alaejos-Algarra F, Mareque-Bueno J, Ferre´s- Padro E, Hernandez-Alfaro F. Thermal changes and drill wear in bovine bone during implant site preparation. A comparative in vitro study: twisted stainless steel and ceramic drills. Clin Oral Implants Res. 2011:23(8):963-969.
106. Udiljak T, Ciglar D, Skoric S. Investigation intobonedrillingand thermal bone necrosis. Adv Prod Eng Manag. 2007;2:103-112.
107. Branemark PI. Osseointegration and its experimental background. J Prosthet Dent. 1983;50:399-410.
108. Itay S, Tsur H. Thermal osteonecrosis complicating Steinmann pin insertion in plastic surgery. Plast Reconstr Surg. 1983;72:557-561.
109. Kirschner H, Meyer W. Entwichlung einer innenkuhlung fur chirurgische bohrer. Dtsch Zahnaztl Zeitschrift. 1975;30:436-438.
110. Lavelle C, Wedgwood D. Effect of internal irrigation on frictional heat generated from bone drilling. J Oral Surg. 1980;38:499-503.
111. Gupta V, Pandey PM, Gupta RK, Mridha AR. Rotary ultrasonic drilling on bone: A novel technique to put an end to thermal injury to bone. Proc Inst Mech Eng Part H J Eng Med. 2017;231(3):189–96.

112. Wootton R, Reeve J, Veall N. The clinical measurement of skeletal blood flow. Clin Sci Mol Med. 1976;50:261-268.
113. Ong FR, Bouazza-Marouf K.. 1998. Drilling of bone: a robust automatic method for the detection of drill bit break-through. Proc Inst Mech Eng H J Eng Med. 1998; 212 (3): 209–221.
114. Mitsuishi M, Warisawa S, Sugita N. Determination of the machining characteristics of a biomaterial using a machine tool designed for total knee arthroplasty. CIRP Ann-Manuf Technol. 2004; 53 (1): 107–112.
115. Pandey RK, Panda SS. A feasibility investigation for modeling and optimization of temperature in bone drilling using fuzzy logic and Taguchi optimization methodology. Proc Inst Mech Eng Part H J Eng Med. 2014;228(11):1135–1145.
116. Pandey RK, Panda SS. Modeling of Temperature in Orthopaedic Drilling Using Fuzzy Logic. Appl Mech Mater. 2012;249–250:1313–1318.
117. Li X, Zhu W, Wang J, Deng Y. Optimization of bone drilling process based on finite element analysis. Appl Therm Eng. 2016;108:211–220.
118. Gok K, Gok A, Kisioglu Y. Optimization of processing parameters of a developed new driller system for orthopedic surgery applications using Taguchi method. Int J Adv Manuf Technol. 2014;76(5–8):1437–48.
119. Ueda T, Wada A, Hasegawa K ichi, Endo Y, Takikawa Y, Hasegawa T, et al. Design optimization of surgical drills using the Taguchi method. J Biomech Sci Eng. 2010;5(5):603–14.

120. Izamshah R, Noorazizi M., Kasim MS, Che Haron C. Influence of Orthopaedic Drilling Parameters on Surface Roughness and Cutting Force of Bone Drilling Process. Proc Int Conf Electron Mech Cult Med (Emcm 2015). 2016:752-758.
121. Akhbar MFA, Yusoff AR. Optimization of drilling parameters for thermal bone necrosis prevention. Technol Heal Care. 2018:1–15,(pre-press).
122. Pandey RK, Panda SS. Optimization of bone drilling using Taguchi methodology coupled with fuzzy based desirability function approach. J Intell Manuf. 2015; 26(6):1121-1129.
123. Schwieger K, Carrero V, Rentzsch R, Becker A, Bishop N, Hille E, et al. Abrasive water jet cutting as a new procedure for cutting cancellous bone--in vitro testing in comparison with the oscillating saw. J Biomed Mater Res B Appl Biomater . 2004;71(2):223–228.
124. Biskup C, Hover M. Heat Generation during Abrasive Water-Jet Osteotomies Measured by Thermocouples. Strojniki vestnik-Journal of Mechanical Engineering.2006; 52: 451-457.
125. Dunnen S.D. et al. Waterjet drilling in porcine bone: The effect of the nozzle diameter and bone architecture on the hole dimensions. journal of the mechanical behavior of biomedical materials.2013;27: 8 4 –93.
126. Eshet Y. et al. Microwave Drilling of Bones. IEEE transactions on biomedical engineering. 2006; 53(6):1174-1182.
127. Khademi V, Akbari J, Farahmand J, Ultrasonic-Assisted Drilling of Bone, Patent date Issued Jan 18, 2009 Patent issuer and number ir 5644.

128. Khademi V, Akbari J, Farahmand F, Masoumi E, Experimental Investigation of Ultrasonic-Assisted Bone Drilling, International Conference on Orthopaedic Surgery, Biomechanics & Clinical Application, Brunel university, London, UK, 2010.
129. Ito K, Ishizaka S, Sasaki T, Miyahara T, Horiuchi T, Sakai K, et al. Safe and minimally invasive laminoplastic laminotomy using an ultrasonic bone curette for spinal surgery: technical note. Surg Neurol. 2009 ;72(5):470–475.
130. Wang Y, Cao M, Zhao X, Zhu G, McClean C, Zhao Y, et al. Experimental investigations and finite element simulation of cutting heat in vibrational and conventional drilling of cortical bone. Med Eng Phys. 2014;36(11):1408–15.
131. Gupta V, Pandey PM. Experimental investigation and statistical modeling of temperature rise in rotary ultrasonic bone drilling. Med Eng Phys. 2016;38(11):1330–1338.
132. Gupta V, Pandey PM, Silberschmidt V V. Rotary ultrasonic bone drilling: Improved pullout strength and reduced damage. Med Eng Phys. 2017;41:1–8.
133. Boskey AL, Coleman R. Aging and Bone. J Dent Res. 2010; 89(12):1333-1348.
134. Ding M. Age variations in the properties of human tibial trabecular bone and cartilage. Acta Orthop Scand (Suppl 292) 2000; 71.
135. Ding M, Dalstra M, Danielsen CC, et al., Age Variations In The Properties Of Human Tibial Trabecular Bone. J Bone Joint Surg [Br] 1997;79-B:995-1002.
136. Huttner EA, Machado DC, de Oliveira RB, Antunes AG, Hebling E. Effects of human aging on periodontal tissues. Spec Care Dentist. 2009; 29:149-155.
137. Ding M, Dalstra M, Linde F, Hvid I. Changes in the stiffness of the human tibial cartilage-bone complex in early-stage osteoarthrosis. Acta Orthop Scand 1998; 69: 358-362.

138. Richards JB, Kavvoura FK, Rivadeneira F, Styrkársdóttir U, Estrada K, Halldórsson BV, et al. Collaborative meta-analysis: associations of 150 candidate genes with osteoporosis and osteoporotic fracture. Ann Intern Med, 2009; 151: 528-537.
139. Ding M, Dalstra M, Linde F, Hvid I. Mechanical properties of the normal human tibial cartilage-bone complex in relation to age. Clinic Biomech 1998; 13: 351-358.
140. Brain, E.B. in: The preparation of decalcified sections. Springfield, Ill, Charles C Thomas, ; 1966:121–136.
141. Callis G.M, strechi D.L, decalcification of bone: literature review and practical study of various decalcifying agents, methods and their effects on bone histology. Journal of Histotechnology. 1998; 21(1):49-58.
142. Culling C.F.A. Handbook of Histopathological and Histochemical Techniques (Third Edition). Butterworth. London, 1974.
143. Taguchi G. Introduction to Quality Engineering. Asian Productivity Organization, Tokyo, 1990.
144. Roy RK.. Design of experiments using the Taguchi approach: 16 steps to product and process improvement. 2001.
145. Albright J, Johnson T, Saha S. Principles of internal fixation. Ortho Mech: Proced devices, Acad. Lond 1978, 123–229.
146. Fluhrer J. DEFORM-3D Version 11.0 user‘s manual. Scientific Forming Technologies Corporation, 2013.
147. Ahmed N, Mitrofanov AV, Babitsky VI, Silberschmidt VV: 3D finite element analysis of ultrasonically assisted turning. Computational Materials Science 2007;39:149–154.

148. Mitrofanov AV, Babitsky VI, Silberschmidt VV: Finite element simulations of ultrasonically assisted turning. Computational Materials Science 2003;28:645– 653.
149. Alam K, Mitrofanov A V., Silberschmidt V V. Finite element analysis of forces of plane cutting of cortical bone. Comput Mater Sci. 2009;46(3):738–743.
150. Alam K, Mitrofanov AV, Silberschmidt V. . Thermal analysis of orthogonal cutting of cortical bone using finite element simulations. Int J Exp Comput Biomech. 2010;1(3):236-251.
151. Huiskes J. Some fundamental aspects of human joint replacement. Acta. Orthop. Scand. Suppl. 1980; 185: 1-208.
152. Feldmann A., Zysset P. Experimental determination of the emissivity of bone. Medical Engineering & Physics. 2016; 38(10): 1136–1138.
153. Shih AJ, Yang HTY. Experimental and finite element predictions of residual stresses due to orthogonal metal cutting, International Journal for Numerical Methods in Engineering 1993;36(9):1487–1507.
154. Lotfi M, Amini S. Experimental and numerical study of ultrasonically-assisted drilling. Ultrasonics. 2017;75:185–193.

PUBLICATIONS

- **Singh G**, Jain V, Gupta D. Parametric Effect of Vibrational Drilling on Osteonecrosis and Comparative Histopathology Study with Conventional Drilling of cortical bone. Proc IMechE Part h: J Of Engg In Med. 2018; 232(10): 975-986. **(Sage Publications) (SCI I.F.: 1.13).**
- **Singh G,** Jain V, Gupta D. Multi-Objective Performance Investigations Of Orthopedic Bone Drilling Using Taguchi Membership Function. Proc IMechE Part h: J Of Engg In Med. 2017; 231(12):1133-1139. **(Sage Publications*)* (SCI I.F: 1.13).**
- **Singh G**, Jain V, Gupta D, Ghai A. Optimization Of Process Parameters For Drilled Hole Quality Characteristics During Cortical Bone Drilling Using Taguchi Method. J of mech. Behv. of biomed matr. 2016; 62: 355-365 **(Elsevier) (SCI I.F.: 3.45).**
- **Singh G,** Jain V, Gupta D. Comparative Study for Surface Topography of Bone Drilling Using Conventional Drilling and Loose Abrasive Machining. Proc IMechE Part h: J Of Engg In Med. 2015; 229(3):225-231. **(Sage Publications) (SCI I.F: 1.13)**
- **Singh G,** Ghai A, jain V, Gupta D, Investigation on thermal necrosis during bone drilling. J of Machg and Machb of Matr. 2016; 18(4): 341-349. **(SCOPUS).**

- **Singh G**, Jindal R, Jain V, Gupta D. Effect of tool and drilling parameters on surface topography of bone drilled holes: an invitro study. The International Conference for Students on Applied Engineering, **Newcastle, United Kingdom**, 20-21 October 2016. **(published with IEEE digital library)**
- **Singh G**, Ghai A, Jain V, Gupta D, Investigations for Bone Surface Damage during Orthopaedic Bone Drilling. 4th International Conference on Orthopedics & Rheumatology-2015, **Baltimore, Maryland, USA.**

- **Singh G**, Jain V, Gupta D. Comparison for Pullout Strength of Bone Joint Using Conventional and Non-Conventional Drilled Hole. Moratuwa Engineering Research Conference-2017. University of Moratuwa, Srilanka. **(Best poster presentation award).**

Articles under review

- **Singh G,** Jain V, Gupta D. Analytical Validation For Thrust Force And Heat Generation During Cortical Bone Drilling. Journal of the Brazilian Society of Mechanical Sciences and Engineering. **(Springer)** (under review) **(SCI I.F.: 1.6).**
- **Singh G,** Jain V, Gupta D. influence of drill rotational speed on thermal damage in bone: an assessment using thermal imaging camera and histopathology. Acta orthopaedic beligica. (under review) **(SCI I.F.: 0.48)**
- **Singh G,** Jain V, Gupta D. histopathology of drilled bone specimen to evaluate the thermal damage with various drilling conditions. Medical Engineering & Physics. **(Elsevier) (SCI I.F.: 2.2)**

APPENDIX-A

Figure A-1: Coordinate Measuring Machine (Courtesy: Advanced metrology lab, Thapar Institute of Engineering &Technology, Patiala)

Figure A-2: Scanning Electron Microscopy (SEM) (Courtesy: SAI lab, Thapar Institute of Engineering &Technology, Patiala)

Figure A-3: 3-axis vertical milling center (Courtesy: CNC lab, Thapar Institute of Engineering &Technology, Patiala)

Figure A-4: Nikon microscope (Courtesy: maharishi Markandeshwer University, Mullana-Ambala)